Journal Name

Review—Electrolytes for Electrochemical Energy Storage

Lan Xia,[a] Linpo Yu,[a] Di Hu[a] and George Z. Chen[a,b,*]

Received 00th January 20xx,
Accepted 00th January 20xx

DOI: 10.1039/x0xx00000x

www.rsc.org/

Electrolyte is a key component of electrochemical energy storage (EES) devices and its properties greatly affect the energy capacity, rate performance, cyclability and safety of all EES devices. This article offers a critical review of recent progresses and challenges in electrolyte research and development particularly for supercapacitors and supercapatteries, recharegable batteries (such as lithium-ion and sodium-ion batteries), and redox flow batteries (including fuel cells in a broad sense). The review will focus on liquid electrolytes, particularly aqueous and organic electrolytes, ionic liquids and molten salts. Influences of electrolyte properties on the performances of different EES devices are discussed in detail.

Table of contents

[a] *Department of Chemical and Environmental Engineering, and Centre for Sustainable Energy Technologies, Faculty of Science and Engineering, University of Nottingham Ningbo China, Ningbo, 315100 China*
[b] *Department of Chemical and Environmental Engineering, Faculty of Engineering, University of Nottingham, Nottingham, NG7 2RD UK*
** Email: george.chen@nottingham.ac.uk*

1. Introduction

Great concerns are growing on the accelerating exhaustion of fossil resources, mainly consumed in various forms of energy, and the associated climate and environmental issues, creating a great demand for energy storage devices at different scales. Of all on-going developments, electrochemical energy storage (EES) technologies have attracted worldwide attention for portable consumer products, electric or hybrid electric vehicles and integration with the power grid and renewable energy sources. These uses are based on the fact that EES devices, e.g. rechargeable batteries, supercapacitors and redox flow batteries (including fuel cells in a broad sense), are manufactured in units or modules which can offer flexible combinations to meet demands for high energy capacity, fast charging-discharging, improved safety, and long service life.[1-9]

Nevertheless, EES also faces challenges. For example, as a relatively new member of the EES family, electric double layer capacitors (EDLCs) store energy through the electrostatic interaction between electrodes and ions in electrolyte. They offer fast dis-/charging capability (i.e. high power capability, >100 kW/kg), high energy efficiency (close to 100 %), and long cycle life (>500,000 cycles), promising for advanced and highly efficient energy storage management. However, compared to the rechargeable batteries, including redox flow batteries, EDLCs have much lower energy capacity (usually <30 Wh/kg in aqueous devices).

It is well known that raising the operating voltage is an effective strategy to increase both the energy and power density of EES devices.[10-12] Such an approach needs new electrode and electrolyte materials that are physically, chemically, particularly electrochemically stable against the high operating voltage. Specifically for new liquid electrolytes, they need to offer low or zero flammability and beneficial interactions with the electrode materials, in addition to other properties as discussed below. Surprisingly, compared to the active and dynamic research on electrode materials, research on electrolytes received relatively less attention.[13-18]

Electrolyte is an indispensable constituent, liquid in most cases, in all types of EES devices and helps conduct electricity by means of the transportation of ions, but not electrons. Because the electrolyte is placed between, and in close interaction with the positive electrode (**positrode**) and

negative electrode (**negatrode**), its identification is the key to a safe and high performance EES device. (Note: The use of **cathode** and **anode** to describe the electrodes in rechargeable EES devices, lithium ion batteries in particular, is inappropriate and confusing because the same positrode is an anode in charging but a cathode in discharging. However, the positrode retains its positive polarity in both the charging and discharging processes. The case is similar for the negatrode.)

Basically, electrolyte is an ionic conductor but electronic insulator, and it is practically either a solid or more often a liquid which usually works with a porous membrane or gel in EES devices. A liquid electrolyte commonly refers to a solution comprising salts and solvents, and functional additives, but it can also be a pure liquid salt, such as ionic liquid or molten salt. In accordance with the principle and purposes of EES devices, the electrolyte generally should meet the following requirements:[19,20] (1) wide electrochemical window; (2) high ionic conductivity; (3) high chemical and thermal stability; (4) chemical inertness to other cell components such as the separator, electrode substrates and cell packaging materials; (5) safe, non-toxic, and economical affordability. Actually, it is very challenging to find an electrolyte matching perfectly with all these prerequisites. Tremendous and continuous research efforts were made in the past, and will continue in the future.

In this article, we offer a review on recent research progresses in optimisation of liquid electrolytes for several important EES devices, including supercapacitors, lithium ion and sodium ion batteries, magnesium batteries, as well as redox flow batteries and others. The discussion will be mainly on aqueous and organic electrolytes with brief introductions of ionic liquids and molten salts. Some recently reported new electrolytes (such as high voltage and highly concentrated electrolytes) and relevant interesting results are also included.

2. Aqueous electrolytes

Aqueous electrolytes are historically the basis of battery research and commercialisation. In the first electrochemical battery, i.e. the so called voltaic pile developed by Alessandro Volta, brine was used as the electrolyte. The ammonium chloride aqueous solution was used as the electrolyte in the first Leclanché cell whose dry cell form is the forerunner of the neutral Zn-MnO_2 battery. Until now, aqueous electrolytes are still widely used in various traditional and new EES devices.

2.1. Aqueous alkali metal ion batteries

Traditional rechargeable Li-ion batteries or Na-ion batteries use organic electrolytes to achieve high working voltages (> 3.0 V). Compared with their aqueous counterparts, organic electrolytes are more expensive, toxic, and flammable. Slow charging and discharging is another disadvantage of Li-ion batteries with organic electrolytes. An aqueous rechargeable Li-ion battery consisting of VO_2 negatrode and $LiMn_2O_4$ positrode was developed to bypass the safety concern of the organic electrolytes.[21] However, the cycling life of this VO_2/$LiMn_2O_4$ aqueous Li-ion battery was poor. The capacity retention was less than 50 % after 100 cycles. The attempt on replacing the electrode materials could hardly improve the poor cycling life of aqueous Li-ion batteries. A recent study on the electrolyte of aqueous Li-ion batteries revealed the mechanism of capacity fading during cycling. The discharged state of all the negatrode materials suitable for aqueous Li-ion batteries reacted with water and O_2, independent of the pH of the electrolyte.[22] Fig. 1 shows the typical charge/discharge curves of the negatrode material, $LiTi_2(PO_4)_3$, in the presence/absence of O_2. The experiment was done in an aqueous Li_2SO_4 electrolyte. As shown in Fig. 1a, the coulombic efficiency of $LiTi_2(PO_4)_3$ at a 4 C rate in the aqueous electrolyte was 99 % in the absence of O_2 and 92 % in the presence of O_2. This discrepancy in coulombic efficiency as shown in Fig. 1b became more significant when cycled at a 1 C rate. The coulombic efficiency was 98 % in the absence of O_2 versus 77 % in the presence of O_2.

This observation suggests that the reduced state, $Li_{3-x}Ti_2(PO_4)_3$, can be chemically oxidised, leading to capacity fading upon charge-discharge cycling the aqueous Li-ion battery.

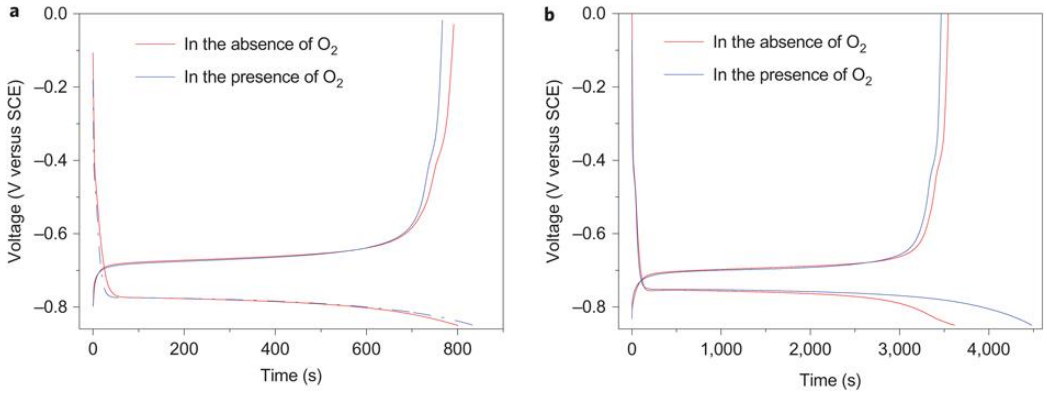

Fig. 1 Typical charge/discharge curves of $LiTi_2(PO_4)_3$ in aqueous 1.0 mol L^{-1} Li_2SO_4 electrolyte at (**a**) 4 C and (**b**) 1 C charge/discharge rates in the presence and absence of O_2.[22] (Reproduced with permission from Nature Publishing Group. Copyright 2010.)

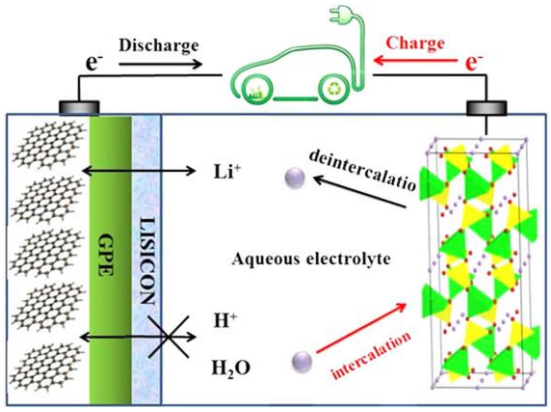

Fig. 2 Schematic illustration of an aqueous Li-ion battery using the graphite coated by GPE (gel polymer electrolyte) and LISICON as the negatrode, $LiFePO_4$ in 0.5 mol L^{-1} Li_2SO_4 aqueous electrolyte as the positrode.[23]

Based on this understanding, the $LiTi_2(PO_4)_3/Li_2SO_4/LiFePO_4$ aqueous batteries were fabricated by eliminating oxygen, adjusting the pH values of the electrolyte, and using carbon-coated electrode materials. The capacity of such aqueous Li-ion batteries remained over 90 % after 1,000 cycles when the batteries were fully charged/discharged in 10 min., and 85 % after 50 cycles even when fully charged/discharged at a very low current for 8 h. Another work on assembling aqueous Li-ion batteries by using graphite coated with gel polymer electrolyte (GPE) and LISICON as the negatrode, and $LiFePO_4$ in aqueous solution as the positrode was published recently.[23] A LISICON film consisting of Li_2O-Al_2O_3-SiO_2-P_2O_5-TiO_2-GeO_2 was simply put on the GPE to be a solid separator to keep water away and allow only the passage of Li^+ ions. The mechanism of this type of aqueous Li-ion battery is illustrated in Fig. 2. When the cell is charging, Li^+ ions will deintercalate from the $LiFePO_4$ olivine structure, and then pass through the aqueous solution, LISICON film, and then GPE in sequence. The Li^+ ions will finally intercalate in the graphite during the charging process. The reversed process will take place during discharging. The average discharging voltage of this LISICON film based aqueous Li-ion battery is up to 3.1 V, which leads to a specific energy value of 258 Wh kg^{-1}. The average discharging voltage of aqueous Li-ion batteries with the LISICON film coated Li metal negatrode and a $LiMn_2O_4$ positrode can be up to 4.0 V, which leads to a specific energy value of 446 Wh kg^{-1}.[24] The Mg metal was also considered to replace the Li metal in similar aqueous batteries. The Grignard reagent of PhMgBr was used to stabilise the Mg metal negatrode, whilst the positrode was still made of $LiFePO_4$ to construct a novel Mg metal and Li-ion hybrid rechargeable aqueous battery.[25] The specific energy value of this interesting hybrid reached 245 Wh kg^{-1}. Similar to the aforementioned $LiTi_2(PO_4)_3/Li_2SO_4/LiFePO_4$ aqueous batteries, the aqueous Li_2SO_4 solution was also used as the electrolyte in these LISICON film based Mg metal and Li-ion hybrid aqueous batteries. In addition to its high ionic conductivity, the Li_2SO_4 aqueous electrolyte does not change the nature of LISICON as a solid-state electrolyte.

Although rarely reported in the literature, aqueous Na-ion batteries are also being developed to fulfil the demand of EES devices with low cost, safety, and abundant resource. Similar to the investigation of aqueous Li-ion batteries, most work on aqueous Na-ion batteries has been focused on the electrode materials. A recent study revealed that hollow $K_{0.27}MnO_2$ nanospheres can facilitate the electron/ion transport kinetics in the negatrode, leading to long cyclability and high rate capability.[26] A coin cell consisting of the hollow $K_{0.27}MnO_2$ nanospheres negatrode and $NaTi_2(PO_4)_3$ positrode with 1.0 mol L^{-1} Na_2SO_4 aqueous electrolyte could exhibit a specific capacity of 84.9 mAh g^{-1} at 150 mA g^{-1}, and the capacity of 56.6 mAh g^{-1} could be still maintained when the current was increased to 600 mA g^{-1}. The capacity retention of the full cell was 83 % at 200 mA g^{-1} after 100 cycles. It is obvious that more attention should be paid to investigation of the electrolytes of aqueous Na-ion batteries.

2.2. Aqueous Zn-ion batteries

The potential of Zn^{2+}/Zn is negative enough to make Zn a preferred negatrode material, particularly in various aqueous batteries. In some aspects, Zn-ion rechargeable batteries can also be competitive with Li-ion batteries. For example, Zn is more abundant in the earth's crust, and has a higher theoretical volumetric charge capacity (5854 mAh/mL-Zn vs. 2062 mAh/mL-Li). Also, aqueous Zn-ion batteries are intrinsically safer due to their incombustible electrolytes. However, Zn dendrite formation and the increased irreversibility of the Zn/Zn^{2+} redox couple during the charge/discharge processes decrease critically the cycle life of Zn-ion batteries and worsen their discharge performance.

A recent study revealed that a $Zn//Co_3O_4$ battery can overcome the drawbacks of conventional Zn rechargeable batteries mentioned above by electrodeposition of Zn on carbon fibres (CFs) with the Zn@CF core-shell structure to achieve dendrite-free cycling behaviour and flexible negatrode. Similarly, electrodeposition of ultrathin porous Co_3O_4 nanosheets on a Ni foam achieved a highly conductive and flexible positrode in the electrolyte of 1.0 mol L^{-1} KOH and 0.01 mol L^{-1} $Zn(Ac)_2$ (Ac = acetate).[27] The battery presented excellent cycling performance with capacity retention of 80 % after 2000 full cycles as shown in Fig. 3a. Fig. 3b demonstrates the assembling of a flexible $Zn//Co_3O_4$ battery, which powered a red LED. Other Zn battery designs were also reported, such as the Prussian blue/Zn rechargeable battery with a mixture of bio-ionic liquid and water as the electrolyte, and the Zn-ion battery based on NASICON structured $Na_3V_2(PO_4)_3$.[28,29] The aqueous electrolyte compositions in these two reports were different, while both of the reported Zn batteries had an effective cycle life of more than 100 cycles. In both cases, the electrolytes affected the performance of the Zn-ion batteries.

2.3. Redox flow batteries

In a redox flow battery (RFB), redox couples that are soluble in the electrolyte are used to store and release energy when the battery is charging and discharging. In most cases, the redox couple, or the electrolyte determines the specifications of the

RFB. It is worth highlighting that all known RFBs are based on aqueous electrolytes. In a previous review,[28] specifications and operation performances of the most developed and commercially available RFBs are compared. The so called all-vanadium RFB has the highest efficiency and the longest cycle life, while the zinc-cerium and bromide-polysulfide RFBs have advantages in power density and cost, respectively. Here, we are not going to provide a comprehensive review of RFBs, but pick up some recent developments in large-scale devices and scientific frontiers. Some large scale RFBs (>10 kW) were reported in the literature.[28, 29] Such a large output of the device is due to the stacked RFB cells. In the all-vanadium case, a 1 kW class RFB stack consisted of 14 cells, and a 10 kW class RFB stack composed of eight 1 kW class stack modules with a configuration of 4 × 2 (serial × parallel).[29] A recent report demonstrated an integration of dual-silicon photoelectro-chemical cell into an RFB for unassisted photocharging by using the redox couples of Br_3^-/Br^- and AQDS/$AQDSH_2$ (cf. Fig. 4).[30] The authors named this device solar rechargeable flow cell (SRFC). Fig. 4 illustrates the SRFC configuration. In the SRFC, the photoelectrochemical cell and RFB are connected through electrolyte circuit loops. First, AQDS is reduced to $AQDSH_2$ on the photocathode and Br^- is oxidised to Br_3^- on the photoanode simultaneously in the photoelectrochemical cell by short-circuiting the two photoelectrodes under illumination. The photoelectrochemical products AQDSH2 and Br_3^- are then stored in two individual reservoirs that can be used by the RFB in the SRFC. A commercial Nafion membrane was used as the separator in each cell. The SRFC could be self-photocharged to 0.8 V under simulated AM 1.5-G illumination and delivered a discharge capacity of up to 730 mAh L^{-1} after photocharging for 2 h.

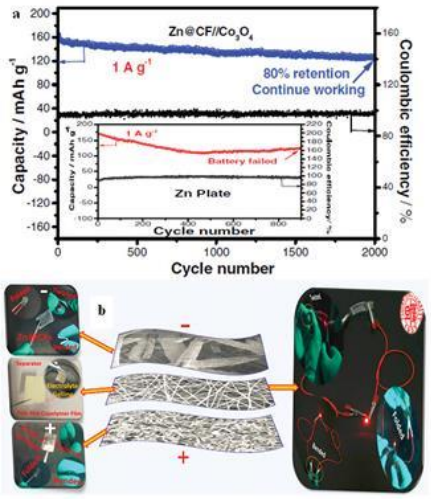

Fig. 3 (a) Cycling performance of the Zn//Co_3O_4 battery at 1 A g^{-1} assembled with Zn@CF and Zn plate (insert); (b) Structure of flexible Zn//Co_3O_4 battery and optical photographs of a flexible battery working at different states.[27] (reprinted with permission, copyright 2016, John Wiley & Sons, Inc.)

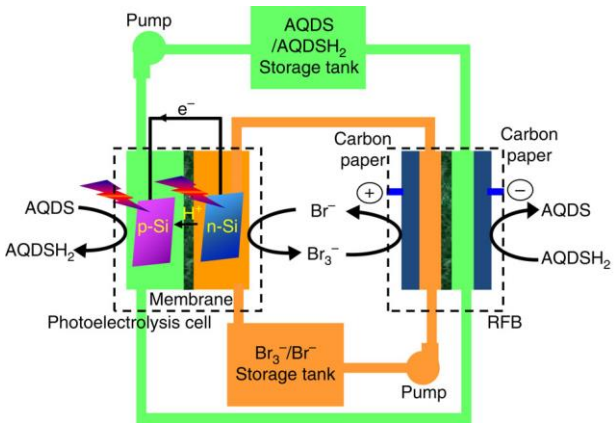

Fig. 4 Schematic configuration of the solar rechargeable flow cell (SRFC), AQDS: 9,10-anthraquinone-2,7-disulphonic sodium. $AQDSH_2$: 1,8-dihydroxy-9,10-anthraquinone-2,7-disulphonic sodium.[30]

2.4. Aqueous supercapacitors and supercapatteries

Similar to the aforementioned batteries, the standard electrolytes used in supercapacitors or supercapatteries (which is a hybrid of **supercapa**citor and ba**ttery**) can be either aqueous or organic. In all variants, the device contains one or occasionally multiple species of supporting electrolytes that are not electroactive within the working voltage range, which is essential for electrolyte stability.

Aqueous electrolytes, compared to their organic counterparts, are advantageous in terms of affordability, conductivity, heat capacity and environmental impact. The solutes of the aqueous electrolytes in either a supercapattery or supercapacitor can be any salt, acid, base, or their combination, but must be carefully selected to be harmonious with electrode materials. For example, a HCl solution is suitable for the CNT/PAn composite as the positrode,[31-33] but a KCl solution is preferred for the CNT/PPy composite.[32,34-37] The pH of an aqueous electrolyte can be greatly deterministic to the performance of electrode materials. A good example of this effect is the capacitive behaviour of MnO_2 under non-stoichiometric conditions. Although MnO_2 is one of the most widely used positrode materials for supercapacitors, it only exhibits a relatively rectangular cyclic voltammogram (CV) in neutral aqueous electrolytes, but presents a bell shaped CV (battery like behaviour) in alkaline solutions. The cause for these apparent dynamic responses is that within the MnO_2 positrode the redox transition between MnO_2 and MnOOH contributes to the observed pseudocapacitance which is featured by the rectangular CV. In neutral aqueous electrolytes, MnO_2 is in the semiconductor state, leading to the relatively rectangular CV. However, MnO_2 is reduced to $Mn(OH)_2$ which is a poor conductor in alkaline solutions.[38] Formation of the insulating $Mn(OH)_2$ occurs because the solubility of MnOOH becomes significant in concentrated alkaline solutions.[39, 40] The dissolved Mn(III) species in turn undergo a reduction process to form Mn(II) species at low voltages and eventually into insoluble $Mn(OH)_2$ by combining

with OH^- ions.[38] In this case, the neutral aqueous electrolytes, such as Li_2SO_4, Na_2SO_4, K_2SO_4, and KCl solutions, are widely used in the MnO_2 based supercapacitor and electrode materials studies.[41-44] It has been found that the supercapacitor using a K_2SO_4 electrolyte can exhibit a specific energy value of 17.6 Wh kg^{-1} at a specific power of 2 kW kg^{-1}, which is higher than the similarly designed supercapacitor using a Li_2SO_4 electrolyte.[43] As to the cycling performance, it was recently reported that an asymmetrical supercapacitor consisting of α-MnO_2/CNT as positrode and activated carbon as negatrode with Na_2SO_4 aqueous electrolyte can retain 77 % of its initial capacity after 20,000 charge-discharge cycles at 50 A g^{-1}.[42]

Another factor affecting the performance of supercapacitor and supercapattery is the size of the hydrated ionic sphere (anion and cation). Regardless of what solutes are in the aqueous electrolytes, the real charge carriers are the hydrated ions, instead of the ions themselves. It is generally accepted that the ions of smaller spheres enhance the diffusion and intercalation rates due to their better kinetic movements.[45, 46] Furthermore, smaller spheres are able to travel deeper into the pores and hence access more active sites in the electrode material than larger spheres. This understanding is particularly important when considering the contribution of double layer capacitance. The Li^+ ion is a typical example. Its salt is widely used in organic electrolytes because it is the smallest alkali metal ion. However, potassium and sodium salts (whose cations are larger than the Li^+ ion) are often more commonly utilised in aqueous electrolytes because the sizes of hydrated K^+ and Na^+ spheres are much smaller than the hydrated Li^+ sphere. Water has also a relatively narrow thermal window, which affects application of aqueous electrolytes at low or sub-zero temperatures. However, many wind farms which require high speed energy storage are built in places where winds are more frequent and stronger in cold winter. A recent study on using the organoaqueous solutions of chloride salts, e.g. $CaCl_2$ and KCl, has revealed promising results, decreasing the working temperature of CNTs and carbon electrodes to below –60 °C.[47] This achievement may be explained by the unique affinity between Ca^{2+} ions and the oxy-groups on the surfaces of carbon nanotubes or activated carbon.

3. Organic electrolytes

3.1. Supercapacitors

Supercapacitors can offer high specific power (> 10 kW kg^{-1}), long cycle life (>500,000 cycles), and have been considered recently as a promising device in advanced and highly efficient energy storage management.[48-50] Of different supercapacitors, electrical double-layer capacitors (EDLCs) are currently dominating the supercapacitor markets. The EDLC stores energy through the electrostatic interaction between electrodes and electrolyte ions. Thus, selection of the correct electrolyte matching with the electrode materials is the key for a successful EDLC.

Electrolytes used in supercapacitors must have high ionic conductivity and wide electrochemical window, which impact the power capability and energy capacity, respectively. Compared to aqueous electrolytes, organic electrolytes composed of a salt and organic solvents provide a wider electrochemical window (>2.8 V), which enables higher specific energy.[51-53] Based on the operating voltage, in this section, the authors will describe mainly recent progresses in the research and development of organic electrolytes used in some high voltage EDLCs and a special type of supercapattery, the so called Li-ion capacitors.[52]

Typical organic electrolytes such as tetraethylammonium tetrafluoroborate ($TEABF_4$) dissolved in acetonitrile (AN) or propylene carbonate (PC) are widely used in commercial EDLCs and research, and generally operate up to 2.8 V. EDLCs using AN-based electrolytes demonstrate higher power and better low temperature performance compared to those in PC-based electrolytes.[54-56] In 2010, NASA Tech Briefs reported an organic electrolyte with freezing temperatures as low as –85.7 °C. It was formulated by addition of $TEABF_4$ to mixed AN and 1, 3-dioxolane (DOL) at 1:1 by volume ratio. The cells filled with this electrolyte showed highly linear discharge curves over a wide range of temperatures.[57] However, AN has not been used in Japan for many years due to its toxicity and low flash point. Thus, PC is usually considered to be a promising alternative solvent for commercial EDLCs. Without the toxicity of AN, PC is more preferred because of its wide electrochemical window, high electrolytic conductivity, wide liquid temperature range and resistance against hydrolysis.[58, 59]

It is also noteworthy to mention that the properties of the salt in the electrolyte may play a crucial role in the development of high performance EDLCs. Many research efforts have been focused on the selection and synthesis of the supporting salts. It was reported that among various known salts, Et_4NBF_4 due to its wide electrochemical window, high solubility and ion conductivity in most solvents was the most common supporting salt for the organic electrolyte of EDLCs .[59-61] However, in many common organic solvents, $TEABF_4$ can only dissolve up to 1.0 mol L^{-1} which is not sufficient for the desired high conductivity. Some asymmetric tetraalkylammonium salts and cyclic quaternary ammonium salts were thus explored, including triethylmethylammonium ($TEMABF_4$), 1-ethyl-1-methyl-pyrrolidinium ($MEPYBF_4$), and tetramethylenepyrrolidinium ($TMPYBF_4$). These salts have higher concentrations and hence offer high conductivities.[62-66] Indeed, $TEMABF_4$ showed higher solubility in PC, which may be used as an alternative to $TEABF_4$.

Since energy capacity of a supercapacitor is the product of capacitance and squared voltage, the most effective strategy to increase both the energy and power densities of EDLCs is to raise the operating voltage.[67] Many studies have shown that it is highly challenging to increase the operating voltage beyond 3 V for EDLCs using any known commercial electrolyte. In fact, the choices of supporting salts, solvents, and impurities of the electrolytes have profound influences on the electrochemical window of the organic electrolyte.[59,68] On the one hand,

research has identified that the ionic size and type of different salts have great influences on the capacitance and power performance of EDLCs.[69-71] It was observed that quaternary ammonium salts with small cations could achieve a high EDLC specific capacitance.[69] Furthermore, the salt also plays an important role in affecting the electrochemical window of organic electrolytes.[63,72,73] The ionic liquid, N-butyl-N-methylpyrrolidinium bis(trifluoromethanesulfonyl) imide ($PYR_{14}TFSI$) was used to formulate the electrolyte, and EDLCs containing $PYR_{14}TFSI$ in PC exhibited a high operating voltage (up to 3.5 V) and excellent cycling stability. A small capacitance loss of only 5 % was also achieved after 100,000 cycles carried out at 3.5 V.[74,75] Additionally, the spiro-(1,1')-bipyrolidinium tetrafluoroborate (SBP-BF_4) salt was also tested, confirming that the novel SBP-BF_4/PC electrolyte in activated carbon based EDLCs had a high withstand voltage of up to 3.2 V and good capacitor behaviour. Unfortunately, these new organic salts are expensive compared to $TEABF_4$, which inhibits practical applications.[76] For the normal EDLCs with AN- or PC-based electrolytes, a voltage over 2.7 V may cause serious decomposition of electrolyte and impurities (e.g. water), and irreversible reactions at the activated carbon electrode. Such unwanted reactions can result in gas evolution and passive film formation on the electrode surface.[77-80] In the case of PC-based electrolytes, the gas evolution has been experimentally analysed using an H-type cell as illustrated in Fig. 5, which is capable of separately collecting gases from the positive and negative compartments.[81] The analysis revealed CO_2 and CO from the positrode, while H_2, and other gases, like propylene, CO_2, ethylene and CO, were found on the negatrode after a float-test applied at cell voltages above 3.0 V.[81,82]

Many efforts have been focused on the implementation of novel solvents with wider operating voltage ranges. In 2011, new electrolytes based on linear sulfones were reported, showing that ethyl isopropyl sulfone (EiPS)-based electrolytes have high voltage durability of 3.7 V with high cycling stability.[83] Also, it was reported that alkylated cyclic carbonates had a withstand voltage higher than 3.0 V.[84] Particularly, the 2,3-butylene carbonate (2,3-BC) electrolyte could withstand up to 3.5 V because of mainly the outstanding oxidation resistance of 2,3-BC.

On the other hand, fluorinated solvents possess remarkably higher chemical and electrochemical stability owing to the high electronegativity and low polarizability of the fluorine atom.[85] For example, a fluorinated solvent, fluoroacetonitorile (FAN) was investigated to offer a wide electrochemical window. However, the findings also showed that the 1.0 mol L^{-1} $TEABF_4$/FAN electrolyte had a lower ionic conductivity compared to the 1.0 mol L^{-1} $TEABF_4$/AN solution.[86] Similarly, in an effort to address the low flash point and relatively low electrochemical stability of AN-based electrolytes, adiponitrile (ADN) was studied as a possible solvent for EDLCs.[87] It was found that EDLCs using 0.7 mol L^{-1} $TEABF_4$/ADN as the electrolyte showed a higher operating voltage of 3.75 V, and a high capacitance retention over 35,000 cycles carried out at a cell voltage as high as 3.5 V. However, the ionic conductivity of this new electrolyte needs further improvement because it is much lower than that of AN-based electrolytes. Although these novel electrolytes have significantly increased operating voltages, their relatively high viscosity and low ionic conductivity, especially at room temperature, reduce the power performance of such EDLCs.

To further increase the working voltage, extensive efforts have been devoted to the development of the so called Li-ion capacitor (LIC). Typically, an LIC combines a Li-ion battery electrode and an EDLC electrode, and is hence, in principle, a supercapattery. It usually displays a high working voltage of ~4.0 V, leading to higher energy capacity (>30 Wh kg^{-1}). Because of the smaller size of solvated Li^+ ion in organic solvents than in water, organic electrolytes composed of $LiClO_4$ or $LiPF_6$ and mixtures of two or more carbonate solvents (e.g., EC+DMC) have been widely used in LICs. In a few previous studies on degradation mechanisms, it was found that 4.3 and 1.5 V versus Li^+/Li were the critical potentials for the positrode and negatrode of EDLCs, respectively.[88] Coupled with an activated carbon (AC) negatrode, many battery positrode materials such as $LiMn_2O_4$, $LiFePO_4$ and $LiCoO_2$ were investigated.[89-91] An example cell of AC/1.0 mol L^{-1} $LiClO_4$-AN/$LiMn_2O_4$ showed specific energy of 45 Wh kg^{-1} at an power output of 0.03 kW kg^{-1}.[90, 92]

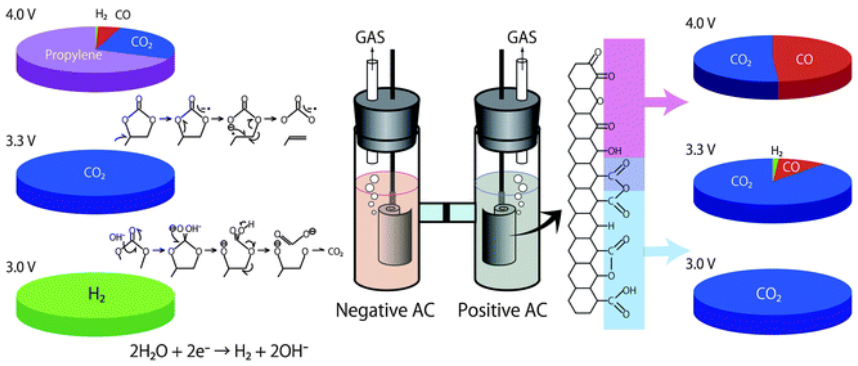

Fig. 5 Illustration of gas evolution from an EDLC cell upon application of different voltages.[78] (Reproduced with permission from The Royal Society of Chemistry. Copyright 2012.)

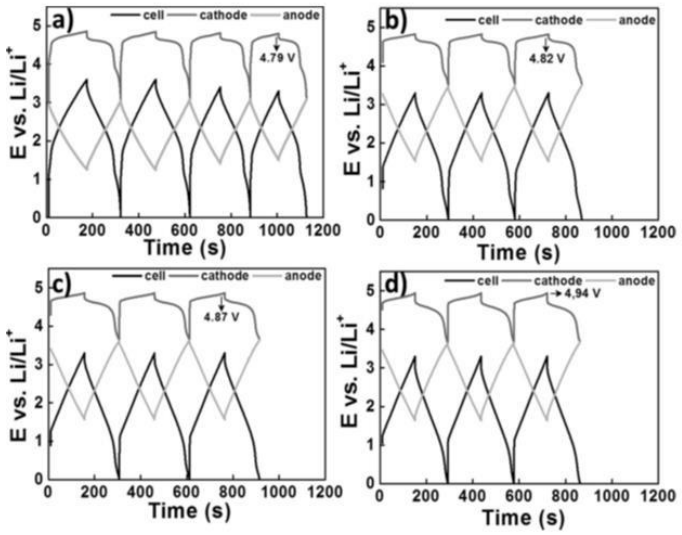

Fig. 6 Charge-discharge profiles of the LNMO/AC LIC with a cell voltage of 3.3 V at the a) beginning, b) after 1,000 cycles, c) 2,000 cycles and d) 3,000 cycles. It can be seen that the potential of the LNMO plateau is relatively low (4.79 V) at the beginning, but gradually increases to higher potentials (4.82 → 4.87 → 4.94 V) during cycling which leads to an increase in the capacity.[95] (Reprinted with permission from The Electrochemical Society, Copyright 2014.)

Using a 1.0 mol L^{-1} $LiPF_6$/EC+DMC electrolyte, a 5.0 V positrode, $LiNi_{0.5}Mn_{1.5}O_4$ (LMNO), was demonstrated in similar configurations.[93,94] These cells display a sloping voltage profile from 1.0 to 3.0 V, high specific energy of 56 Wh kg^{-1}, and excellent capacity retention of 95 % after up to 1000 cycles.

A later investigation used the same electrode combinations and electrolyte, but a higher cell voltage of 3.3 V. Some of the findings are presented in Fig. 6. A promising capacity retention of 89 % was observed even after 4000 cycles with average specific energy and power of about 50 Wh kg^{-1} and 1100 W kg^{-1}.[95] Unfortunately, the capacity fading of this cell became more pronounced with increasing the cell voltage. For example, the cells at 3.4 V and 3.5 V showed capacity retention of only 58 % and 23 % after 4000 and 2000 cycles, respectively. This phenomenon may be ascribed to the constant shifting of the LNMO plateaus to higher potentials as a result of Li loss upon the surface layer formation which in turn leads to the degradation of electrolyte. Remarkably, in a 2006 report,[96] In another study, AC and graphite were used as the negatrode and positrode materials to fabricate a simple capacitor containing the electrolyte of 1.5 mol L^{-1} $TEMABF_4$/PC or 1.5 mol L^{-1} $TEMAPF_6$/PC. This AC/graphite capacitor was tested to show that the electrolyte composition and weight ratio of AC to graphite had a profound influence on the performance of the capacitor. Further investigations confirmed the effect of other factors,[97-103] including the type of salts,[98,99] solvents,[100-102] and weight ratios of AC/graphite,[103] on the performance of this asymmetric AC/graphite capacitor. Specially, it was noticed that EC had an extraordinarily retardant tendency towards anions (e.g. PF_6^-, ClO_4^-, $DFOB^-$ and BF_4^-) intercalating into the interlayer space of graphite. This behaviour was attributed to the strong solvation of some anions by EC (see Fig. 7).[100-102] It should be mentioned that the investigated LICs with an AC negatrode had a medium operating voltage in the range of 2.5-3.5 V, and their energy capacity is rather limited.

LICs employing a combination of AC positrode and Li-ion battery negatrode were also studied, revealing working voltages higher than 4.0 V. Fig. 8 illustrates a case with a Li^+ intercalation graphite negatrode. As a result, these LICs could offer higher energy densities and long cycle life.[104-108] Battery negatrode materials such as carbon-based materials (mostly graphite) and $Li_4Ti_5O_{12}$ were proposed and investigated. Typical compositions of the reported electrolytes used in LICs were based on solutions of $LiPF_6$ or $LiClO_4$ dissolved in mixtures of two or more solvents. These electrolytes are also mainly used in Li-ion batteries (LIBs).[106, 107, 109] A LIC cell of hard carbon (HC)/1.3 mol L^{-1} $LiPF_6$/EC-DEC-PC/AC was reported to show high specific energy of 82 Wh kg^{-1} at 2.4 C. Another LIC cell with 1.0 mol L^{-1} $LiPF_6$ in EC+DMC (1:1, v/v) exhibited the highest specific energy of 103.8 Wh kg^{-1} and a good capacity retention of over 85 % after 10,000 cycles in a voltage range from 1.5 V up to 4.5 V.[110] Since the graphite negatrode did not initially contain Li, pre-lithiation of the graphite negatrode was a key aspect of this LIC.[111] It was also reported that capacity loss of the LICs during charge-discharge cycling was obviously reduced by addition of Li metal into the cell.[112,113]

The highest potential of the AC electrode should be lower than 4.5 V vs Li^+/Li, while the lowest potential of the HC/stabilized Li metal powder (SLMP) electrode should be greater than 0.1 V vs. Li^+/Li. Moreover, the capacitance degradation of this LIC was less than 1 % after 1300 cycles in a voltage range of 2.0 to 4.1 V.[114]

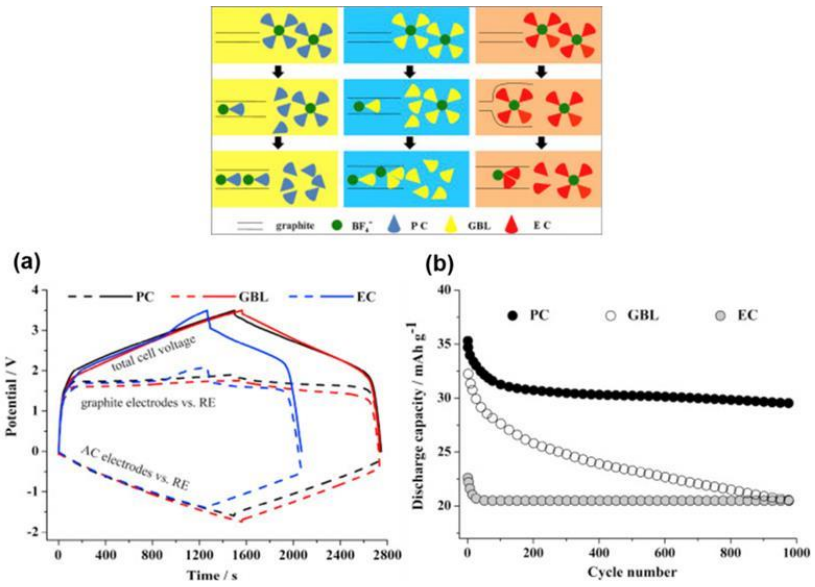

Fig. 7 (a) Potential profiles of graphite positrode and AC negatrode vs. AC quasi-reference electrode in the AC/graphite capacitors using the electrolytes of 1.5 mol L^{-1} $SBPBF_4$–PC, –GBL and –EC, respectively, during the 1st galvanostatic charge–discharge. (b) Cycling performance of AC/graphite capacitors using different electrolyte solutions.[102] (Reprinted with permission from Elsevier. Copyright 2015)

Additionally, it was proposed to use quaternary alkyl ammonium and PC based organic electrolytes in LICs. The result showed that the sizes of quaternary alkyl ammonium cations played a very important role in the performance of LICs.[115] Nonetheless, based on Li-salt electrolytes, the shortcomings of LICs were found to be a poor performance at low temperatures[116] and a low rate capability resulting from the low ionic conductivity and the battery-type graphite negatrode. Therefore, more studies should be focused on the development of new LIC electrolytes to solve the above-mentioned drawbacks in the future. It is generally known that a number of electrolyte additives can be used in Li-ion batteries and also supercapacitors as discussed below.

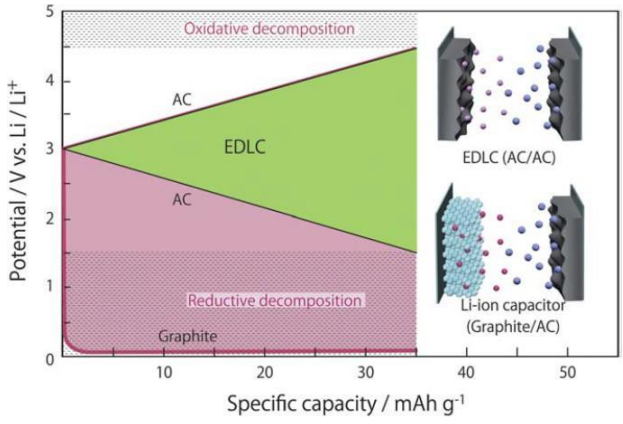

Fig. 8 Typical voltage profiles for an EDLC cell and an LIC cell composed of an AC positrode and a graphite negatrode.[78] (Reproduced with permission from The Royal Society of Chemistry. Copyright 2012.)

There are a few reports on improving the properties of the supercapacitors with the help of functional additives.[117-123] For example, the electrochemical characteristics of EDLCs consisting of electrodes of microporous titanium carbide derived carbon (TiC-CDC) were studied in 1.0 mol L^{-1} $(C_2H_5)_3CH_3NBF_4$/PC solutions with several additives, such as diethyl sulfite (DES) and 1, 3-propylene sulfite (PS).[117-120] These additives are actually well-known for LIBs. The results showed that DES and PS additives could obviously change both the viscosity and conductivity of PC-based electrolytes, affecting the capacitance and the characteristic time constant, and the power and energy values of the obtained EDLCs (see Fig. 9). Regarding EDLCs, upon addition of Li_2O_2 into the 1.5 mol L^{-1} $TEABF_4$/AN electrolyte, the electrochemical window was increased to over 4.0 V. The EDLC adopting this electrolyte could obtain higher specific capacitance at high scan rates of 10-500 mV s^{-1}.[121]

Another electrolyte additive, 1,3,5-trifluorobenzene (TFB) was found to be able to improve the mobility of BF_4^- ions near the microporous electrode, and can enhance the high rate performance of the AC/Li high voltage capacitors.[122] In situ formation of fluorophosphates additives in the commercial 1.0 mol L^{-1} $LiPF_6$/EC+DMC electrolyte was tested in LICs to create a stable layer of solid electrolyte interphase (SEI) on the electrode surface and broaden the operating voltage window to 4.8-1.2 V.[123] This finding indicates a new strategy for designing proper electrolyte additives to further widen the electrochemical window of existing electrolytes and enhance the performances of the supercapacitors.

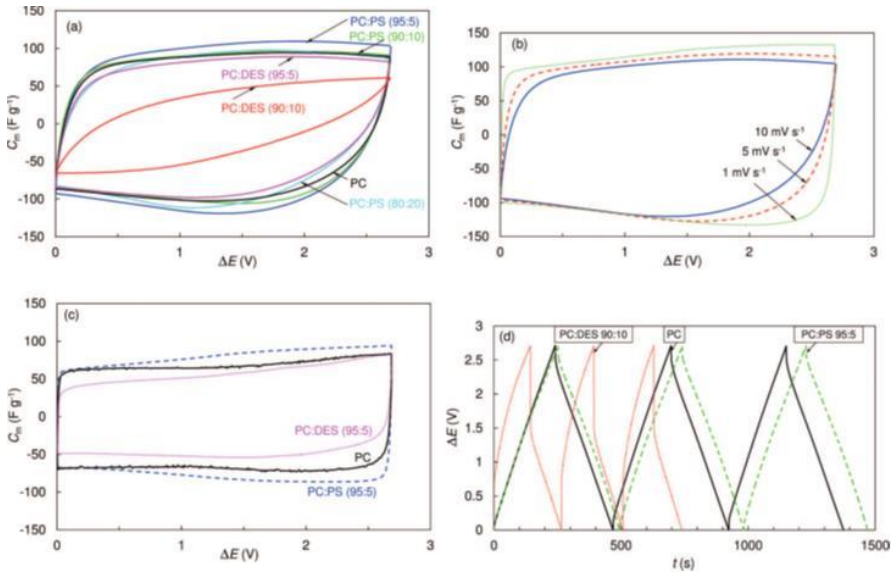

Fig. 9 Cyclic voltammograms expressed as specific capacitance vs. cell voltage for EDLCs with different solvents and addition of 1.0 mol L^{-1} $(C_2H_5)_3CH_3NBF_4$ at 10 mV s^{-1} and −20°C (a), at different voltage scan rates with mixed PC:PS (95:5) (b), and at 1 mV s^{-1} and 0°C (c). Galvanostatic charging-discharging cycles (ΔE = 3.0 V, j = 10 mA cm^{-2}) for electrolytes with different solvents (d).[117] (Reprinted with permission from The Electrochemical Society. Copyright 2014.)

3.2. Lithium ion batteries

Among all rechargeable batteries, LIBs are the most popular EES devices because they have high energy density, acceptable cycle life, no memory effect, and low self-discharging.[124-126] As mentioned above, an electrolyte functions to conduct ions but insulate electrons, and can be in various forms such as ionic liquid, molten salt, or a solid ionic conductor, but more often a salt dissolved in a solvent. Some EES devices, such as supercapacitor, can work with almost any liquid electrolyte, but LIBs would refuse to work properly if the electrolyte used were incorrect.[127-129] In this section, we review recent progresses in organic electrolytes for currently prevailing LIBs, focusing on conventional electrolytes, high voltage electrolytes and highly concentrated electrolytes.

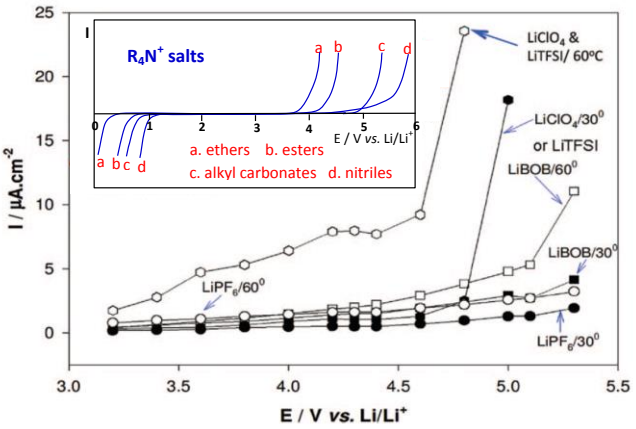

Fig. 10 Anodic behaviour of Al foils (current collector for positrode) in various Li salt solutions (alkyl carbonates). The inset includes schematic potentio-dynamic behaviour of an inert Pt or glassy carbon electrode in various organic solutions containing tetra-alkyl ammonium salts, e.g. $(C_4H_9)_4NClO_4$. When the anodic stability is high, the cathodic stability is low and vice versa.[129] (Reprinted with permission from The Electrochemical Society. Copyright 2015.)

3.2.1 Conventional electrolytes

During the past three decades, extensive efforts have been devoted to investigating new electrode materials, while there is little work about improvements in electrolytes. In principle, new electrodes would have incurred new electrolyte compositions. However, these new materials still use the conventional electrolytes, which are typically solutions of lithium hexafluorophosphate ($LiPF_6$) dissolved in mixed organic carbonate solvents such as PC, ethylene carbonate (EC), either dimethyl carbonate (DMC), ethyl methyl carbonate (EMC) or diethyl carbonate (DEC).

Alkyl carbonates are considered to be the most suitable solvents for dissolution of lithium salts, because they have acceptable electrochemical stability, high ionic conductivity, wide operating temperature range and sufficiently low toxicity.[127-129] It is well known that due to carbon atoms being at an oxidation state of +4, alkyl carbonates have high anodic and low cathodic stability. For example, the oxidation potential of EC-based electrolytes can reache up to 4.5 V vs. Li^+/Li on a spinel positrode surface.[130, 131]

Meanwhile, the EC-based electrolytes show an excellent compatibility with a graphite negatrode because the reduction of EC on graphite electrodes can lead to formation of a protective SEI film.[132-136] Thus, EC is a critical component to obtain sufficient passivation of a graphite negatrode in standard electrolyte solutions for LIBs.[137]

Like EC as a mandatory component, the $LiPF_6$ salt has also become an indispensable solute in almost all LIBs. $LiPF_6$ is well known for its high solubility and conductivity, great anodic stability, and good capability of passivating Al current collectors at positive potentials.[138] However, $LiPF_6$ has a main disadvantage: it is easy to decompose to LiF and PF_5 at temperatures higher than 60 °C. The PF_5 can then cause a series of irreversible reactions on both the positrode and negatrode, resulting in performance deterioration.[139, 140] $LiN(SO_2CF_3)_2$ (LiTFSI) and $LiC(SO_2CF3)_3$ (LiTFSM) show good thermal and chemical stability compared to $LiPF_6$.[141-144] Unfortunately, they are highly corrosive to the Al positrode current collector. As shown in Fig. 10, corrosion of Al was typically observed at potentials above 4.25 V vs Li^+/Li.[145] Therefore, the most common electrolyte solutions for LIBs are composed of 1.0 mol L^{-1} $LiPF_6$ and binary mixtures of EC combined with a linear carbonate with low viscosity, e. g. dimethyl carbonate (DMC), ethyl methyl carbonate (EMC) or diethyl carbonate (DEC).

Besides $LiPF_6$ and carbonate solvents, various electrolyte additives have been proposed and tested to improve the battery performance and safety. The progresses and prospective in functional additives for LIBs are reviewed recently, ranging from negatrode additives, positrode additives, safety additives, and salt type additives.[146]

3.2.2. High voltage electrolytes

High-voltage Li-ion batteries have been a focus in the current energy storage research due to their potential application in transportation and grid load levelling.[147] Recently, positrode materials with high operating potential of ~4.7 V vs. Li^+/Li, such as $LiNi_{0.5}Mn_{1.5}O_4$, $LiMPO_4$ (M=Mn, Co, V), Li_2MPO_4F (M=Ni, Co) and Li-rich layer oxides, xLi_2MnO_3• (1-x) $LiMeO_2$ (Me=Mn, Co, Ni), have been investigated extensively.[148,149] However, a major difficulty in using these positrode materials is the anodic instability of conventional carbonate-based organic electrolytes at operating potentials over 4.5 V.[127, 150, 151] It was shown that the conventional EC-based electrolyte was not stable around 4.5 V, resulting in severe oxidative decomposition into a resistive and unstable surface film of inorganic Li salts and organic carbonates in the positrode, and deterioration of the cycling performance. Moreover, the transition-metal ions could catalyse the oxidation reaction and accelerate the decomposition of electrolytes at potentials higher than 4.5 V, leading to rapid capacity fading.[152-155] Therefore,

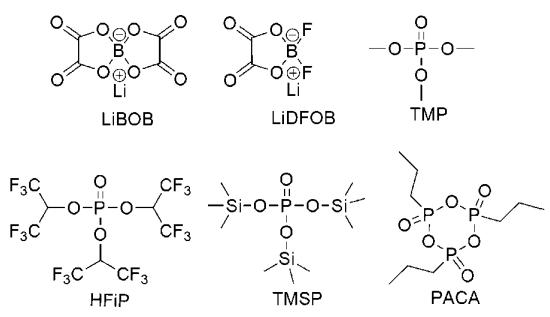

Fig. 11 Chemical structures of additives for high voltage LIBs.

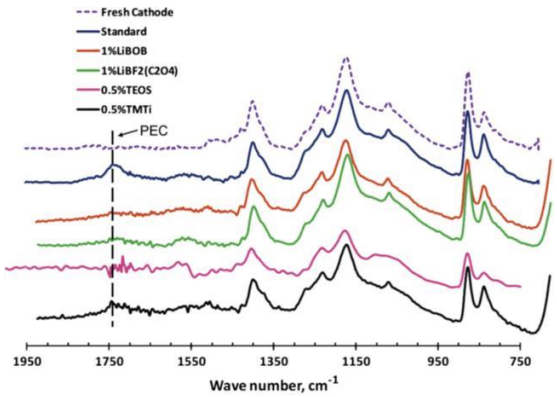

Fig. 12 FTIR-ATR spectra of the $Li_{1.17}Mn_{0.58}Ni_{0.25}O_2$ positrode after charging-discharging cycling in different additives-containing electrolytes.[157] (Reprinted with permission from Elsevier. Copyright 2011.)

research and development of high voltage electrolytes for high energy density LIBs is an urgent demand for a number of high-technology applications.[147, 151]

One of the most economic and easiest strategies to improving the stability of the positrode-electrolyte interface is using additives. The mechanism is that additives are preferably oxidised on the positrode surface to generate a stable interfacial layer, which inhibits the detrimental reaction of electrolytes at high positive potentials. Reported additives include (1) inorganic compounds such as lithium bis(oxalato)borate (LiBOB)[152-158] and lithium difluoro(oxalato)borate (LiDFOB)[159], (2) phosphite-derivatives such as trimethyl phosphite (TMP)[160], tris(hexafluoro-iso-propyl) phosphate (HFiP)[161,162], tris(trimethylsilyl) phosphite (TMSP)[163-166], (Ethoxy) pentafluorocyclotriphosphazene (PFPN),[167] and 1-propylphosphonic acid cyclic anhydride (PACA)[168], (3) sulfonate esters such as 1,3-propane sultone (PS)[169], 1,3-propanediol cyclic sulfate (PCS)[170], and (4) some carboxyl anhydrides[169, 171, 172]. These additives, some of which are shown wither their molecular structures in Fig. 11, are all very effective in alleviating decomposition of the electrolyte at the highly charged positrode.

Among these additives, LiBOB has been recognised as a highly promising multifunctional additive. The oxidation of LiBOB on the positrode could generate a thin surface film to inhibit further oxidation of the electrolyte.[156] Meanwhile, the presence of LiBOB could also prevent the dissolution of Mn or Ni from the positrode surface, which might originate from the inhibition of formation of acidic species, e.g. HF or PF_5.[156] Additionally, a robust and stable SEI film on graphite produced by the reduction of LiBOB was observed.[173,174] Compared to LiBOB, LIB cells with LiDFOB showed a greatly improved capacity retention of more than 92 % after 100 cycles, which might be ascribed to the more stable SEI film with lower interfacial resistance on the negatrode surface.[175] The LiDFOB-containing electrolyte was also found to work well with the high voltage positrode $LiCoPO_4$, leading to higher reversible charge/discharge capacity and better cycling stability. XPS and FTIR-ATR analyses further confirmed that LiDFOB was helpful to form a

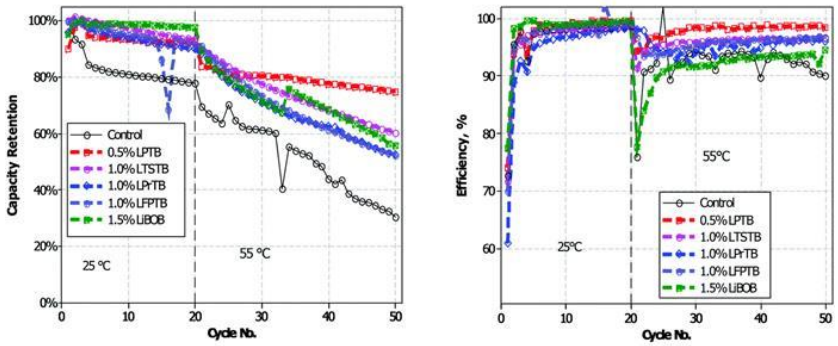

Fig. 13 Cycling performance of graphite/$LiNi_{0.5}Mn_{1.5}O_4$ cells at 25 and 55 °C in electrolytes with and without added lithium 4-pyridyl trimethyl borate (LPTB).[176] (Reproduced with permission from The Royal Society of Chemistry. Copyright 2016.)

stable interphase film with borates, suppressing the decomposition of EC to form PEC (see Fig. 12).[157]

Recently, a series of novel lithium alkyl/aryl trimethyl borates were designed and prepared as positrode film forming additives.[176] The cycling performance of graphite/$LiNi_{0.5}Mn_{1.5}O_4$ cells with the electrolyte containing such additives is presented in Fig. 13. It can be seen that incorporation of lithium organoborate additives into 1.0 mol L^{-1} $LiPF_6$ in EC/EMC results in improved capacity retention and efficiency of the graphite/$LiNi_{0.5}Mn_{1.5}O_4$ cells. As confirmed by ex situ surface analyses via TEM, SEM, XPS and IR-ATR, the improvement was because incorporation of lithium 4-pyridyl trimethyl borate (LPTB) led to the generation of a borate rich passivation layer on the surface of both the positrode and negatrode. The mechanism is that the tetraalkyl borate is oxidised by the metal oxide surface to irreversibly generate a metal oxide borate complex, which in turn can inhibit electrolyte oxidation and Mn/Ni dissolution from the positrode, resulting in improved capacity retention and efficiency.

Based on the discussion above, these additives generally tend to be electrochemically oxidised during charging the cell to high voltages, and form a passivation layer on the positrode surface, and then suppress the reactivity of the charged electrode and electrolyte. The result has shown that the addition of these high voltage additives could enhance the cycling performance of the high voltage cells.

A recent study of the 5 V $LiNi_{0.4}Mn_{1.6}O_4$ positrode with 40 different additives, such as fluoroethylene carbonate (FEC), PS and LiBOB, revealed that these additives could retard self-discharge. This improvement may be also related to oxidative electrolyte decomposition due to the high lithium (de-)insertion potentials. The study showed that among the 40 additives, only one compound, succinic anhydride (SA) helped a decreased capacity loss per cycle and an enhanced coulombic efficiency. Therefore, SA is the promising candidate as a high voltage additive to realise rechargeable LIB with high energy density.

On the other hand, it is a major challenge to develop novel stable solvents with intrinsic anodic ability for high voltage electrolytes that have good compatibility with electrodes. Many novel solvents with a high anodic potential have been reported, including dinitriles,[177-182] sulfones,[183-194] and fluorinated solvents[195-198]. For example, in 1994, gluotaronitrile (GLN) and adioponitrile (ADN) were reported to offer exceptionally high anodic stability at ~8.3 V vs. Li^+/Li.[61, 199, 200]

In general, dinitriles are known for their extra anodic stability on positrode surfaces, high dielectric constant and excellent thermal properties (high boiling point and flash point). However, they cannot be used alone in LIBs owing to their high melting point, high viscosity and poor wettability with the separator. Therefore, dinitriles can be used as a co-solvent with others such as EC or EMC to improve the physical properties of dinitrile-based electrolytes. The 1.0 mol L^{-1} $LiBF_4$/EC+DMC+sebaconitrile (25:25:50, by vol.) showed an excellent high oxidation stability above 6.6 V vs. Li^+/Li on glassy carbon. On the $Li_2Ni_{0.98}Co_{0.02}PO_4F$ positrode, this electrolyte was found to be stable at ca. 5.3 V vs. Li^+/Li.[177,178] It should be noticed that these dinitrile-based electrolytes are incompatible with graphite-based negatrodes, which result from the easy reduction of nitriles (C=N) on common negatrode materials such as Li metal or graphite, leading to a deterioration of the cycling performance.

To improve the compatibility of these electrolytes with graphite negatrode, LiBOB,[180, 181] VC and FEC[182] have been studied as additives. The findings showed evidence for the formation of a stable SEI on the graphitic negatrode that protected the dinitrile solvent from undergoing reductive decomposition. Fairly good capacity and cycling behaviour were observed upon addition of VC and FEC to the electrolyte of 1.0 mol L^{-1} LiTFSI, 0.25 mol L^{-1} $LiBF_4$/ADN in the mesoporous carbon microbeads (MCMB) half-cell and the MCMB/$LiCoO_2$ full cell.[182]

Sulfones with high oxidation potentials continued to attract attention as possible electrolyte solvents for LIBs. Electrolytes formed with ethylmethyl sulfone (EMSF) as the solvent exhibited an extraordinary anodic stability at ca. 5.8 V vs. Li^+/Li, promising a wide range of possible high voltage applications.[183] This finding agreed well with computed oxidation potentials for a series of sulfone-based molecules functionalised with fluorine, cyano, ester, and carbonate groups.[201, 202] In addition, it was found that sulfones with strong electron-withdrawing groups (such as -F and -CN) have higher oxidation potentials than the non-functionalised ones. An

investigation of the electrochemical stability of five sulfone-based electrolytes by cyclic voltammetry found that among these solvents, tetramethylene sulfone (TMS) and EMS showed the highest anodic stability on Pt working electrodes (see Fig. 14).[203] The $Li_4Ti_5O_{12}/LiMn_2O_4$ full cell with the 1.0 mol L^{-1} $LiPF_6$/TMS+EMC blended electrolyte exhibited a fairly long cycle life of 1000 cycles at the 2 C rate. However, their application in actual LIBs was limited by their inability to form a stable SEI layer on graphitic negatrodes. It has also been reported that the introduction of additives such as VC[186-188], LiBOB,[189, 190] *p*-toluenesulfonylisocyanate (PTSI)[191] and hexamethylenediisocyanate (HDI)[192] can promote SEI film formation in sulfone-based electrolytes, giving a cycling performance equal to the conventional carbonate electrolytes. Molecular dynamic simulations suggested that in the 1.0 mol L^{-1} $LiPF_6$/TMS+DMC electrolyte, TMS tended to preferentially adsorb on the positrode surface. Thus, the anodic stability of this mixture was dominated by sulfone instead of carbonate.[194] This conclusion is consistent with experimentally observed increased oxidative stability of sulfone-based electrolytes. Based on the above mentioned results, although dinitriles and sulfones exhibit high anodic stability on various positrode surfaces and low flammability, they suffer from their intrinsic high viscosity, low conductivity and poor wettability toward the electrodes and separators, which cause poor rate performance of the battery. More importantly, they do not form a protective SEI film on graphite negatrode, which severely hinder their application in commercial LIBs.

At present, fluorinated electrolytes appear more appropriate for high voltage LIBs. Owing to the high electronegativity and low polarisability of the fluorine atom, fluorinated solvents possess increased oxidative or anodic stability.[203, 204] However, they also have poorer resistance against reduction. The first comparison of the high voltage cyclability between $Li/LiCoO_2$ batteries containing FEC-based electrolytes and EC-based electrolytes concluded that the cell with the FEC-base electrolytes delivered a higher and more stable discharge capacity at a high cut off voltage of 4.5 V.[195] This conclusion also agreed with results from later electrochemical evaluation of the $Li/LiNi_{0.5}Mn_{1.5}O_4$, $Li_4Ti_5O_{12}/LiNi_{0.5}Mn_{1.5}O_4$ and $Si/LiCoPO_4$ cells.[196,197,205] These high voltage batteries demonstrated significantly improved capacity retention, which was attributed to the high anodic stability of the fluorinated electrolytes. However, because fluorinated solvents have less negative reduction potentials, they generally have poorer compatibility with

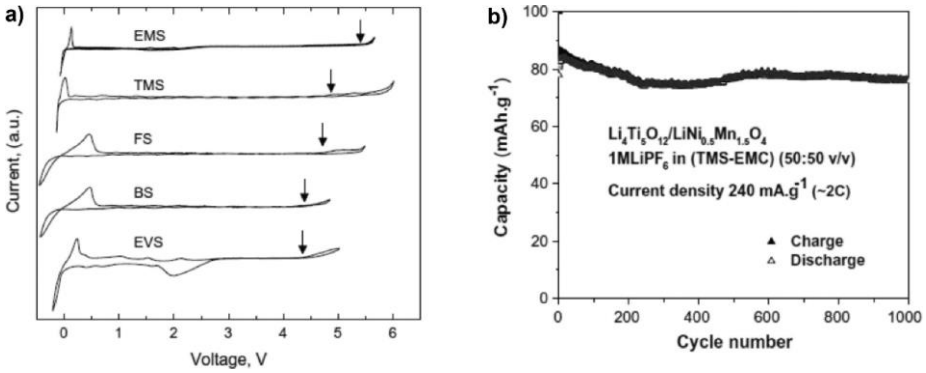

Fig. 14 Sulfone-based electrolytes: (a) Cyclic voltammograms of 1.0 mol L^{-1} LiTFSI in various neat sulfones on Pt working electrode; and (b) cycling performance of a full lithium ion cell based on $LiNi_{0.5}Mn_{1.5}O_4/Li_4Ti_5O_{12}$ in 1.0 mol L^{-1} $LiPF_6$/tetramethylene sulfone/DMC.[193] (Reprinted with permission from Elsevier. Copyright 2009.)

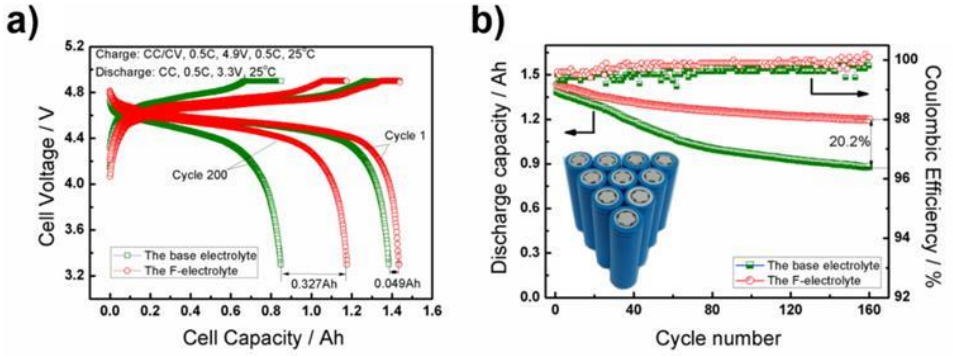

Fig. 15 a) Voltage profiles for the charge–discharge cycles and b) cycling performance according to the CC–CV protocol of the 18650 MCMB/$LiNi_{0.5}Mn_{1.5}O_4$ battery in the voltage range of 3.3–4.9 V at the 0.5 C rate.[198] (Reproduced with permission from The Royal Society of Chemistry. Copyright 2015.)

graphite based negatrodes. To improve the stability of the graphite/F-electrolyte interface, a new solvent, 1,1,1,3,3,3-hexafluoroisopropyl methyl ether (HFPM) with a more negative reduction potential was prepared and used as the co-solvent to prepare a fluorinated electrolyte of 1.0 mol L^{-1} $LiPF_6$/FEC+DMC+EMC+HFPM (2:3:1:4, by vol.), leading to a remarkable anodic stability at 5.5 V vs. Li^+/Li, and good compatibility with the graphite negatrode. Particularly, as shown in Fig. 15, high-voltage MCMB/$LiNi_{0.5}Mn_{1.5}O_4$ 18650 cells containing this F-electrolyte exhibited good capacity retention of 82 % after 200 cycles, promising enhanced safety and longevity.[198]

3.2.3. Highly concentrated electrolytes

Highly concentrated electrolytes (HCEs) are emerging as a new class with various unusual functionalities (see Fig. 16), such as high reductive and oxidative stability, and reduced corrosion to Al,[206] which are not realised in conventional $LiPF_6$/EC-based electrolytes. Solution structures of HCEs are totally different from that of the dilute counterparts, thus resulting in various unusual properties.[207] As shown in Fig. 17, Raman spectroscopy and molecular dynamics (MD) simulations revealed that increasing the concentration of Li salt decreases the number of free solvent molecules because most, if not all, solvent molecules are participating in solvation of the Li^+ ions. Ultimately, at the high concentration of 4.2 mol L^{-1}, all solvent molecules will coordinate to Li^+ ions to form contact ion pairs and aggregates, instead of solvent separated ion pairs, resulting in their unusual properties.

HCEs could affect other electrode processes in LIBs. For example, a PC solution of the LiBETI (that is $LiN(SO_2C_2F_5)_2$) salt could significantly improve the reversibility of Li metal deposition and stripping.[208] After this path-breaking work, it was reported that stable Li metal deposition and stripping reactions in HCEs with ether solvents were observed.[209-211] At high concentrations, the LiTFSI/DOL+DME electrolyte could not only effectively suppress dendrite formation at the metallic Li negatrode but also inhibit the dissolution of lithium polysulphide, resulting in excellent cycling performance and improved safety.[209] In this case, for unknown reasons, a rather low columbic efficiency of ca. 71 % during the Li

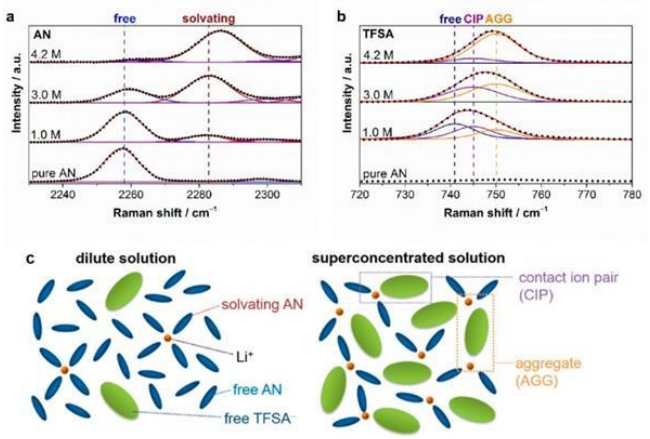

Fig. 17 Raman spectra of LiTFSA/AN solutions in (a) 2230–2310 cm^{-1} (C≡N stretching mode of AN molecules) and (b) 720–780 cm^{-1} (S–N stretching, C–S stretching, and CF_3 bending mode of $TFSA^-$). Points and solid lines denote experimental spectra and fitting curves, respectively. (c) Representative environment of Li^+ in a conventional dilute solution (i.e., ~1.0 mol dm^{-3}) and a salt-superconcentrated solution (i.e., 4.2 mol dm^{-3}).[207] (Reprinted with permission from American Chemical Society. Copyright 2014.)

plating/stripping processes was obtained. On the contrary, very high coulombic efficiency of up to 99.1 % at 10 mA cm^{-2} for > 6000 cycles in a Li/Li cell, and an average efficiency of 98.4 % at 4 mA cm^{-2} for > 1000 cycles in a Li/Cu cell were reported in the 4.0 mol L^{-1} LiFSA/DME (lithium bis(fluorosulfonyl)imide/ 1,2-dimethoxyethane) electrolyte (see Fig. 18).[210] The excellent high-rate cycling stability of the Li metal negatrode in the HCE of 4.0 mol L^{-1} LiFSI/DME was attributed to the selection of a reduction-stable solvent, a highly dissociated Li salt, and a high electrolyte concentration.

It is widely known that the graphite negatrode prefers to working in EC-based electrolytes. This is primarily because only EC-based electrolytes allow for highly reversible Li^+ intercalation into graphite. Other popular solvents such as PC, DME, acetonitrile (AN) and dimethyl sulfoxide (DMSO) easily destroy the graphite crystalline structure by the co-intercalation of solvent molecules and Li^+ ions into graphite.[212-215]

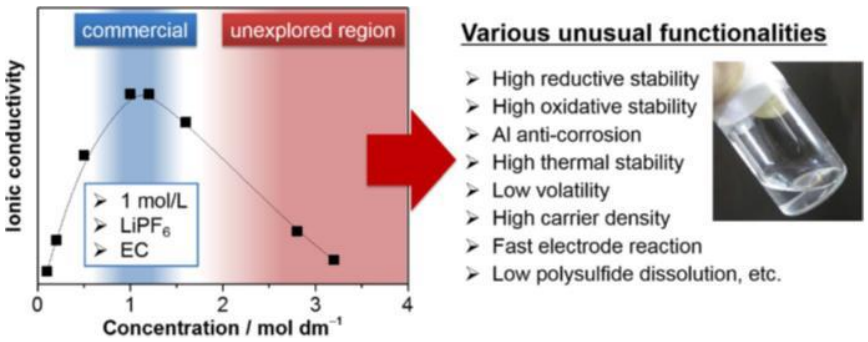

Fig. 16 Typical ionic conductivity curve of Li salt-aprotic solvent mixture. Highly concentrated electrolytes, having been outside the research mainstream due to decreased ionic conductivity, are recently receiving intensive attention because of various unusual functionalities beneficial for battery applications.[206]

Recently, several reports confirmed that HCEs containing these popular solvents showed enhanced reductive stability, suppressing the co-intercalation of solvent to allow reversible lithium intercalation into the interlayers of graphite.[207,216-219] Unusual reductive stability of a super-concentrated LiTFSA/AN electrolyte (4.2 mol L^{-1}) was investigated, revealing the origin by first-principle calculations combined with spectroscopic analyses.[207,220] As shown in Fig. 19, the obtained reversible capacity of the cell using the 4.2 mol L^{-1} LiTFSA/AN electrolyte was ca. 330 mAh g^{-1}, which was close to the theoretical capacity (372 mAh g^{-1}) based on fully lithiated carbon, LiC_6. This is indication of a reversible operation of the graphite negatrode in an AN-based electrolyte. The enhanced reductive stability can be linked to the excellent and compact SEI film with high ionic conductivity, which was due to the reductive decomposition of the $TFSA^-$ anion, instead of the AN solvent. The DFT-MD simulation results confirmed that the sacrificial anion reduction hindered electron reductive decomposition of AN, leading to improved electrochemical stability (see Fig. 20).[220] Interestingly, it was also found that Li^+ intercalation into graphite in HCEs could be ultrafast with either LiTFSI or LiFSI and AN or DME, even exceeding that in currently used commercial EC-based electrolytes, for example, 1.0 mol L^{-1} $LiPF_6$-EC/DMC.[207, 218]

Thanks to the unique solution structure with anions and solvent molecules coordinating strongly to Li^+ ions, HCEs exhibit enhanced oxidative stability, and inhibit the dissolution of the Al current collector.[221-225] It was shown that the 4.45 mol L^{-1} $LiPF_6$/PC electrolyte improved the cycling performance of the 5.0 V $LiNi_{0.5}Mn_{1.5}O_4$ positrode, while the corresponding dilute electrolyte was easily oxidised and decomposed at such high positive potentials.[221]

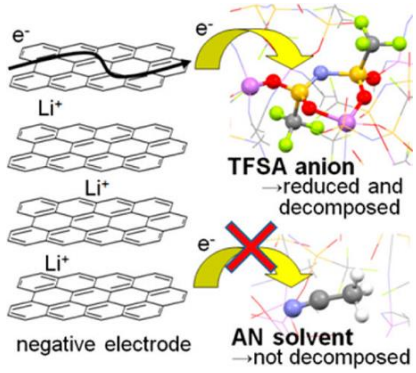

Fig. 20 Schematic description of the reductive decomposition near the negatrode in highly concentrated Li-salt electrolyte.[220] (Reprinted with permission from American Chemical Society. Copyright 2014.)

Specially, the simple formulation of the superconcentrated $LiN(SO_2F_2)_2$/DMC (LiFSA/DMC) electrolyte exhibited remarkably high anodic stability at 5.5 V vs. Li^+/Li. Progressive inhibition of anodic Al dissolution was proven by the SEM images (see Fig. 21).[222] A high-voltage $LiNi_{0.5}Mn_{1.5}O_4$/graphite battery with this superconcentrated electrolyte exhibited excellent cycling durability with over 90 % capacity retention after 100 cycles at 40 °C. In contrast, the cell using the commercial electrolyte retained only 18 % of the initial capacity after 100 cycles, indicating a severe capacity decay. Besides, compared to the dilute electrolytes, the concentrated 1:1.1 LiFSA/DMC electrolytes also showed superior thermal stability and flame retardancy, contributing to the remarkably improved safety properties.

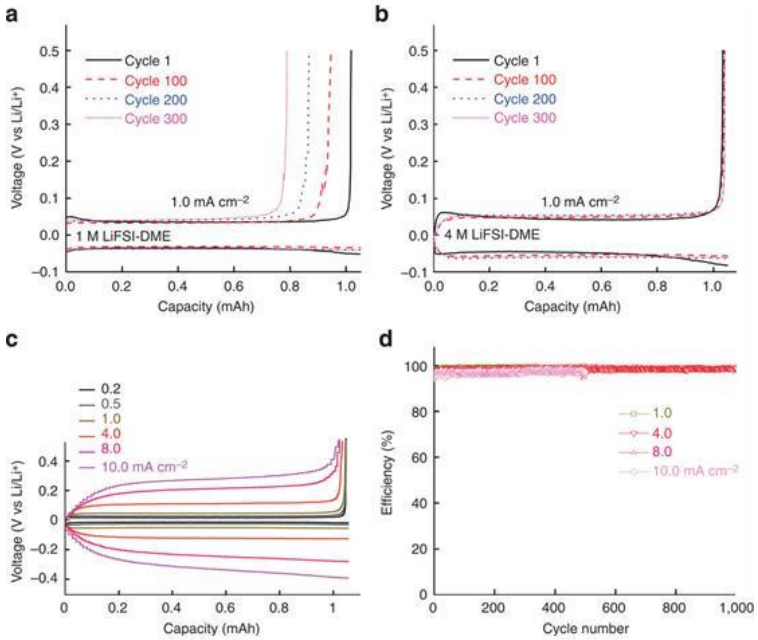

Fig. 18 Electrochemical performance of Li metal plating/stripping on a Cu working electrode. (a) Voltage profiles for the cell cycled in 1.0 mol L^{-1} LiFSI-DME; (b) Voltage profiles for the cell cycled in 4.0 mol L^{-1} LiFSI-DME; (c) Polarization of the plating/stripping for the 4.0 mol L^{-1} LiFSI-DME electrolyte with different current densities. (d) CE of Li deposition/striping in 4.0 mol L^{-1} LiFSI-DME at different current densities.[210]

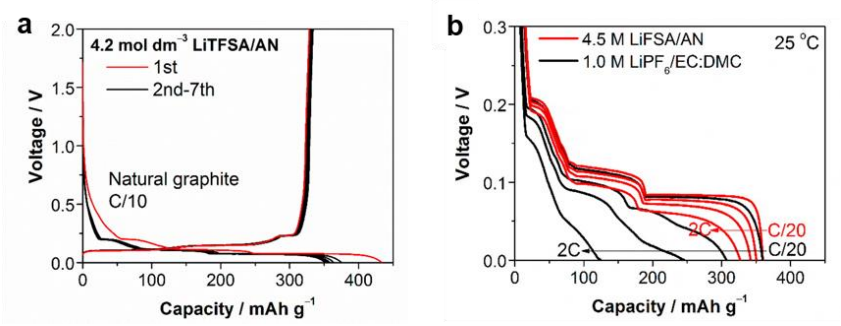

Fig. 19 (a) Charge–discharge curves of natural graphite/Li metal cell with 4.2 mol L^{-1} LiTFSA/AN electrolyte at 1/10 C rate. (b) Lithium intercalation voltage curves of a natural graphite/lithium metal half-cell with superconcentrated 4.5 mol L^{-1} LiFSA/AN and commercial 1.0 mol L^{-1} $LiPF_6$/EC:DMC (1:1, by vol.) electrolytes at various C-rates (1/20, 1/2, 1, and 2 C) at 25 °C.[207] (Reprinted with permission from American Chemical Society. Copyright 2014.)

In addition to the aforementioned HCEs, a new class of highly concentrated Li salt-glyme complexes was established and named as "solvate ionic liquids" with clear classification criteria, because various physicochemical features of such electrolytes were similar to those of ionic liquids.[226-232] The Li salt-glyme equimolar mixture had many desirable properties, including ionicity, Li^+ ion transference number, Li^+ ion concentration, and oxidative stability, in addition to the common properties of ionic liquids. Considering the competition of different glyme solvents and anions (X^-) for interactions with Li^+ ions, a variety of Li(glyme)]X complexes could form with different glyme solvents and Li salts. It was found that ([Li(glyme)]X with weakly Lewis basic anions (e.g. $TFSA^-$ or ClO_4^-) and longer glymes (e.g. triglyme=G3 or tetraglyme=G4) could form fairly stable complexes.[229,231] For example, the electro-oxidation of $[Li(glyme)_1][TFSA]$ (triglyme or tetraglyme) took place at ca. 5.0 V vs. Li^+/Li, which is obviously more positive than the oxidation potential (ca. 4.0 V) of solutions containing excess glyme molecules ($[Li(glyme)_x][TFSA]$, X>1) (see Fig. 22).[227] A further study by ab initio molecular orbital calculations showed that the enhanced oxidative stability could be ascribed to the donation of lone pair electrons of the ether oxygen atom to the Li^+ ion, which lowered the highest occupied molecular orbital (HOMO) energy level of the glyme molecule. Additionally, these solvate ionic liquids could be also used as efficient electrolytes for Li-ion, Li-S and Li-O_2 batteries.[226-232]

Owing to their unique solution structures at certain high concentrations, HCEs have various unusual properties compared to their dilute counterparts, making it unnecessary to rely on the $LiPF_6$ salt for the passivation of the Al current collector, or on the EC solvent for formation of the SEI film on the graphite surface, and providing more design considerations in future battery technologies. Similarly, Na salts based highly concentrated electrolytes may also offer new opportunities in building stable and safe Na-ion batteries.

Safety issue is still a challenge for LIBs because of the intrinsic flammability of organic liquid electrolyte and possibility of leakage. Replacing the organic electrolytes with gel polymer electrolytes (GPEs) delivers a promising solution to improve safety by avoiding these crucial issues.[233-235] There are extensively explored GPEs based on polymer matrices that are capable of immobilizing a large amount of liquid electrolyte. These GPEs offer both the flexibility of the polymer and the high ionic conductivity of the liquid electrolyte, and enable wide electrochemical windows, excellent cycling durability and improved thermal stability. GPEs can be formed on different polymer matrices, such as poly(ethylene oxide) (PEO), poly(vinylidene fluoride) (PVDF), PVDF-HFP, and poly(methyl methacrylate) (PMMA).[236-237] However, the inferior mechanical strength of most GPEs fail to block effectively dendrite growth.[238]

In this regard, PVDF-based composite GPEs with a cross-linked structure[239-240] or a nonwoven fabric[241-242] or glass fiber mats (GFMs)[243] as a reinforcement scaffold could be a promising solution to improve the mechanical strength. Considering their low cost and high safety, these modified GPEs with enhanced mechanical properties show great possibilities for large-scale and high safety energy storage applications.

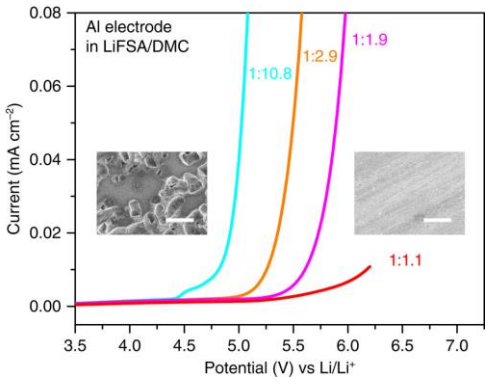

Fig. 21 LSV of an Al electrode in LiFSA/DMC electrolytes of various concentrations in a three-electrode cell. The scan rate was 1.0 mV s^{-1}. The insets are SEM images of the Al surface polarised in the dilute 1:10.8 (left) and superconcentrated 1:1.1 (right) electrolytes. Many corroding pits cover the surface of the Al electrode polarized in the dilute electrolyte, showing a severe anodic Al dissolution. In contrast, no corroding pits appear on the surface of the Al electrode polarised in the superconcentrated electrolyte, indicating a good inhibition of anodic Al dissolution. The white scale bars in the SEM images represent 20 µm.[222]

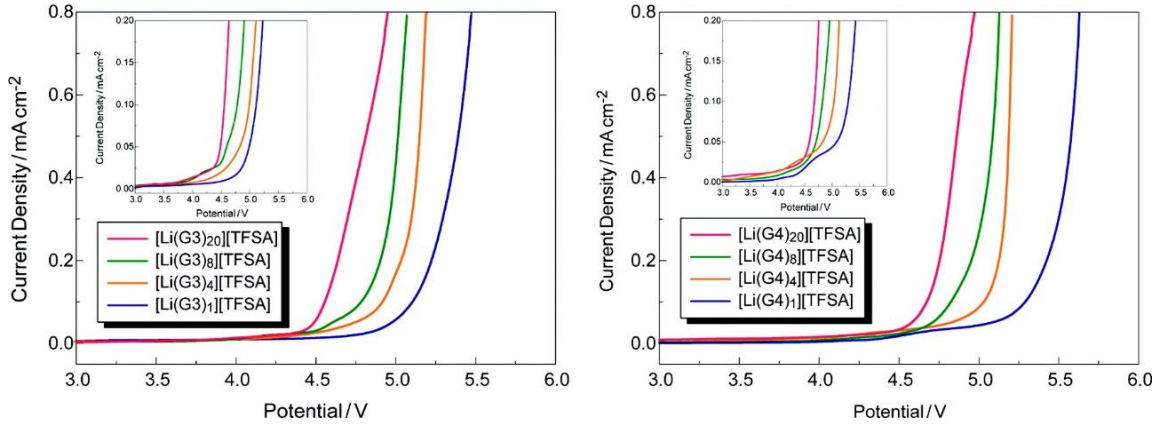

Fig. 22 Linear sweep voltammograms of [Li(glyme)$_x$][TFSA] (x = 1, 4, 8, and 20) at a scan rate of 1 mV s^{-1} at 30°C. Each inset depicts an enlarged view of current density.[227] (Reprinted with permission from American Chemical Society. Copyright 2011.)

3.3. Sodium-ion batteries

Ambient temperature sodium-ion (Na-ion) batteries (SIBs) are promising for large-scale grid energy storage applications based on the wide availability and low cost of sodium.[244-246] Although there are many publications on the research and development towards different electrode materials, little is given to new electrolytes used in SIBs.[20, 247, 248] Additionally, it is necessary to design appropriate liquid electrolyte compositions to minimise unwanted interface reactions and to enhance the electrochemical performance and safety in SIBs. Among various aqueous,[249, 250] organic[251] and ionic liquid based choices[252-254], organic electrolytes are more promising owing to their high ionic conductivity, wide electrochemical window and good electrochemical performance.[255]

The most common electrolyte formulations for SIBs include $NaClO_4$ or $NaPF_6$ dissolved in carbonate ester solvents, particularly EC and/or PC.[256-259] Various organic electrolytes for SIBs with hard-carbon electrodes have been investigated. The electrochemical properties of hard-carbon in EC: DMC, DME, tetrahydrofuran (THF) and EC:THF solvents containing 1.0 mol L^{-1} $NaClO_4$ were studied.[260] In comparison with carbonate only solvents, THF and the EC:THF mixture were capable of improving the electrochemical performance of hard-carbon electrodes. Unfortunately, oxidation current was observed in the 1.0 mol L^{-1} $NaClO_4$-THF electrolyte at an onset potential of ca. 4.26 V vs. Na$^+$/Na, indicating the instability of THF-based electrolytes against anodic oxidation.[261] Probably because of a combination of historical and cost reasons, most publications on SIB electrolytes are based on $NaClO_4$ as the electrolyte salt. The performance of the hard carbon electrode in cyclic alkylene carbonate and binary solvent electrolyte based on EC and linear carbonate esters containing $NaClO_4$ were studied. It was found that the Na/hard carbon cells with PC and EC:DEC solutions demonstrated a highly reversible capacity of >200 mAh g^{-1} with excellent capacity retention during 100 cycles.[262] A comparative study of diverse electrolyte formulations with different Na salts ($NaClO_4$, $NaPF_6$ and NaTFSI) and solvents (PC, EC, DMC, DME, DEC, THF and Triglyme) or solvent mixtures (EC:DMC, EC:DME, EC:PC and EC:Triglyme) were reported in terms of ionic conductivity, viscosity, electrochemical window and thermal stability.[261] The results showed that the binary EC:PC mixture with dissolved $NaClO_4$ or $NaPF_6$ might be the best electrolyte formulation for the Na/hard carbon cells (see Fig. 23). The same results were confirmed by another group.[263] The introduction of dimethyl carbonate (DMC) into EC:PC was found to improve the performance of electrolytes containing these two salts, which was mainly ascribed to the enhanced conductivity resulting from the decrease in viscosity without inducing any significant modification of the SEI composition on the negatrode (Fig. 24).[264] Recently, the electrode/electrolyte interface for lithium and sodium metal negatrodes were compared in the 1.0 mol L^{-1} $LiPF_6$/EC+DMC and 1.0 mol L^{-1} $NaPF_6$/EC+DMC electrolytes, respectively. Symmetric Li/Li cells exhibited low polarisation and smooth charge-discharge curves at current densities of 0.1 and 1.0 mA cm^{-2}. In contrast, large overpotentials were observed even at 0.1 mA/cm^2 in symmetric Na/Na cells, indicating slower electrode kinetics and larger interfacial resistance.[265]

Apart from $NaClO_4$ and $NaPF_6$, other salts, such as sodium bis(trifluoromethane) sulfonimide (NaTFSI), sodium fluorosulfonyl (trifluoromethanesulfonyl)imide (NaFTFSI), sodium bis(fluoro-sulfonyl)imide (NaFSI), $NaSO_3CF_3$ (NaOTf), sodium 4,5-dicyano-2-(trifluoromethyl)imidazolate (NaTDI), sodium 4,5-dicyano-2-(pentafluoroethyl)imidazolate (NaPDI), and sodium difluoro-(oxalato)borate (NaDFOB) were also investigated.[251, 266, 267] Of these salts, NaTDI and NaPDI were both found to be thermally stable up to more than 300 °C, and the measured conductivity of their solutions in PC (about 4 mS cm^{-1}) was slightly lower than that of the market available salt, $LiClO_4$ (8 mS cm^{-1}).[266]

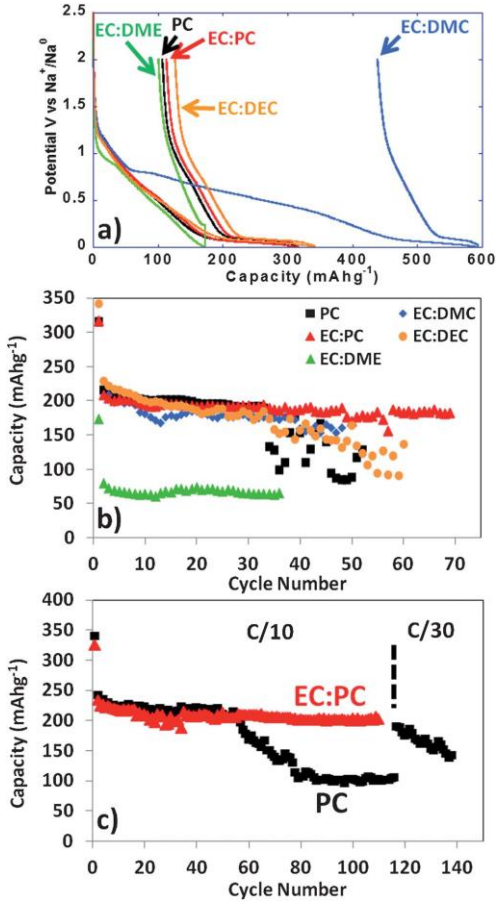

Fig. 23 Profiles of (a) first cycle potential vs. capacity, and (b) discharge capacity vs. cycle number for hard carbon in 1.0 mol L^{-1} $NaClO_4$ in various solvent mixtures at C/20. (c) Discharge capacity vs. cycle number for tape-cast hard carbon electrodes in 1.0 mol L^{-1} $NaClO_4$ in PC alone and EC: PC at C/10 up to 110 cycles and further at 1/30 C.[261] (Reproduced with permission from The Royal Society of Chemistry. Copyright 2012.)

Comparative studies were reported on electrolytes based on commercially available sodium salts, namely $NaPF_6$, $NaClO_4$ and $NaCF_3SO_3$ in a binary mixture of EC and DMC. [268] It was found that the ionic conductivity of the two solutions of 0.6 mol L^{-1} $NaPF_6$ and 1.0 mol L^{-1} $NaClO_4$ in EC and DMC were 6.8 and 5.0 mS cm^{-1}, respectively. These values are somewhat higher than that of NaOTf (3.7 mS cm^{-1}, 0.8 mol L^{-1}). Unfortunately, NaOTf, NaFSI and NaTFSI - based electrolytes had the major drawback of being unable to form a passivation layer on the Al current collector.[268, 269] A systematic evaluation of the intrinsic Al stability in electrolytes based on various NaX [X=PF_6, ClO4, TFSI, FTFSI, FSI] salts dissolved in solvent mixtures showed a trend of the Al dissolution increasing in an order of $NaPF_6$ < $NaClO_4$ < NaTFSI < NaFTFSI < NaFSI.[270]

When adding 5 wt.% $NaPF_6$ to the base electrolyte, the stability of Al in imide-based electrolytes could be improved, which may be attributed to the formation of a protection passivation layer on the Al surface. Notably, compared to $NaClO_4$ and $NaPF_6$ (see Fig. 25), NaDFOB not only possesses excellent compatibility with various common solvents used in SIBs, but also has good stability. It will also not generate toxic or dangerous products when exposed to air and water, indicating that NaDFOB may be a prospective Na salt for application in high performance electrolytes for future SIBs.[271]

A new high-voltage electrolyte was developed from $NaClO_4$ in mixed ethyl methanesulfonate (EMS) and FEC.[272] The anodic stability of this electrolyte could be increased to 5.6 V vs. Na^+/Na, which is higher than that of the PC-based electrolyte of 4.5 V. Moreover, the EMS-based electrolyte had a slightly higher ionic conductivity of 6.3 mS cm^{-1} at 25 °C. In this high-voltage electrolyte, the 4.0 V positrode of $Na[Ni_{0.25}Fe_{0.5}Mn_{0.25}]O_2$ was found to have much improved electrochemical performance.

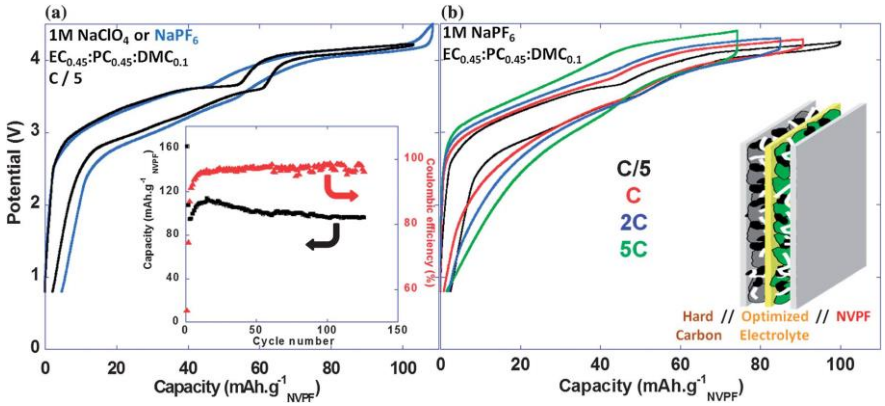

Fig. 24 (a) Voltage vs. capacity profiles for NVPF//HC ($Na_3V_2(PO_4)_2F_3$//Hard carbon) full Na-ion cells in 1.0 mol L^{-1} $NaPF_6$ or 1.0 mol L^{-1} $NaClO_4$ in $EC_{0.45}$:$PC_{0.45}$:$DMC_{0.1}$ recorded at C/5 (the inset displays plots of the charge capacity and coulombic efficiency vs. cycle number (C/5; 1.0 mol L^{-1} $NaClO_4$ in $EC_{0.45}$:$PC_{0.45}$:$DMC_{0.1}$)). (b) Voltage vs. capacity profiles for NVPF//HC full Na ion cells in 1.0 mol L^{-1} $NaPF_6$ in $EC_{0.45}$:$PC_{0.45}$:$DMC_{0.1}$ recorded at different rates.[264] (Reproduced with permission from The Royal Society of Chemistry. Copyright 2013)

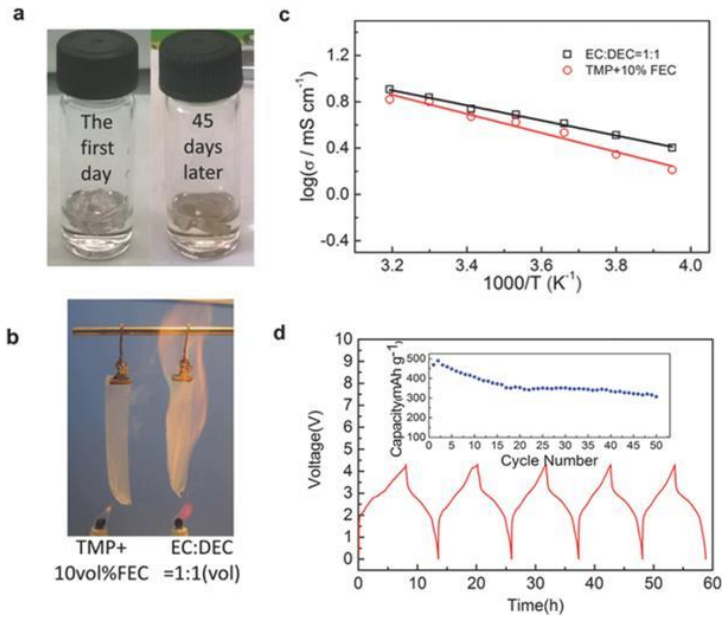

Fig. 26 a) Room temperature storage behaviour of the TMP + 10 vol% FEC electrolyte. b) Combustion behaviour of the TMP electrolyte and carbonate electrolyte. c) Temperature dependence of the ionic conductivities of 0.8 mol L^{-1} $NaPF_6$/TMP + 10 vol% FEC electrolyte. The ionic conductivity of 1.0 mol L^{-1} $NaPF_6$ EC/DEC (1:1) electrolyte is also shown for comparison. d) Charge/discharge curves and cycling performance of Sb/$NaNi_{0.35}Mn_{0.35}Fe_{0.3}O_2$ cells in the 0.8 mol L^{-1} $NaPF_6$/TMP + 10 vol% FEC electrolyte.[273]

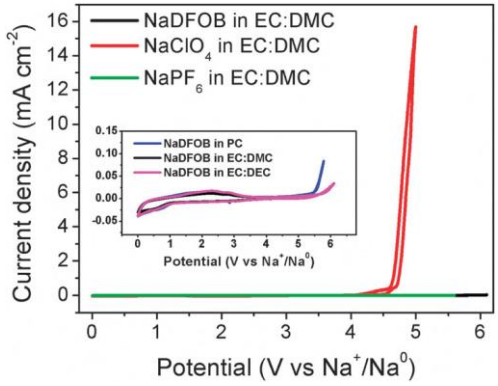

Fig. 25 CVs of Na-ion cells with electrolytes of 1.0 M NaX (X = DFOB, ClO_4, and PF_6) in EC:DMC at room temperature at a scan rate of 1.0 mV s^{-1}. The inset shows the CVs of the cells with electrolytes of NaDFOB in PC, EC:DEC, and EC:DMC, respectively.[271] (Reproduced with permission from The Royal Society of Chemistry. Copyright 2015.)

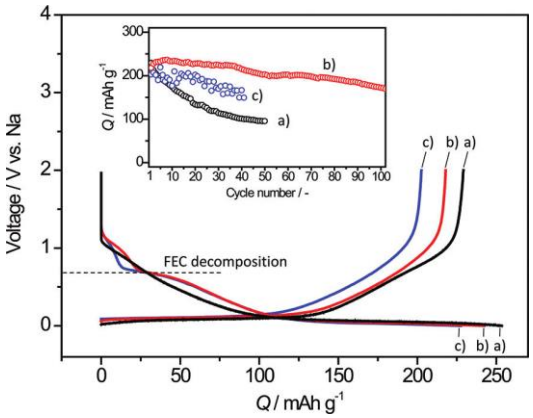

Fig. 27 Initial reduction/oxidation curves of hard-carbon electrodes in 1.0 mol L^{-1} $NaClO_4$ PC solution (a) without and with (b) 2.0 vol % and (c) 10.0 vol % FEC at a rate of –25 and +25 mA g^{-1} in coin-type Na-ion cells. Inset shows the variation of reversible oxidative capacities of hard carbon during successive cycling test.[280] (Reprinted with permission from American Chemical Society. Copyright 2011.)

On the other hand, to bypass the flammability of organic carbonate electrolytes, a safer Na-ion battery was proposed and demonstrated based on a nonflammable electrolyte of trimethyl phosphate (TMP) coupled with a $NaNi_{0.35}Mn_{0.35}Fe_{0.3}O_2$ positrode and a Sb-based negatrode (see Fig. 26).[273] The results showed that the TMP-based electrolyte with FEC additive was totally nonflammable. It also offered a wide electrochemical window of 4.5 V and good compatibility with both the Sb-based negatrode and $NaNi_{0.35}Mn_{0.35}Fe_{0.3}O_2$ positrode, promising a new technical prospect to meet the high-capacity and high-safety requirements for large-scale energy storage applications.

The progress in development of electrolyte additives for SIBs is even slower than that for LIBs. Currently, hard carbon is the most widely used negatrode material in SIBs, exhibiting an initial reversible capacity of 300 mAh g^{-1} in 1.0 mol L^{-1} $NaClO_4$/EC+DEC (3:7, by vol.) in the potential range of 0 to 2.0 V vs. Na^+/Na.[274]

However, the hard carbon electrode showed a significant loss of capacity as galvanostatic cycling continued. It may be due to the high reactivity of sodium inserted hard carbon (Na@HC) which suffered from continuous and corrosive attack by the commonly

used organic electrolytes, rather than forming a stable SEI, resulting in degradation of cell performance.[275]

It is commonly known that addition of film-forming additives in electrolyte can be an effective and easiest strategy to improve the electrode performance in LIBs.[276-279] A comparative study was carried out to understand how different electrolyte additives, such as FEC, trans-difluoroethylene carbonate (DFEC), ethylene sulfite (ES) and vinylene carbonate (VC), could affect the electrochemical performance of hard carbon electrodes in SIBs.[280] It was found that only FEC could help form a stable passivation film at ca. 0.7 V on the hard carbon or sodium metal surfaces, resulting in sufficiently suppressed capacity degradation in comparison with electrolytes without FEC (Fig. 27). Later, the influence of the addition of FEC into the 1.0 mol L^{-1} $NaClO_4$/EC+PC electrolyte on the electrochemical performance of hard carbon electrodes was reported.[281] In the presence of 2.0 % FEC additive, a decrease of the reversible capacity and Coulombic efficiency was observed. Additionally, FEC was used as an SEI formation additive for Sb/C,[282, 283] amorphous P,[284] Sn_4P_3,[285] and other negatrodes[286], and demonstrated a variety of benefits in terms of the cycling performance and effective passivation of SIB negatrodes.

Recently, a double-layer SEI film mechanism was proposed for the Sb-based alloy negatrodes in the FEC-containing electrolyte. According to this mechanism, the presence of FEC in the electrolyte first decomposes to form a dense and thin SEI film (first-layer film), and then other solvents further decompose on the first-layer film to form a double-layer SEI film in the more negative potential region, resulting in improved performance of the negatrodes (see Fig. 28).[283] Thereby, FEC is an effective film-forming additive for modifying the SEI film and improving the cyclability of the negatrode materials in SIBs. It is also noted that only 5 % ethoxy(penta-fluoro)cyclotriphosphazene (EFPN) addition is sufficient to make the carbonate-based electrolyte totally non-flammable, which can help improve the safety of organic SIBs.[287] On the other hand, the use of gel polymer electrolytes (GPEs) to replace flammable organic electrolytes has also been proposed to address the safety concerns and avoid liquid leakage for SIBs.[288-290] The first report indicated that a Na^+ ion conducting GPE based on poly(vinylidene difluoride-co-hexafluoropropylene) (PVDF-HFP) was prepared by a simple phase separation process, and showed an acceptable ionic conductivity of 0.60 mS cm^{-1}, good mechanical properties and good electrochemical stability.[288] Then, a Na-ion capacitor assembled with this GPEs provided high specific energy of 168 Wh kg^{-1} and stable cycling with 85 % of the specific capacitance maintained after 1200 cycles.[234] Also, a Na-ion battery $Sb/Na_3V_2(PO_4)_3$ with a low-cost GPE based on cross-linked PMMA was demonstrated. The cell exhibited a highly reversible electrochemical reaction and a stable cycle performance, which was attributed to the enhanced interfacial properties of the gel-polymer electrolyte, especially at the evaluated temperature.[290]

For development of SIBs, there is more research needed to design and prepare new electrolyte,s and improve existing ones in terms of sodium salts, solvents and additives. Theoretically, it is important to understand the reaction mechanisms at the electrode/electrolyte interface, and to enable more stable cycling properties of organic SIBs.

3.4. Magnesium batteries

The first rechargeable battery with a Mg metal negatrode and a Mo_6S_8 positrode, as shown in Fig. 29, was only demonstrated recently,[293] but has gained increasing attention due to the high volumetric capacity of Mg = Mg^{2+} + 2e (3832 mAh cm^{-3}), abundant resource, low material cost, and more importantly easier control of the electrodeposition of Mg metal without dendrite formation.[291-293] The last point differentiates Mg from both Li and Na in that it is unnecessary to use an intercalation host, but the Mg metal itself can be used directly as the negatrode to couple with a suitable positrode in a rechargeable battery. For this reason, the term “magnesium battery” is more appropriate than “magnesium ion battery”. This nature of Mg electrochemistry brings about other benefits, such as higher device energy density (no interaction host material), and safer operation (no short circuit due to dendrite growth).

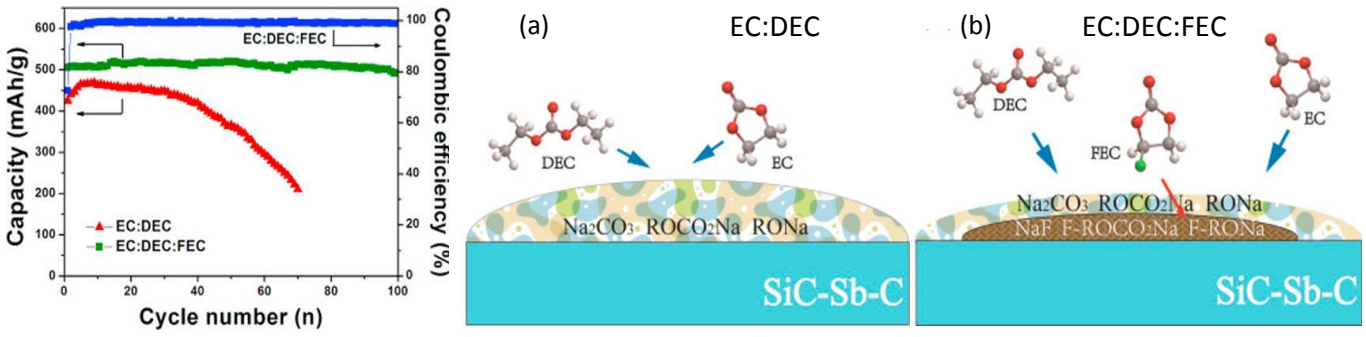

Fig. 28 Left: Cycling performance of the SiC–Sb–C electrode at a cycling current of 100 mA g^{-1} in FEC-free and FEC-containing electrolytes; Right: Structural scheme of the film-forming mechanism of the SiC–Sb–C electrode in the FEC-free (right-a) and FEC-containing electrolyte (right-b).[283] (Reprinted with permission from Elsevier. Copyright 2016.)

However, since the nonconductive ion-blocking layers formed on the Mg surface in non-aqueous, polar aprotic electrolytes cannot transport Mg^{2+} ions effectively, it is crucial to develop a suitable solvent-salt combining with reversible Mg electrodeposition and stripping, and wide electrochemical windows.[294,295] The challenge to commercialise rechargeable Mg batteries is to develop anodically stable, and Mg^{2+} ion conducting electrolytes which govern the electrode and cell performances.[296] In fact, it was known long ago that the solutions of organomagnesium salts and complexes in ethers or tertiary amines were compatible with the Mg negatrode, allowing for reversible Mg deposition and dissolution.[297] Afterwards, highly inert ethereal solvents, such as tetrahydrofuran (THF), dimethoxyethane (DME) and tetraglyme become the more popular solvents that are compatible with Mg and all other battery components.[298,299]

Extensive research efforts have been dedicated to designing the salts, which must be highly soluble in these nonpolar solvents and electrochemically stable. Early studies indicated that although offering high charge density by the Mg^{2+} ion, simple Mg salts such as $Mg(ClO_4)_2$ or $Mg(PF_6)_2$ failed to work in Mg batteries as the respective anions decomposed on, and passivated the Mg metal surface.[300,301]

Interestingly, nearly 100 years ago, the Grignard reagent was studied as an electrolyte that allowed etching of the passivating oxide coating, and hence reversible deposition and dissolution of Mg on the negatrode.[302] However, Grignard reagents (RMgX, where R is an alkyl or aryl group, and X is Cl or Br) cannot be used in batteries due to its intrinsic reducing power. The first non-Grignard electrolyte comprised of $Mg(BR_2R'_2)_2$ (where R and R' can be various organic groups) in THF, which has been considered as the first major breakthrough in Mg battery electrolytes.[297] Later on, a family of dichloro complexes (DCC) electrolytes were proposed based on products of the transmetalation reaction of the Lewis base R_xMgCl_{2-x} with a variety of Lewis acids R'_yAlCl_{3-y} (R, R'=n-butyl and or ethyl, x=0~2, y=0~3) in THF.[303-306] In 2000, the first prototype of the rechargeable Mg battery was demonstrated, signifying the second breakthrough in this area.[307] This prototype with a DCC ($Mg(AlCl_2BuEt)_2$=Bu_2Mg•2$EtAlCl_2$) as the electrolyte achieved high coulombic efficiency up to 99 %.This electrolyte has an acceptable conductivity of few mS cm^{-1} but unfortunately a narrow electrochemical window of ca. 2.2 V which is incompatible with high-voltage positrode materials.

To enlarge the electrochemical window of DCC electrolytes without hampering the ionic conductivity, more varieties of DCC were synthesised by substituting the ethyl groups on the Lewis acid with a methyl or phenyl group.[308-310] For example, the optimal composition of the THF solution of the $(PhMgCl)_2$•$AlCl_3$ complex showed an improved anodic stability up to 3.0 V.[308] When using the phenyl group as the organic ligand, the DCC comprising the products of the reaction between Ph_xMgCl_{2-x} and Ph_yAlCl_{3-y} is known as all phenyl complex (APC, see Fig. 30) electrolytes.[308-310]

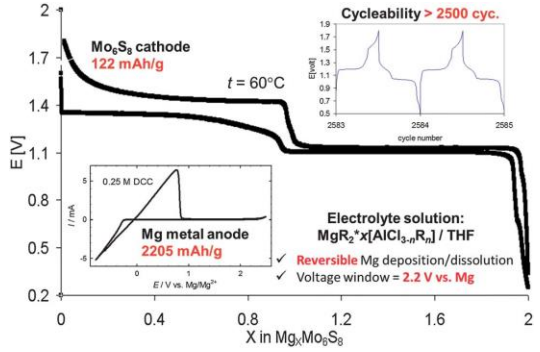

Fig. 29 Operation scheme of the first working rechargeable Mg battery prototype[292] (Reproduced with permission from The Royal Society of Chemistry. Copyright 2013.)

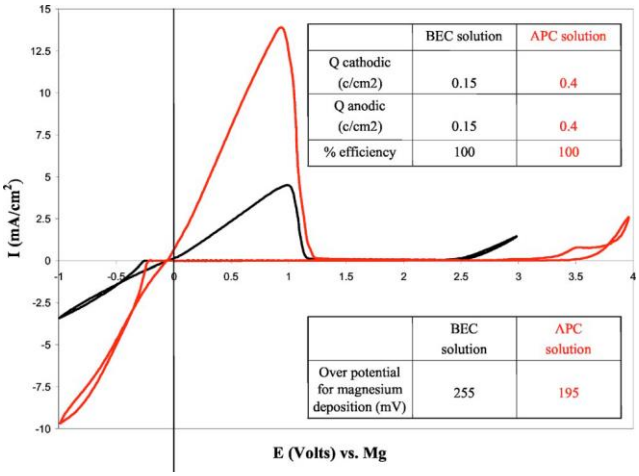

Fig. 30 Comparison between cyclic voltammograms (CVs) of THF solutions containing 0.25 mol L^{-1} of the reaction product between 1:2 $MgBu_2$ and $AlCl_2Et$ (ethyl-butyl complex, standard solutions, black line) and 0.4 mol L^{-1} of the reaction product between 1:2 $AlCl_3$ and PhMgCl (all phenyl complex electrolyte, red line) as indicated. 25 mV s^{-1}, Pt wire working electrode, 25°C. Right insert: Enlargement of the CVs near 0 V vs. Mg, comparing the over-potential for Mg deposition in the two solutions. Left insert: The charge balance upon typical Mg deposition-dissolution cycles in these solutions (100 % cycling efficiency of Mg deposition).[308] (Reprinted with permission from The Electrochemical Society. Copyright 2008.)

In particular, the APC-THF electrolyte containing the reaction product (0.4 mol L^{-1}) between 1:2 $AlCl_3$ and PhMgCl displayed a significantly broader electrochemical window up to 3.3 V on a Pt working electrode and a coulombic efficiency of 100 % for reversible deposition of Mg. Additionally, this APC electrolyte exhibited conductivity of 2 mS cm^{-1}.[311]

The reaction of Grignard hexamethyldisilazide magnesium chloride (HMDSMgCl) with a Lewis acid $AlCl_3$ in a 3:1 ratio led to a product that could significantly raise the oxidation potential to 3.2 V without compromising the coulombic efficiency.[312] The product was isolated as crystals of [$Mg_2(\mu$-$Cl)_3$·6THF] ($HMDSAlCl_3$) with a structure as shown in Fig. 31.

In addition, it should be noted that the electrolyte of tri(3,5-dimethylphenyl)borane $(Mes_3B)\bullet(PhMgCl)_2$ in THF exhibited a wide electrochemical window >3.5 V. It was found to be capable of assisting very well the electrochemical performance of the Mg/Mo_6S_8 battery.[313]

Very recently, the first inorganic compound, magnesium aluminium chloride complex (MACC), was synthesised via the acid-base reaction of $MgCl_2$ with Lewis acidic compounds such as $AlCl_3$, which demonstrated a high coulombic efficiency (up to 99 %), low deposition overpotential (<200 mV), and good anodic stability (3.1 V vs. Mg/Mg^{2+}). Despite of the good performance achieved with all the above reported electrolytes, corrosion of aluminium and stainless steel current collectors posed by the presence of halide ions had hampered the commercialisation of these batteries.[314] Therefore, the development of halide-free salts with high reductive stabilities is crucial for realising a practical rechargeable Mg battery. A new class of $Mg(BH_4)_2$ based electrolytes was proposed for use in rechargeable Mg batteries.[315] When dissolved in both THF and DME, the electrolyte enabled reversible Mg deposition and stripping, and enhanced stability on the current-collector materials. However, the oxidative stability on Pt at 1.7 V vs. Mg limits the use of $Mg(BH_4)_2$ with high-voltage positrodes.

A later study on synthesis and test of closo-borane magnesium dodecahydrododecaborate ($MgB_{12}H_{12}$) found high stability for use in Mg batteries, but it was virtually insoluble in ethers. In contrast, another synthetic salt, [1-(1,7-$C_2B_{10}H_{11}$)]MgCl, showed good solubility in THF with remarkably high anodic stability (ca. 3.2 vs. Mg).[316] Further, a new boron cluster anion, monocarborane $CB_{11}H_{12}^-$, which was compatible with Mg (> 99% coulombic efficiency), showed great anodic stability at 3.8 V vs. Mg, and was non-corrosive (see Fig. 32).[317] A MnO_2 positrode using the $Mg(CB_{11}H_{12})_2$/tetraglyme electrolyte could be charged up to 3.5 V, while the cell using the APC electrolyte could only be charged to around 2.5 V due to corrosion. Owing to its outstanding properties, $Mg(CB_{11}H_{12})_2$ salt-based electrolytes are very promising for future design of high voltage Mg batteries.

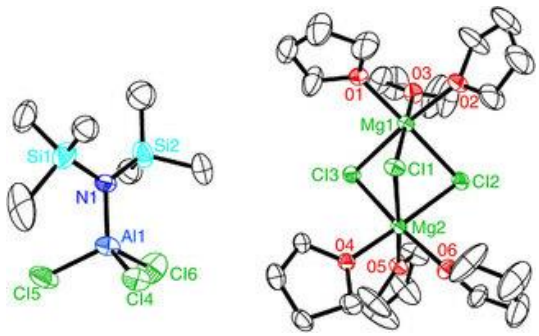

Fig. 31 ORTEP plot (25 % thermal probability ellipsoids) of the crystallised product, $(Mg_2(\mu\text{-}Cl)_3\cdot 6THF)(HMDSAlCl_3)$.[311]

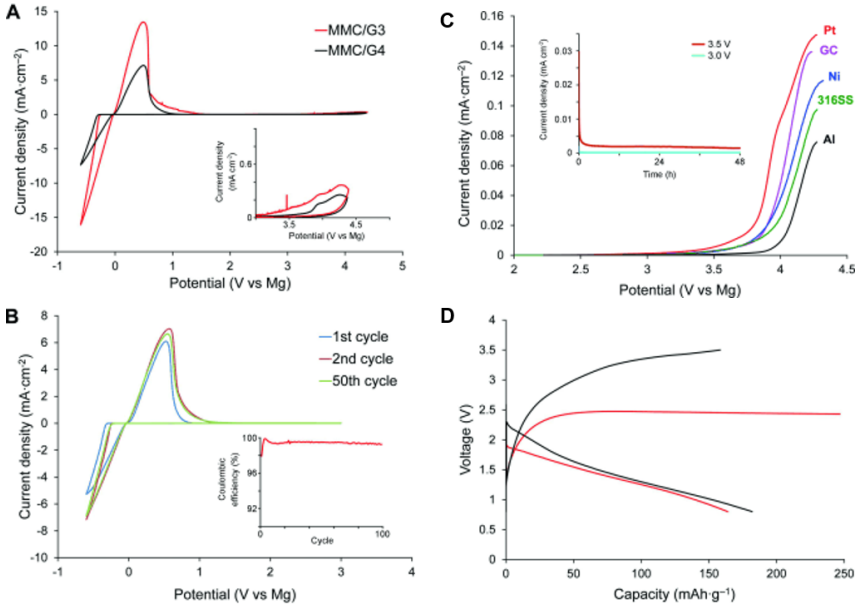

Fig. 32 A) First scan CVs of 0.75 mol L^{-1} MMC/G3 and 0.75 mol L^{-1} MMC/G4 on Pt electrode collected at 5 mV s^{-1} (inset: enlargement of the 3.0 to 5.0 V region). B) Selected CVs of 0.75 mol L^{-1} MMC/G4 electrolyte on Pt electrode collected within the potential range of −0.6 to 3.0 V (vs. Mg/Mg^{2+}) at 5 mV s^{-1} (inset: cycling efficiencies of Mg deposition and dissolution). C) Linear sweep voltammograms of different electrode materials in 0.75 mol L^{-1} MMC/G4 electrolyte at a scan rate of 5 mV s^{-1} (inset: chronoamperometry of a 316 stainless steel disk electrode (area = 1.33 cm^2) in 0.75 mol L^{-1} MMC/G4 electrolyte at 3.0 V (light blue) and 3.5 V (brown) vs. Mg/Mg^{2+}. D) Initial discharge–charge profiles of a rechargeable Mg battery with 0.75 mol L^{-1} MMC/G4 (black line) and 0.2 mol L^{-1} APC (red line) as the electrolyte, a Mg negatrode, and an α-MnO_2 positrode under a constant current density of 0.2 mA cm^{-2}.[317] (Reprinted with permission from WILEY-VCH Verlag GmbH & Co. KGaA, Weinheim. Copyright 2007.)

4. Ionic liquid electrolytes

Although organic electrolytes can offer wide operating voltages which are beneficial to EES devices, they show several significant problems, such as maintenance difficulty (volatile, tedious purification processes), higher environmental impact, higher cost (both materials and manufacture), safety issues (explosion risks due to the poor thermal stability), and low ionic conductivity (diminished power capability).

Among all the available electrolytes, ionic liquids show the highest operating voltage up to 6.0 V, although the working range is often from 2.5 V to 4.0 V. It is directly related to the energy capacity and performance of EES devices, particularly supercapacitors. Unfortunately, ionic liquids are usually less conductive than their high temperature counterpart, molten salts as discussed in the next section. The reason is mainly that ions in ionic liquids are very large and hence unable to move fast. A recently produced graphene based supercapacitor with an ionic liquid as the electrolyte has demonstrated a specific energy of up to 136 Wh / kg at 80 °C, comparable to that of a commercial Li-ion battery.[318] This high specific energy is mainly due to the high working voltage of 4.0 V. Fig. 33 demonstrates the galvanostatic charge-discharge curve of a curved graphene electrode (6.6 mg) at a constant specific current of 1 A g^{-1}, and CVs for the graphene electrode at different scan rates. All these electrochemical tests were done in an ionic liquid, 1-ethyl-3-methylimidazolium tetrafluoroborate ($EMIMBF_4$), as the electrolyte.

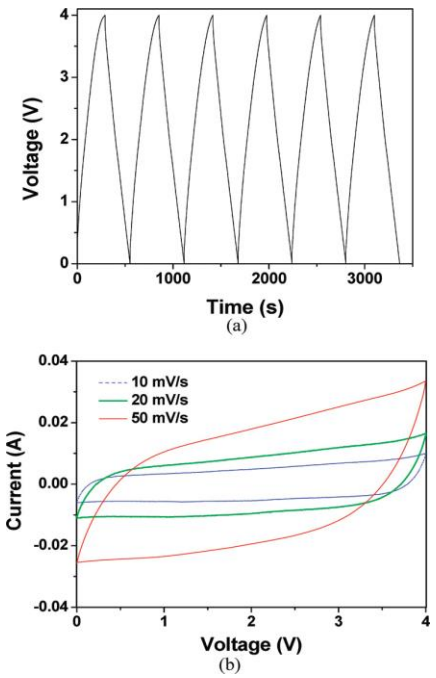

Fig. 33 (a) Galvanostatic charge-discharge curve at 1 A g^{-1} and (b) CVs at different scan rates recorded on a curved graphene electrode in an ionic liquid, $EMIMBF_4$.[318] (Reproduced from with permission from American Chemical Society. Copyright 2010.)

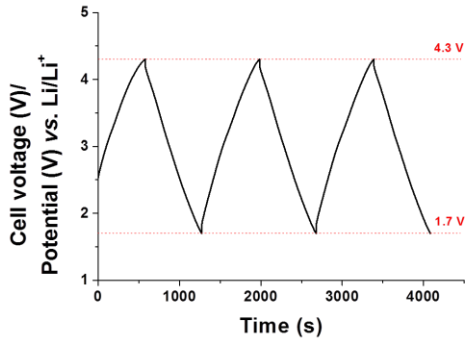

Fig. 34 Galvanostatic charge-discharge curves of a demonstrative ionic liquid based supercapattery cell at 1 mA cm^{-2}.[320]

In this example, the mesoporous graphene electrode enabled fast capacitive charging and discharging, and unusually high specific capacitance. Coupled with this electrode material, the ionic liquid electrolyte supported an operating voltage of 4.0 V, pushing the specific energy of the EDLC to an unprecedented level at the time of the report.

Similar applications of ionic liquids as the electrolyte in supercapacitors and supercapatteries were also reported.[319, 320] Fig. 34 shows a very recent study demonstrating a supercapattery based on an activated carbon positrode and a Li negatrode in an ionic liquid, 1-butyl-1-methylpyrrolidinium tri(pentafluoroetnyl)tri-fluorophosphate (BMPyrrFAP), containing gamma-butyrolactone (γ-GBL) and $LiClO_4$.[320] The remarkably high specific energy of 230 Wh kg^{-1} can be mainly attributed to the broad operating voltage up to 4.3 V. However, simply substituting an aqueous or organic electrolyte with an ionic liquid would not always lead to a high energy capacity. Inferior results from ionic liquid electrolytes in supercapacitors are not uncommon and largely related to a reduced specific capacitance of the electrode materials in the ionic liquid, highlighting the significance of a considered and synergistic approach to materials choice and cell design.

It is commonly thought that dendrite formation is inevitable when metal is used as the negatrode in batteries or supercapatteries, which could shorten the cycling life of the devices. The worst scenario is that the dendrite penetrates through the separator membrane, short-circuit between positrode and negatrode and lead fire or explosion. However, a recent study has shown that pre-treatment of the Li metal in ionic liquids containing an appropriate lithium salt can effectively supress the formation of the Li metal dendrite during charge-discharge cycling.[321]

Typical results from this study are presented in Fig. 35 which plots the discharge capacity and coulombic efficiency of several "Li(–)|Li-salt + ionic liquid|$LiFePO_4$(+)" cells against the charge-discharge cycle number at a rate of 1 C. The low viscosity ionic liquid used in the cell was *N*-propyl-*N*-methyl-pyrrolidinium bis(fluorosulfonyl)imide, [C_3mPyr^+][FSI^-]. A Li-salt, LiFSI (Fig. 35a, b), $LiPF_6$ (Fig. 35c) or $LiAsF_6$ (Fig. 35d), was added to the ionic liquid to form the electrolyte. The negatrode was either pristine, untreated Li metal (Fig. 35a), or

pre-treated Li metal (Fig. 35b-d) by immersing it in the respective electrolytes for 12 days.

It can be seen in Fig. 35 that the four cells all show initially unstable and then gradual declining discharge capacity which becomes stable beyond about 500 cycles. This unstable initial behaviour corresponded possibly to the variation of the SEI layer on the Li negatrode. For the cell with the untreated Li metal negatrode (Fig. 35a), the stable discharge capacity is just below 60 mAh g^{-1}, whilst all the other cells with the pre-treated Li metal negatrode exhibit notably higher stable discharge capacities. The more significant difference is shown on the coulombic efficiency profiles. For untreated Li metal negatrode, the coulombic efficiency becomes widely scattered after about 600 cycles, indicating gradual formation of dendrites which are unfavourable to maintaining the dynamic stability of the SEI layer. However, the coulombic efficiency remains much more constant for the cells with the pre-treated Li negatrode. This change can be attributed to the pre-formed SEI on the Li negatrode contributing to eliminating dendrite formation during charge-discharge cycling. It should be mentioned that Fig. 35d also shows some scattered points on the coulombic efficiency profile after about 820 cycles. This is evidence that anions in the ionic liquid electrolyte can impact the SEI stability, suggesting the FSI^- and PF_6^- ions to be more effective for stabilising the SEI layer on the Li negatrode.

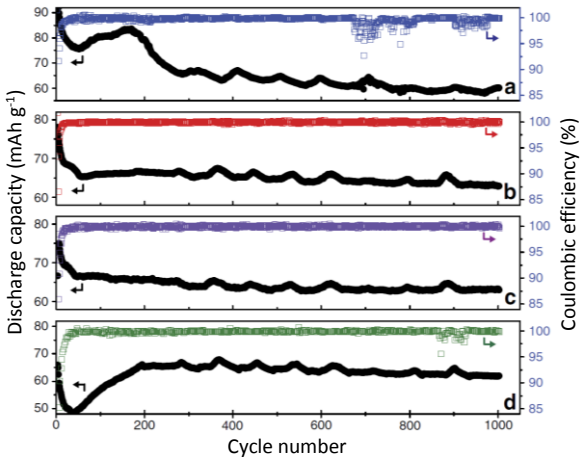

Fig. 35 Variations of discharge capacity and coulombic efficiency with the cycle number of charging and discharging the "Li | Li-salt + [C_3mPyr^+][FSI^-] | $LiFePO_4$" cell at a rate of 1 C under different conditions: (a) Pristine Li metal, LiFSI; (b-d) Li metal immersed in [C_3mPyr^+][FSI^-] containing (b) LiFSI, (c) $LiPF_6$, or (d) $LiAsF_6$ for 12 days before cell assembly.[321]

5. Molten salt electrolytes

Molten salts are classified as 'high-temperature' liquid salts with reference to ionic liquids that are in the liquid state at

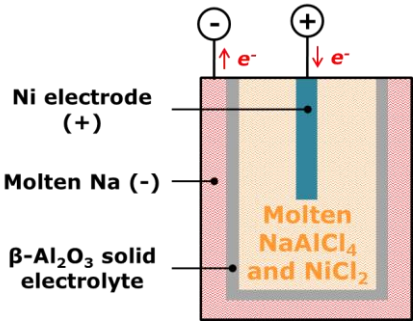

Fig. 36 Schematic drawing of a ZEBRA molten salt battery.

room temperatures. The distinguished properties of molten salts, which include but not limit to high ionic conductivity, high chemical and thermal stability, and high mutual solubility, enable their wide applications in construction of EES devices. Molten salt electrolytes offer many advantages over their aqueous counterparts, such as higher working voltage and no detrimental effects from hydration of ions. Because molten salts based EES devices operate at elevated temperatures, both kinetic and thermodynamic barriers can be minimised, and hence a relatively high efficiency for energy conversion is expected. This section describes and analyses four typical examples of molten salts based EES devices, which are ZEBRA molten salt batteries, liquid metal batteries, carbonate fuel cells, and direct carbon fuel cells.

5.1. ZEBRA molten salt batteries

Named after a technical project, Zero Emissions Batteries Research Activity,[322] the ZEBRA molten salt battery has been considered as one of the most attractive EES devices for both transportation (e.g., automobile) and stationary (e.g., renewable energy storage) applications.[323,324] The working mechanism of the ZEBRA molten salt battery can be described by the following electrochemical reactions:

(+) positrode: $NiCl_2 + 2Na^+ + 2e^- = Ni + 2NaCl$
(–) negatrode: $2Na = 2Na^+ + 2e^-$
Cell: $NiCl_2 + 2Na = Ni + 2NaCl$

According to the cell reaction and thermodynamic data at 300 °C ($\Delta G^o = -138.51$ Wh), the theoretical cell voltage and specific energy of the ZEBRA molten salt battery can be respectively calculated to be 2.584 V and 789 Wh kg^{-1} (counting only the total mass of the active materials on both electrodes). In practical cells, the use of electrolyte, current collectors, and thermal insulating and packaging materials are inevitable. As a result, the reported specific energy of real ZEBRA batteries ranged from 90 to 120 Wh kg^{-1} with the energy efficiency close to 100 %.[323]

As can be seen from Fig. 36, the construction of the ZEBRA battery is similar to that of a sodium-sulphur battery in that both use a liquid sodium negatrode and the β-Al_2O_3 solid electrolyte. This makes the development of the ZEBRA battery much easier as it can adopt the existing mature technologies. On the other hand, in comparison with the sodium-sulphur battery, the ZEBRA battery

uses an additional molten salt electrolyte to bridge between the β-Al_2O_3 solid electrolyte and positrode. The molten salt is $NaAlCl_4$ which enables not only ionic conduction, but also the reversible conversion between Ni and $NiCl_2$ in solid state on the positrode during discharging and charging. The operating temperature of a ZEBRA battery is between 170 °C and 400 °C, which helps high power capability.[323] By taking advantage of the molten $NaAlCl_4$, the corrosion issue arose from the sodium polysulfides in the sodium-sulphur battery can be avoided. This property of $NaAlCl_4$ also contributes, at least partly, to the long cycle life of the ZEBRA battery which is typically designed to work over 10 years.[323,324]

5.2. Liquid metal batteries

Due to the unique liquid-liquid electrode-electrolyte interfaces and highly conductive molten salt electrolytes, the liquid metal batteries endow ultrafast electrode charge-transfer kinetics and superior ion transport properties.[325] The structure of a liquid metal battery is illustrated in Fig. 37.

As can be seen from Fig. 37, the molten salt electrolyte in a typical liquid metal battery is sandwiched between two liquid-metallic electrodes, i.e., positrode and negatrode. Therefore, the liquid metal battery cell can be described as follows:[325]

A(l) | AX_z(l) | A-B(l)

where A and B represent the two different metals on the negatrode and positrode, respectively, and AX_z the alkali or alkaline-earth molten salt electrolyte.

The electrochemical reactions in a liquid metal battery during discharging can be written as follows:

(+) positrode: $A^{z+} + B(l) + ze^- = A\text{-}B(l)$

(–) negatrode: $A(l) = A^{z+} + ze^-$

Cell: $A(l) + B(l) = A\text{-}B(l)$

According to the construction shown in Fig. 37, the characteristics of the molten salt electrolyte have to meet some specific criteria. First, the density of the electrolyte should fall in between those of the positrode and negatrode, with the intention of self-segregation of the three liquid layers. Second, the ionic conductivity of the molten salt should be high, which is crucial for increasing the energy efficiency and power capability. Thirdly, the solubility of metallic electrodes in the electrolyte should be as low as possible. The high solubility of metallic electrodes in the molten salt will bring about electronic conduction and self-discharge, leading to low current and energy efficiency.

The solubilities of alkali and alkaline-earth metals in their respective halide salts have been evaluated and summarised by many researchers.[325-328] It has been found that with increasing the atomic number, the solubility of both liquid alkali and alkaline-earth metals in their respective halide salts increases, i.e., Li < Na < K < Rb < Cs, and Mg < Ca < Sr < Ba, respectively.

In the same way, the liquid metal solubility also increases with increasing the halide atomic number, i.e., F < Cl < Br < I.[325] In order to minimise the solubility of metals in the molten salt, the cell operating temperature should be maintained at a relatively low value. Therefore a relatively low melting point of the molten salt electrolyte is vital. In the interest of the low melting point, eutectic mixtures of salts (binary, ternary, and quaternary) have been investigated intensively,[325, 329, 330] which could also help to minimise the associated issues with the high operating temperatures, including side reactions, high cost of refractory cell materials, difficulties in device sealing, and safety concerns. During recent years, a unique binary electrolyte consisting of NaOH and NaI (molar ratio of ca. 0.8 to 0.2) has been developed, which shows a low eutectic melting temperature of 220 °C.[331] Another characteristic of the molten salt electrolyte, which should be considered, is the decomposition voltage. A high decomposition voltage is desired as it could render high charging and discharging voltages.[325] Table 1 lists the properties of some commonly used low melting point molten halide salt electrolytes.

Recently, there are several types of molten salts based liquid metal batteries being developed, including Mg | $MgCl_2$-KCl-NaCl | Sb,[332] Ca | LiCl-NaCl-$CaCl_2$ | Bi,[334] CaLiCl-NaCl-$CaCl_2$ | Sb,[334] Na | NaOH-NaI | Pb-Bi[335] and Li | LiCl-LiF | Bi[336]. In these liquid metal batteries, Mg, Ca, Na, and Li have been used as the reactive elements on the negtrode, whereas Sb, Bi, and Pb-Bi have been utilised as the positrode materials due to their relatively low melting temperatures. These molten salts based liquid metal battery systems exhibited remarkable performances, e.g. long life cycle, high efficiency, and low fading rate (i.e. high capacity retention). Fig. 38 shows the full cell cycling performance of a Li | LiCl-LiF | Bi cell.[336] After 1000 cycles, 99.9 % of the coulombic efficiency remained, and only 4 % loss of capacity was observed. This cell was even tested by cooling to the solidified state, followed by heating and recycling.[336]

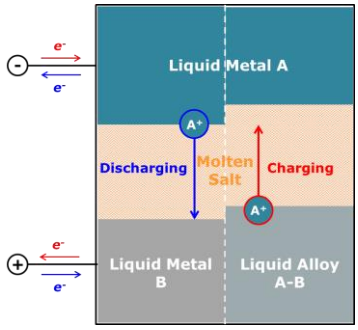

Fig. 37 Illustration of a liquid metal battery upon charging and discharging.

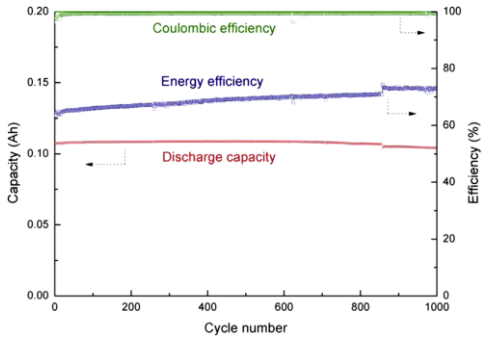

Fig. 38 Full cell cycling performance for a Li|LiCl-LiF|Bi cell at 550 °C. Cell diameter: 1.2 cm, theoretical capacity: 0.115 Ah, at 0.3 A cm^{-2}.[336]

Table 1 Properties of typical commonly used multicomponent molten salt electrolytes at the specified temperature, T_0.[325]

Cation	Electrolyte	Composition, mol%	T_m, °C	$\rho(T_0)$, g cm^{-3}	$\sigma(T_0)$, S cm^{-1}	T_0, °C
Li^+	LiCl-KCl	41:59	353	1.63	1.7	476
	LiF-LiCl-LiI	20:50:30	430			
	LiCl-LiI	35:65	368	2.57	3.5	450
Na^+	NaF-NaCl-NaI	15:16:53	530	2.54	1.7-2.0	560
Mg^{2+}	NaCl-KCl-$MgCl_2$	30:20:50	396			
Ca^{2+}	LiCl-NaCl-$CaCl_2$-$BaCl_2$	29:20:35:16	390	2.28	1.9	527

5.3. Molten carbonate fuel cells

Current designs of various fuel cells are form primary use, i.e. they function only to convert chemical energy to electricity (discharging), but not able to reverse the process (charging). Thus, fuel cells are not, strictly speaking, EES devices. This is particularly the case when the fuel is of small organic molecules, such as methanol and formic acid, and the fuel oxidation reaction is practically not possible to reverse electrochemically, and not even chemically. However, when the fuel is of hydrogen or carbon, the oxidation reaction can be chemically or even electrochemically reversed. Therefore, these fuel cells present good opportunities for EES applications. Two examples that are relevant to molten salts are explained in this and next sections: molten carbon fuel cells and direct carbon fuel cells.

The molten carbonate fuel cells (MCFCs) use hydrogen as the fuel and have an exclusive superiority over other types of fuel cells. It is their ability to capture CO_2 and regenerate it in a more concentrated form.[337] This ability of MCFCs is attractive to the ongoing global effort to mitigate the impact of CO_2 emission on climate change. Apart from this, the MCFC has been considered as the most successful major fuel cell. For example, there are more than 50 MCFC based stationary power stations being commissioned around the world producing over 300 MW of clean electric powder.[338] Fig. 39 shows the schematic drawing of an MCFC.

As shown in Fig. 39, CO_2 is consumed by the cathodic reactions on the positrode side (typical positrode material: lithiated nickel oxide). Meanwhile the anodic reactions release CO_2 on the negatrode side (typical negatrode material: Ni, alloyed with chromium or aluminium). A eutectic mixture of Li_2CO_3 and K_2CO_3 is commonly utilised as the electrolyte. In order to balance the molten electrolyte, some of the CO_2 released at the negatrode needs to be recycled for cathodic reactions. It has been reported that the MCFC can operate for up to 40,000 hours without noticeable electrolyte deteriorations, owing to the remarkable long term stability of the molten carbonate salt under CO_2.[337, 339]

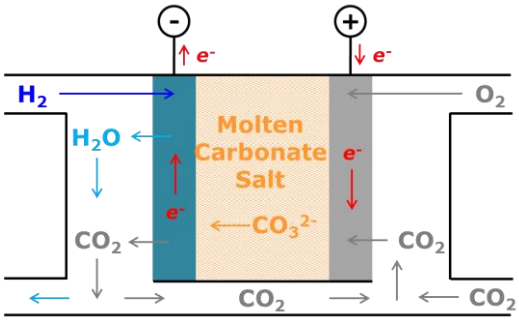

Fig. 39 Schematic drawing of a molten carbonate fuel cell when H_2 is employed as the fuel.

Interestingly, the main issue associated with the prolonged use of MCFCs is the degradation of the cell components instead of the decomposition of molten salt electrolyte. The reason is that the cell operating temperature is relatively high (typically between 600 °C to 850 °C due to the high melting temperature of carbonates)[340] when compared to that of hydroxide based fuel cells,[337, 341-344] which is problematic to the construction materials of the cell components. However, the eutectic carbonate salt mixture is adequately stable at the operating temperatures. There are some other advantages of using the molten carbonate electrolyte, including its ability to catalyse carbon oxidation and high ionic conductivity.[345, 346]

5.4. Direct carbon fuel cells

The configuration and working mechanisms of the direct carbon fuel cells (DCFCs) are similar to the above-mentioned MCFCs as shown in Fig. 40. The most commonly used molten carbonate electrolyte is the eutectic mixture of Li_2CO_3 and K_2CO_3.[347] Therefore, the molten salt electrolyte in the DCFCs shares the same advantages as that used in the MCFCs (see Section 5.3.).

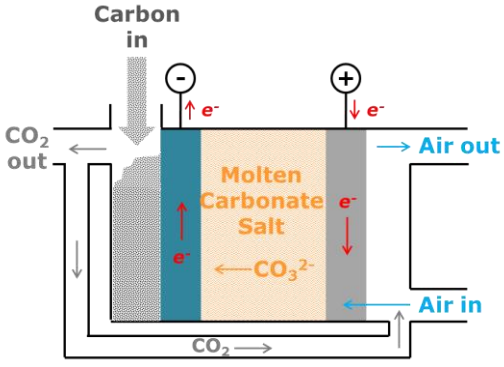

Fig. 40 Schematic drawing of a direct carbon fuel cell.

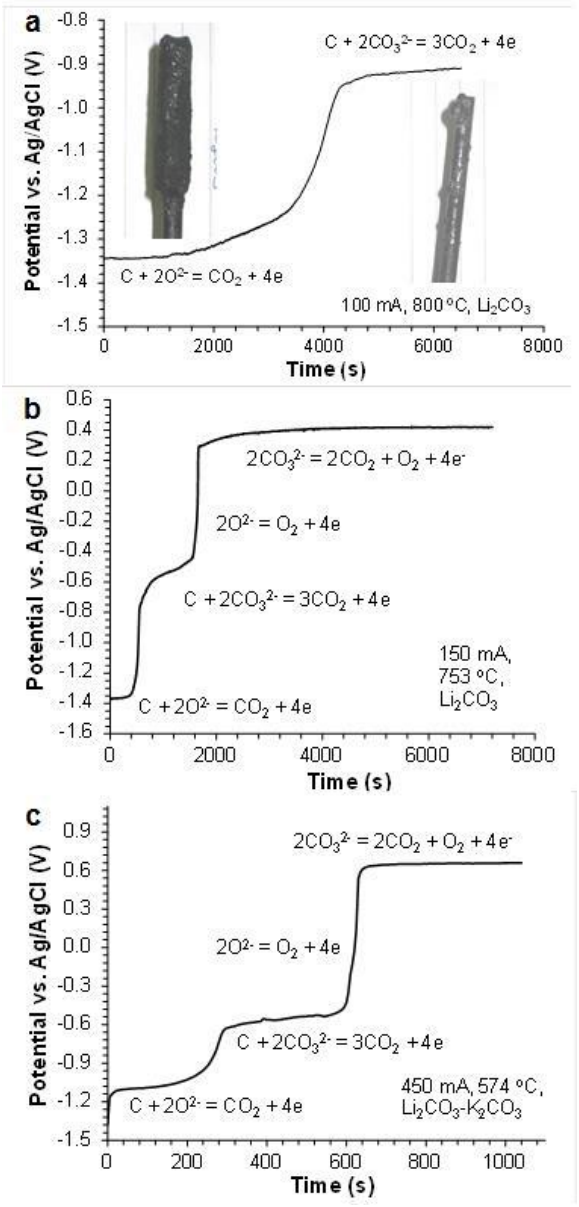

Fig. 41 Potential-time profiles of a mild steel working electrode (5 mm dia. rod) with electro-deposited carbon during anodic oxidation in molten salts under CO_2. (a) Li_2CO_3 at 800 °C and 100 mA for 3600 s deposition at -2.1 V vs. Ag/AgCl (ca. 16000 C in charge), (b) Li_2CO_3 at 753 °C and 150 mA for 600 s deposition at -2.1 V (ca.1200 C), and (c) Li_2CO_3-K_2CO_3 (molar ratio: 62:38) at 574 °C for 600 s deposition at -2.6 V (ca. 850 C). Photographs in (a) show the working electrode with the carbon deposit before (left) and after (right) anodic oxidation, respectively. Counter electrode: 10 mm dia. graphite rod.[355]

Although there are many similarities between DCFCs and MCFCs, the DCFC is the only type of fuel cell that uses a solid fuel (i.e., various forms of solid carbon) instead of using gaseous fuels, such as hydrogen gas and coal gas. Another distinctive characteristic of the DCFC is the fixed chemical potentials of both reactant (carbon) and the product (carbon dioxide), which are irrelevant to the fuel conversion rate or position within the cell. This is attributed to the separate phases of the reactant (pure carbon in solid phase) and the product (pure carbon dioxide in gas phase).[347] Therefore, 100 % fuel conversion efficiency can be expected. Electrode reactions in the DCFC during discharging can be described as follows:

(+) positrode: $O_2 + 2CO_2 + 4e^- = 2CO_3^{2-}$
(–) negatrode: $C + 2CO_3^{2-} = 3CO_2 + 4e^-$
Cell: $C + O_2 = CO_2$

Similar to the MCFCs, in order to achieve mass balance, two molecules of CO_2 for every atom of carbon that is consumed on the negatrode, need to be recycled from the negatrode to the positrode compartment, as shown in Fig. 40. Obviously, to reverse the fuel oxidation reaction in the DCFC, the reduction of CO_2 to carbon, particularly by electrochemical means, needs to be feasible. In fact, electro-reduction of the carbonate ion, CO_3^{2-} to solid carbon in molten carbonate salts has been known since early 1960s.[348-350] However, the research has remained fairly quiet until recent consideration of the process for capture and utilisation of CO_2.[351-360] Particularly, electro-deposition and re-oxidation of carbon in molten carbonate salts under the CO_2 atmosphere have been investigated in order to close the loop of CO_2-carbon cycles via the combination of molten salt electrolysis and DCFCs for energy storage.[355,356] To help understand the carbon deposition process, different salt compositions have been used to investigate the electrochemical deposition and re-oxidation of solid carbon, which are $CaCl_2$-$CaCO_3$-LiCl-KCl (molar ratio of 0.30:0.17:0.43:0.10) and Li_2CO_3-K_2CO_3 (molar ratio of 0.62:0.38) at different temperatures and atmospheres.[355] More importantly, it was confirmed that Li^+ ions play an essential role for carbon electro-deposition in carbonate-only electrolytes.[355,356] Electrochemical oxidation of the deposited carbon was also investigated,[355] and preliminary findings, as shown in Fig. 41, indicate two plateaux on the potential-time profiles related to the anodic oxidation of the deposited carbon. The potential difference between these two plateaux can be over 800 mV in Fig. 41b, but it is about 500 mV in Fig. 41c. This finding suggests a strong influence from both thermodynamic and kinetic causes in relation with the experimental conditions. Reducing this potential difference would benefit the energy efficiency of electrochemical cycling between CO_2 and carbon, which may result from the fast growing interests and activities in this area.[350-360]

6. Conclusions and outlooks

In this review, we have introduced the recent progresses in research and practice of various electrochemical energy storage (EES) devices from the perspective of electrolytes. Properties of typical examples of different types of electrolyte for EES devices are summarised in Table 2 to display both their advantages and limitations. These devices include most recently developed secondary batteries, supercapacitors,

Table 2. Properties of different types of electrolyte used in electrochemical energy storage devices.

Electrolyte	Typical example	Electrode materials	Conductivity, $mS \cdot cm^{-1}$	Cell voltage, V	Advantages	Limitations	Ref.
Aqueous electrolytes	5 mol L^{-1} $LiNO_3$ in water	(+) $VO_2(B)$// $LiMn_2O_4$ (–)	ca. 10^3	1.5	Non-combustible, affordability, high conductivity, low viscosity, non-toxic, low cost	Poor stability, self-discharge, narrower electrochemical window	21
	1 mol L^{-1} Li_2SO_4 aqueous electrolyte at pH=13 in the absence of O_2	(+) $LiTi_2(PO_4)_3$// $LiFePO_4$ (–)		0.9			22
	1 mol L^{-1} Na_2SO_4 in aqueous solution	(+) Hollow $K_{0.27}MnO_2$// $NaTi_2(PO_4)_3$ (–)		0.9			26
	1 mol L^{-1} KOH+0.01 mol L^{-1} $Zn(Ac)_2$ in aqueous solution	(+) Zn@CF// Co_3O_4@Ni (–)		1.78			27
	0.2 mol L^{-1} HBr+0.005 mol L^{-1} Br_2+1.0 mol L^{-1} H_2SO_4 solution on the positive side and 0.05 mol L^{-1} AQDS+1.0 mol L^{-1} H_2SO_4 solution on the negative side	(+) Photo-electrolysis cell//RFB (–)		0.8			30
Organic electrolytes	1.0 mol L^{-1} $TMEABF_4$/AN	(+) AC//AC (–)	50	3	Wide electrochemical window, cyclablity	Highly toxic, flammable, evaporation	69
	PYR_{14}TFSI/PC (1:1 wt.%)		10.3	3.5	Low energy density	High conductivity	74
	0.7 mol L^{-1} Et_4NBF_4 in ADN		4.3	3.75	Wide electrochemical window	Low conductivity	87
	1.0 mol L^{-1} $LiPF_6$ in EC+DMC (1:2, v/v)	(+) AC// $LiNi_{0.5}Mn_{1.5}O_4$ (–)	ca. 10	2.0	Cycle stability	Low working voltage	93
	1.0 mol L^{-1} $LiPF_6$ in EC+DMC (1:1, v/v)	(+) Graphite//AC (–)	12	4.5	wide working voltage	Poor cycle stability	110
	1.0 mol L^{-1} $LiPF_6$ in EC+DMC (1:1, v/v)	(+) Graphite// $LiCoO_2$ (–)	12	4.0	Excellent performance, low self-discharge, wide working voltage	Flammable, leakage	
	1.0 mol L^{-1} $LiPF_6$ in TMS+EMC (1:1, v/v)	(+) $Li_4Ti_5O_{12}$// $LiNi_{0.5}Mn_{1.5}O_4$ (–)	5.1	3.2	Nonflammable	Poor low temperature properties	193
	1.0 mol L^{-1} $LiPF_6$ in FEC+DMC+EMC+HFPM (2:3:1:4, v/v)	(+) MCMB// $LiNi_{0.5}Mn_{1.5}O_4$ (–)	8.57	4.6	Nonflammable, good wettability, excellent cyclability	High cost, poor high-temperature performance	198
	$LiN(SO_2F)_2$/DMA (1:1.1, molar ratio)	(+) Graphite// $LiNi_{0.5}Mn_{1.5}O_4$ (–)	1.12	5.2	Superior thermal stability, flame retardant ability, effective inhibition of anodic Al dissolution	High viscosity, high cost, low conductivity	222
	1.0 mol L^{-1} $NaClO_4$ in $EC_{0.45}$:$PC_{0.4}$5:$DMC_{0.1}$	(+) Hard C// $Na_3V_2(PO_4)_2F_3$ (–)	18	3.65	High ionic conductivity, low viscosity, good rate capability, excellent capacity retention	Flammable	264
	0.8 mol L^{-1} $NaPF_6$/TMP+10 vol% FEC	(+) Sb-based anode// $NaNi_{0.35}Mn_{0.35}Fe_{0.3}O_2$ (–)	5.41	3.0	Nonflammable	Low operation voltage	273
	0.25 mol L^{-1} $Mg(AlCl_2BuEt)_2$ in THF	(+) Mg// $Mg_xMo_3S_4$ (–)	1.0 to 1.4	1.1	High energy density	Narrow electrochemical window, poor cyclability, low conductivity, high cost	292
	0.75 mol L^{-1} $Mg(CB_{11}H_{12})_2$/tetraglyme (MMC/G_4) electrolyte	(+) Mg//α-MnO_2 (–)	1.8	2.5			317
Ionic liquid electrolytes	0.5 mol L^{-1} $LiClO_4$ in BMPyrrFAP+γ-GBL (1:1, v/v)	(+) Li//AC (–)	--	4.3	Wide electrochemical window, safety	Low conductivity, high cost, complicated synthesis, poor rate capability	320
Molten salt electrolytes	Molten $NaAlCl_4$+β-Al_2O_3 solid electrolyte	(+) Na// $NiCl_2$ (–)	36	2.58	High ionic conductivity, high efficiency, ultrafast electrode charge-transfer kinetics, superior ion transport properties, remarkable long term stability	High operation temperature, the degradation of the cell components	323
	Molten LiCl-LiF (30:70)	(+) Li//Bi (–)	--	0.7			336
	Li_2CO_3, Na_2CO_3 and K_2CO_3 (43.5:31.5:25 mol%)	(+) SnO_2//Ni (-)	--	1.8			353

supercapatteries, fuel cells, and redox flow batteries. Aqueous electrolytes were used in the very first battery in the world, and are still been widely used in various modern EES devices which require safety control and highly conductive electrolytes. Specifically, readers can also find the recent examples of aqueous electrolytes utilised in Li-ion and Na-ion batteries which usually use non-aqueous electrolytes. However, the limitation of the working voltage of the aqueous EES devices is still a drawback when high specific energy of the device is required in real applications. Organic electrolytes can offer wider working potential window than aqueous ones. Although the safety issue is still a barrier for organic electrolytes, they are widely used in the batteries of portable devices due to the high working voltage and high specific energy. Ionic liquids can offer acceptable conductivity and will not suffer from safety issues because of their inflammable and almost non-volatile natures. Recent studies on ionic liquid electrolytes also revealed their potential in EES devices. On the other hand, molten salts for EES devices are also introduced here. Both kinetic and thermodynamic barriers of the molten salt electrolyte based EES devices could be minimised, and hence a relatively high efficiency and high speed for energy conversion could be expected. In this review, we do not intend to downplay the importance of the electrode materials in all these EES devices. Actually in most cases, the typical electrode materials structures could affect the performance of the devices quite significantly. Here, we wish to emphasise the less discussed but important role of electrolytes in EES devices, and introduce some pioneering studies in which the electrolytes contribute greatly to the improvement of the device performance.

We hope more attention will be paid to electrolyte studies to understand the mechanism of the interaction between the electrolytes and the electrode materials, and to improve the performance of the EES devices based on the existing mechanism. Further research needs to be done for electrolyte investigation and selection optimization of different EES devices in order to obtain the desired cycling stability and safety. Since the interphases between electrodes and electrolytes directly affect the performance (affecting the energy capacity, rate performance, cycliability and safety) of EES devices, the fundamental understanding and controlling about the physical and chemical properties of these interphases are vital. The ideal interphase can only form upon well informed selection of solvents, salts and/or additives. Meanwhile, the development of in situ analytical tools to better characterise the composition distribution and properties of the interphase is also important for the design and optimisation of new and better electrolytes for applications in different EES devices. A specific prospect can be related with the molten salts enabled electrochemical cycling between CO_2 and carbon. Because solid carbon is a fuel and stable in air, it is suitable for long term storage and long distance transportation. Therefore, we anticipate that the concepts of “seasonal energy storage” (SES) and “regional energy storage” (RES), as schematically illustrated in Fig. 42 can be tested and demonstrated. The purpose of SES is to store energy harvested in the sunny summer and reuse it in cold winter, whilst the RES aims to collect energy from remote desserts (sunlight to electricity) or mountains (wind to electricity) to urban areas. To achieve these goals, future research and development need to improve the process and energy efficiency of the electrochemical conversion between CO_2 and carbon in molten salts. Obviously, continued research effort plays the key role to better understand the mechanisms and kinetics of electrodeposition and re-oxidation of carbon for technological development. However, financial support, market establishment and public awareness are all equally important to make the process a commercial success.

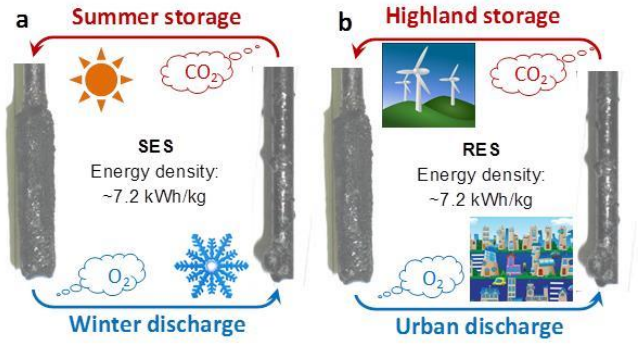

Fig. 42 Schematic illustration of the concepts of (a) seasonal energy storage (SES), and (b) reginal energy storage (RES) based on electrochemical cycling between carbon and CO_2 in molten salts.[353]

Acknowledgements

This work received funding from the Ningbo Municipal Government (3315 Plan and the IAMET Special Fund, 2014A35001-1, and Ningbo Natural Science Foundation Programme, 2016A610114 and 2016A610115), the Zhejiang Provincial Applied Research Programme for Commonweal Technology (2016C31023), the NSFC (21503246), the EPSRC (EP/F026412/1, and EP/J000582/1) and the Royal Society (2007 Brian Mercer Feasibility Award).

List of abbreviations and acronyms

2,3BC	2, 3-butylene carbonate
γ -GBL	gamma-butyrolactone
Ac	acetate
AC	active carbon
ADN	adiponitrile
AGG	aggregate
AN	acetonitrile
APC	all phenyl complex
AQDS	9, 10-anthraquinone-2, 7-disulphonic sodium

$AQDSH_2$	1, 8-dihydroxy-9, 10-anthraquinone-2, 7-disulphonic sodium
BMPyrrFAP	1-butyl-1-methylpyrrolidinium tri(pentafluoroetnyl)tri-fluorophosphate
$CB_{11}H_{12}^-$	monocarborane
CIP	contact ion pair
CFs	carbon fibres
CV	cyclic voltammetry
C=N	nitriles
$[C_3mPyr^+][FSI^-]$	N-propyl-N-methylpyrrolidinium bis(fluorosulfonyl)imide anion
DCC	dichloro complexes
DCFCs	the direct carbon fuel cells
DES	diethyl sulfite
DEC	diethyl carbonate
DFEC	trans-difluoroethylene carbonate
DMC	dimethyl carbonate
DME	1, 2-dimethoxyethane
DMSO	dimethyl sulfoxide
DOL	1, 3-dioxolane
EC	ethylene carbonate
EDLCs	electrical double-layer capacitors
EFPN	ethoxy(penta-fluoro)cyclotriphosphazene
EES	electrochemical energy storage
$EMIMBF_4$	1-ethyl-3-methylimidazolium tetrafluoroborate
EMSF	ethylmethyl sulfone
EMC	ethyl methyl carbonate
EiPS	ethyl isopropyl sulfone
ES	ethylene sulfite
FAN	fluoroacetonitorile
FEC	fluoroethylene carbonate
G3	triglyme
G4	tetraglyme
GFMs	glass fiber mats
GPEs	gel polymer electrolytes
GLN	gluotaronitrile
HC	hard carbon
HCEs	highly concentrated electrolytes
HDI	hexamethylenediisocyanate
HFPM	1, 1, 1, 3, 3, 3-hexafluoroisopropyl methyl ether
HFiP	tris(hexafluoro-iso-propyl) phosphate
HMDSMgCl	hexamethyldisilazide magnesium chloride
HOMO	highest occupied molecular orbital
LNMO	$LiNi_{0.5}Mn_{1.5}O_4$
LPTB	lithium 4-pyridyl trimethyl borate
$LiPF_6$	lithium hexafluorophosphate
LICs	lithium ion capacitors
LIBs	Li-ion batteries
LiTFSI	$LiN(SO_2CF_3)_2$
LiTFSM	$LiC(SO_2CF_3)_3$
LiBOB	lithium bis(oxalato)borate
LiDFOB	lithium difluoro(oxalato)borate
LiBETI	$LiN(SO_2C_2F_5)_2$
LiFSA	lithium bis(fluorosulfonyl)imide
LiFSA	$LiN(SO_2F_2)_2$
MACC	magnesium aluminium chloride complex
MCMB	mesoporous carbon microbeads
MCFCs	the molten carbonate fuel cells
MD	molecular dynamics
$MEPYBF_4$	1-ethyl-1-methyl-pyrrolidinium
Mes_3B	tri(3, 5- dimethylphenyl)borane
$MgB_{12}H_{12}$	closo-borane magnesium dodecahydrododecaborate
NaTFSI	sodium bis(trifluoromethane) sulfonamide
NaFTFSI	sodium fluorosulfonyl (trifluoromethanesulfonyl)imide
NaFSI	sodium bis(fluoro-sulfonyl)imide
NaOTf	$NaSO_3CF_3$
NaTDI	sodium 4, 5-dicyano-2-(trifluoromethyl)imidazolate
NaPDI	sodium 4, 5-dicyano-2-(pentafluoroethyl)imidazolate
NaDFOB	sodium difluoro-(oxalato)borate
Na@HC	sodium inserted hard carbon
PACA	1-propylphosphonic acid cyclic anhydride
PAn	polyaniline
PPy	polypyrrole
PC	propylene carbonate
PS	1, 3-propylene sulfite
PEO	poly(ethylene oxide)
PVDF	poly(vinylidene fluoride)
PVDF-HFP	poly(vinylidene difluoride-co-hexafluoropropylene)
PMMA	poly(methyl methacrylate)
RFB	redox flow battery
PFPN	(ethoxy) pentafluorocyclotriphosphazene
$PYR_{14}TFSI$	N-butyl-N-methylpyrrolidinium bis(trifluoromethanesulfonyl) imide
PS	1, 3-propane sultone
PCS	1, 3-propanediol cyclic sulfate
PTSI	p-toluenesulfonylisocyanate
SA	succinic anhydride
$SBP\text{-}BF_4$	spiro-(1, 1')-bipyrolidinium tetrafluoroborate
SLMP	stabilized Li metal powder
SIBs	sodium-ion batteries
SRFC	solar rechargeable flow cell
$TEMABF_4$	triethylmethylammonium
$TEABF_4$	tetraethylammonium tetrafluoroborate
TFB	1, 3, 5-trifluorobenzene
$TMPYBF_4$	tetramethylenepyrrolidinium
TMP	trimethyl phosphite
TMSP	tris(trimethylsilyl) phosphite
TMS	tetramethylene sulfone
THF	tetrahydrofuran
TiC-CDC	titanium carbide derived carbon
VC	vinylene carbonate
ZEBRA	the Zero Emissions Batteries Research Activity

Notes and references

1 M. Z. Jacobson, *Energy Environ. Sci.*, 2009, **2**, 148.

2 M. He, F. Krzysztof, F. Elżbieta, N. Petr and J. B. Erik, *Energy Environ. Sci.*, 2016, **9**, 623.

3 Z. Yang, J. Zhang, M. C. W. Kintner-Meyer, X. Lu, D. Choi, J. P. Lemmon and J. Liu, *Chem. Rev.*, 2011, **111**, 3577.
4 M. M. Thackeray, C. Wolverton and E. D. Isaacs, *Energy Environ. Sci.*, 2012, **5**, 7854.
5 J. B. Goodenough and K.-S. Park, *J. Am. Chem. Soc.*, 2013, **135**, 1167.
6 T.-H. Kim, J.-S. Park, S. K. Chang, S. Choi, J. H. Ryu and H.-K. Song, *Adv. Energy Mater.*, 2012, **2**, 860.
7 J. B. Goodenough and Y. Kim, *Chem. Mater.*, 2010, **22**, 587.
8 K. Kubota and S. Komaba, *J. Electrochem. Soc.*, 2015, **162**, A2538.
9 R. C. Massé, E. Uchaker and G. Cao, *Sci. China Mater.*, 2015, **58**, 715.
10 K. Fic, L. Grzegorz, M. Mikolaj and F. Elzbieta, *Energy Environ. Sci.*, 2012, **5**, 5842.
11 C. J. Wook and D. Aurbach. *Nat. Rev. Mater.*, 2016, **1**, 16013.
12 Y. Orikasa, *Sci. Rep.*, 2014, **4**, 5622.
13 S. S. Zhang and C. A. Angell, *J. Electrochem. Soc.*, 1996, **143**, 4047.
14 G. ardar, A. E. S. Sleightholme, J. Naruse, H. Hiramatsu, D. J. Siegel and C. W. Monroe, *ACS Appl. Mat. & Interfaces*, 2014, **6**, 18033.
15 D. Monti, A. Ponrouch, M. R. Palacín and P. Johansson, *J. Power Sources*, 2016, **324**, 712.
16 P. G. Bruce, S. A. Freunberger, L. J. Hardwick and J.-M. Tarascon, *Nat. Mater*, 2012, **11**, 19.
17 A. C. Kozen, *ACS Nano*, 2015, **9**, 5884.
18 A. Balducci, B. Ugo, C. Stefano, M. Marina and S. Francesca, *Electrochem. Commun.*, 2004, **6**, 566.
19 D. Aurbach, *Electrochim. Acta*, 2004, **50**, 247.
20 V. Palomares, S. Paula, V. Irune, B. H. Karina, C.-G. Javier and R. Teófilo, *Energy Environ. Sci.*, 2012, **5**, 5884.
21 W. Li, J. R. Dahn, D. S. Wainwright, *Science*, 1994, **264**, 1115.
22 J.-Y. Luo, W.-J. Cui, P. He, Y.-Y. Xia, *Nature Chem.*, 2010, **2**, 760.
23 Z. Chang, C. Li, Y. Wang, B. Chen, L. Fu, Y. Zhu, L. Zhang, Y. Wu, W. Huang, *Sci. Rep.*, 2016, **6**, 28421.
24 X. Wang, Y. Hou, Y. Zhu, Y. Wu and R. Holze, *Sci. Rep.*, 2013, **3**, 1401.
25 Z. Chang, Y. Yang, X. Wang, M. Li, Z. Fu, Y. Wu and R. Holze, *Sci. Rep.*, 2015, **5**, 11931.
26 Y. Liu, Y. Qiao, X. Lou, X. Zhang, W. Zhang, Y. Huang, *ACS Appl. Mater. Interfaces*, 2016, **8**, 14564.
27 X. Wang, F. Wang, L. Wang, M. Li, Y. Wang, B. Chen, Y. Zhu, L. Fu, L. Zha, L. Zhang, Y. Wu, W. Huang, *Adv. Mater.*, 2016, **28**, 4904.
28 P. Leung, X. Li, C. Ponce de Leon, L. Berlouis, C. T. J. Low, F. C. Walsh, *RSC Adv.*, 2012, **2**, 10125.
29 P. Zhao, H. Zhang, H. Zhou, J. Chen, S. Gao, B. Yi, *J. Power Sources*, 2006, **162**, 1416.
30 S. Liao, X. Zong, B. Seger, T. Pedersen, T. Yao, C. Ding, J. Shi, J. Chen, C. Li, *Nat. Commun.*, 2016, **7**, 11474.
31 M. Wu, G. A. Snook, V. Gupta, M. Shaffer, D. J. Fray, G. Z. Chen, *J. Mater. Chem.*, 2005, **15**, 2297.
32 C. Peng, J. Jin, G. Z. Chen, *Electrochim. Acta*, 2007, **53**, 525.
33 C. Peng, S. Zhang, X. Zhou, G. Z. Chen, *Energy Environ. Sci.*, 2010, **3**, 1499.
34 G. Z. Chen, M. S. P. Shaffer, D. Coleby, G. Dixon, W. Zhou, D. J. Fray, *Adv. Mater.*, 2000, **12**, 522.
35 M. Hughes, G. Z. Chen, M. S. P. Shaffer, D. J. Fray, A. H. Windle, *Chem. Mater.*, 2002, **14**, 1610.
36 G. A. Snook, G. Z. Chen, D. J. Fray, M. Hughes, M. Shaffer, *J. Electroanal. Chem.*, 2004, **568**, 135.
37 X. Zhou, C. Peng, G. Z. Chen, *AIChE J.*, 2012, **58**, 974.
38 A. P. Malloy, S. W. Donne, *J. Power Sources*, 2008, **179**, 371.
39 Y. D. Qu, B. E. Conway, L. Bai, Y. H. Zhou, W. A. Adams, *J. Appl. Electrochem.*, 1993, **23**, 693.
40 A. Kozawa, T. Kalnoki-Kis, J. F. Yeager, *J. Electrochem. Soc.*, 1966, **113**, 405.
41 F. X. Wang, S. Y. Xiao, Y. S. Zhu, Z. Chang, C. L. Hu, Y. P. Wu and R. Holze, *J. Power Source*, 2014, **246**, 19.
42 R. T. Vinny, K. Chaitra, K. Venkatesh, N. Nagaraju and N. Kathyayini, *J. Power Source*, 2016, **309**, 212.
43 Q. Qu, L. Li, S. Tian, W. Guo, Y. Wu and R. Holze, *J. Power Source*, 2010, **195**, 2789.
44 X. Jin, W. Zhou, S. Zhang and G. Z. Chen, *Small*, 2007, **3**, 1513.
45 Y. U. Jeong, A. Manthiram, *J. Electrochem. Soc.*, 2002, **149**, A1419.
46 D. W. Kirt, J. W. Graydon, *ECS Trans.*, 2010, **25,** 163.
47 Y. Gao, Z. Qin, L. Guan, X. Wang And G. Z. Chen, *Chem. Commun.*, 2015, **51**, 10819.
48 B. Dunn, H. Kamath and J. M. Tarascon, *Science*, 2011, **334**, 928.
49 Y. Si and E. T. Samulski, *Nano Lett.*, 2008, **8**, 1679.
50 D. Li, M. B. Muller, S. Gilje, R. B. Kaner and G. G. Wallace, *Nat. Nanotechnol.*, 2008, **3**, 101.
51 A. Lewandowski, A. Olejniczak, M. Galinsk and I. Stepniak, *J. Power Sources*, 2010, **195**, 5814.
52 F. Beguin, V. Presser, A. Balducci and E. Frackowiak, *Adv. Mater.*, 2014, **26**, 2219.
53 C. Zhong, Y. Deng, W. Hu, J. Qiao, L. Zhang and J. Zhang, *Chem. Soc. Rev.*, 2015, **44**, 7484.
54 E. Iwama, P. L. Taberna, P. Azais, L. Brégeon, P. Simon, *J. Power Sources*, 2012, **219**, 235.
55 D. E. Jiang, Z. Jin, D. Henderson and J. Wu, *J. Phys. Chem. Lett.*, 2012, **3**, 1727.
56 P. Liu, M. Verbrugge, S. Soukiazian, *J. Power Sources*, 2006, **156**, 712.
57 M. S. Erik Brandon and William West, *NASA Tech. Briefs*, 2010, **34**, 21.
58 M. Ue, *J. Electrochem. Soc.*, 1994, **141**, 3336.
59 M. Ue, K. Ida and S. Mori, *J. Electrochem. Soc.*, 1994, **141**, 2989.
60 M. Ue, *Electrochim. Acta*, 1994, **39**, 2083.
61 M. Ue, M. Takeda, M. Takehara and S. Mori, *J. Electrochem. Soc.*, 1997, **144**, 2684.
62 S. Mori, K. Ida and M. Ue, *U. S. Patent*, 1990, 4892944.
63 M. Ue, *Electrochemistry*, 2007, **75**, 565.
64 M. Ue, M. Takehara, Y. Oura, A. Toriumi, M. Takeda and Denki Kagaku, *Electrochemistry*, 2001, **69**, 458.
65 M. Ue, M. Takehara, M. Takeda and Denki Kagaku, *Electrochemistry*, 1997, **65**, 969.
66 K. Chiba, *US Patent Office*, 2008, US 20060274475 A1.
67 P. Simon and Y. Gogotsi, *Nat. Mater.*, 2008, **7**, 845.
68 P. Kurzweil and M. Chwistek, *J. Power Sources*, 2008, **176**, 555.
69 A. R. Koh, B. Hwang, K. C. Roh and K. Kim, *Phys. Chem. Chem. Phys.*, 2014, **16**, 15146.
70 A. Ja¨nes, H. Kurig, T. Romann and E. Lust, *Electrochem. Commun.*, 2010, **12**, 535.
71 Y. Yokoyama, N. Shimosaka, H. Matsumoto, M. Yoshio and T. Ishiharaa, *Electrochem. Solid-State Lett.*, 2008, **11**, A72.
72 K. Xu, M. S. Ding and T. R. Jow, *J. Electrochem. Soc.*, 2001, **148**, A267.
73 H. Kurig, A. Janes and E. Lust, *J. Mater. Res.*, 2010, **25**, 1447.
74 A. Krause, A. Balducci, *Electrochem. Commun.*, 2011, **13**, 814.

75 S. Pohlmann and A. Balducci, *Electrochim. Acta*, 2013, **110**, 221.
76 X. Yu, D. Ruan, C. Wu, J. Wang and Z. Shi, *J. Power Sources*, 2014, **265**, 309.
77 C. Hu, W. Qu, R. Rajagopalan and C. Randall, *J. Power Sources*, 2014, **272**, 90.
78 K. Naoi, S. Ishimoto, J.-i. Miyamoto and W. Naoi, *Energy Environ. Sci.*, 2012, **5**, 9363.
79 L. He, J. Li, F. Gao, X. Wang, F. Ye and J. Yang, *Electrochemistry*, 2011, **79**, 934.
80 P. W. Ruch, D. Cericola, A. Foelske-Schmitz, R. Kötz and A. Wokaun, *Electrochim. Acta*, 2010, **55**, 4412.
81 S. Ishimoto, Y. Asakawa, M. Shinya and K. Naoi, *J. Electrochem. Soc.*, 2009, **156**, A563.
82 M. Hahn, A. Würsig, R. Gallay, P. Novák and R. Kötz, *Electrochem. Commun.*, 2005, **7**, 925.
83 K. Chiba, T. Ueda, Y. Yamaguchi, Y. Oki, F. Shimodate and K. Naoi, *J. Electrochem. Soc.*, 2011, **158**, A872.
84 K. Chiba, T. Ueda, Y. Yamaguchi, Y. Oki, F. Saiki and Naoi, K., *J. Electrochem. Soc.*, 2011, **158**, A1320.
85 R. Francke, D. Cericola, R. Kötz, D. Weingarth and S. R. Waldvogel, *Electrochim. Acta*, 2012, **62**, 372.
86 K. Suzuki, M. Shin-Ya, Y. Ono, T. Matsumoto, N. Nanbu, M. Takehara, M. Ue and Y. Sasaki, *Electrochemistry*, 2007, **75**, 611.
87 A. Brandt, P. Isken, A. Lex-Balducci and A. Balducci, *J. Power Sources*, 2012, **204**, 213.
88 K. Naoi, *Fuel Cells*, 2010, **10**, 825.
89 A. Du Pasquier, I. Plitz, S. Menocal, G. Amatucci, *J. Power Sources*, 2003, **115**, 171.
90 D. Cericola, P. Novák, A. Wokaun, R. Kötz, *J. Power Sources*, 2011, **196**, 10305.
91 A. Krause, P. Kossyrev, M. Oljaca, S. Passerini, M. Winter and A. Balducci, *J. Power Sources*, 2011, **196**, 8836.
92 S. Liu, S. Liu, K. Huang, J. Liu, Y. Li, D. Fang, H. Wang and Y. Xia. *J. Solid State Electrochem.*, 2011, **16**, 1631.
93 H. Li, L. Cheng and Y. Xia, *Electrochem. Solid-State Lett.*, 2005, **8**, A433.
94 H. Wu, C. V. Rao, B. Rambabu, *Mater. Chem. Phys.*, 2009, **116**, 532.
95 A. Brandt, A. Balducci, U. Rodehorst, S. Menne, M. Winter and A. Bhaskar, *J. Electrochem. Soc.*, 2014, **161**, A1139.
96 H. Wang, M. Yoshio, *Electrochem. Commun.*, 2006, **8**, 1481.
97 H. Wang, M. Yoshio, A. K. Thapa, H. Nakamura, *J. Power Sources*, 2007, **169**, 375.
98 H. Wang, M. Yoshio, *Electrochem. Commun.*, 2008, **10**, 382.
99 Y. Wang, C. Zheng, L. Qi, M. Yoshio, K. Yoshizuka, H. Wang, *J. Power Sources*, 2011, **196**, 10507.
100 J. Gao, S. Tian, L. Qi, H. Wang, *Electrochim. Acta*, 2015, **176**, 22.
101 J. Gao, S. Tian, L. Qi, M. Yoshio and H. Wang, *J. Power Sources*, 2015, **297**, 121.
102 J. Gao, M. Yoshio, L. Qi, H. Wang, *J. Power Sources*, 2015, **278**, 452.
103 H. Wang, M. Yoshio, *J. Power Sources*, 2008, **177**, 681.
104 T. Aida, K. Yamada and M. Morita, *Electrochem. Solid-State Lett.* 2006, **9**, A534.
105 W. J. Cao and J. P. Zheng, *J. Power Sources* 2012, **213,** 180.
106 N. Ogihara, Y. Igarashi, A. Kamakura, K. Naoi, Y. Kusachi and K. Utsugi, *Electrochim. Acta*, 2006, **52**, 1713.
107 S. R. Sivakkumar, J. Y. Nerkar and A. G. Pandolfo, *Electrochim. Acta*, 2010, **55**, 3330.
108 S. R. Sivakkumar and A. G. Pandolfo, *Electrochim. Acta*, 2012, **65**, 280.
109 S. R. Sivakkumar, A. S. Milev and A. G. Pandolfo , *Electrochim. Acta*, 2011, **56**, 9700.
110 V. Khomenko, E. Raymundo-Piñero and F. Béguin, *J. Power Sources*, 2008, **177**, 643.
111 M. Schroeder, M. Winter, S. Passerini, A. Balducci, *J. Electrochem. Soc.*, 2012, **159**, A1240.
112 T. Aida, I. Murayama, K. Yamada and M. Morita, *Electrochem. Solid-State Lett.*, 2007, **10**, A93.
113 T. Aida, I. Murayama, K. Yamada and M. Morita, *J. Electrochem. Soc.*, 2007, **154**, A798.
114 W. J. Cao and J. P. Zheng, *J. Electrochem. Soc.*, 2013, **160**, A1572.
115 H. Wang, M. Yoshio, *J. Power Sources*, 2012, **200**, 108.
116 P. H. Smith, T. N. Tran, T. L. Jiang and J. Chung, *J. Power Sources*, 2013, **243**, 982.
117 A. Jänes, J. Eskusson, T. Thomberg and E. Lust, *J. Electrochem. Soc.*, 2014, **161**, A1284.
118 J. Eskusson, A. Jänes, T. Thomberg and E. Lust, *ECS Trans.*, 2015, **64**, 21.
119 J. C. Burns, A. Kassam, N. N. Sinha, L. E. Downie, L. Solnickova, B. M. Way and J.R. Dahn, *J. Electrochem Soc.*, 2013, **160**, A1451.
120 G. H. Wrodnigg, T. M. Wrodnigg, J. O. Besenhard and M. Winter, *Electrochem. Commun.*, 1999, **1**, 148.
121 H. W. Jung, L. Hamenu, H. S. Lee, M. Latifatu, K. M. Kim and J. M. Ko, *Curr. Appl. Phys.*, 2015, **15**, 567.
122 C. H. Lee, F. Xu and C. Jung, *Electrochim. Acta*, 2014, **131**, 240.
123 W. Qu, E. Dorjpalam, R. Rajagopalan and C. A. Randall, *ChemSusChem*, 2014, **7**, 1162.
124 D. Aurbach, *J. Power Sources*, 2000, **89**, 206-218.
125 P. G. Balakrishnan, R. Ramesh and T. Prem Kumar, *J. Power Sources*, 2006, **155**, 401.
126 V. Etacheri, R. Marom, R. Elazari, G. Salitra and D. Aurbach, *Energy Environ. Sci.*, 2011, **4**, 3243.
127 K. Xu, *Chem. Rev.*, 2014, **114**, 11503.
128 K. Xu, *Chem. Rev.*, 2004, **104**, 4303.
129 E. M. Erickson, E. Markevich, G. Salitra, D. Sharon, D. Hirshberg, E. de la Llave, I. Shterenberg, A. Rozenman, A. Frimer and D. Aurbach, *J. Electrochem. Soc.,* 2015, **162**, A2424.
130 D. Guyomard and J. M. Tarascon, *J. Electrochem. Soc.*, 1992, **139**, 937.
131 J. M. Tarascon, D. Guyomard and G. L. Baker, *J. Power Sources*, 1993, **43-44**, 689.
132 D. Guyomard and J. M. Tarascon, *J. Power Sources*, 1995, **54**, 92.
133 J. M. Tarascon and D. Guyomard, *Electrochim. Acta*, 1993, **38**, 1221.
134 J. O. Besenhard, M. Winter, J. Yang and W. Biberacher, *J. Power Sources*, 1995, **54**, 228.
135 A. M. Andersson, D. P. Abraham, R. Haasch, S. MacLaren, J. Liu and K. Amine, *J. Electrochem. Soc.*, 2002, **149**, A1358.
136 D. Aurbach, B. Markovsky, A. Shechter, Y. Ein-Eli and H. Cohen, *J. Electrochem. Soc.*, 1996, **143**, 3809.
137 D. Aurbach, Y. Talyosef, B. Markovsky, E. Markevich, E. Zinigrad, L. Asraf, J. S. Gnanaraj, H. J. Kim, *Electrochim. Acta*, 2004, **50**, 247.
138 B. Markovsky, F. Amalraj, H. E. Gottlieb, Y. Gofer, S. K. Martha and D. Aurbach, *J. Electrochem. Soc.*, 2010, **157**, A423.
139 E. Sloop, J. K. Pugh, S. Wang, J. B. Kerr, K. Kinoshita, *Electrochem Solid State Lett.*, 2001, **4**, 42.

140 D. Aurbach, K. Gamolsky, B. Markovsky, G. Salitra and Y. Gofer, *J. Electrochem. Soc.*, 2000, **147**, 1322.

141 J. Foropoulos and D. D. DesMarteau, *Inorg. Chem.*, 1984, **23**, 3720.

142 L. Péter and J. Arai, J. Appl. *Electrochem.*, 1999, **29**, 1053.

143 L. A. Dominey, V. R. Koch and T. J. Blakley, *Electrochim. Acta*, 1992, **37**, 1551.

144 M. Ue, A. Murakami and S. Nakamura, *J. Electrochem. Soc.*, 2002, **149**, A1572.

145 K. Kanamura, W. Hoshikawa and T. Umegaki, *J. Electrochem. Soc.*, 2002, **149**, 339.

146 A. M. Haregewoin, A. S. Wotango and B. J. Hwang, *Energy Environ. Sci.*, 2016, **9**, 1955.

147 M. Hu, X. Pang and Z. Zhou, *J. Power Sources*, 2013, **237**, 229.

148 W. Liu, *Angew. Chem. Int. Ed. Engl.*, 2015, **54**, 4440.

149 S. Hy, H. Liu, M. Zhang, D. Qian, B.-J. Hwang, Y. S. Meng, *Energy Environ. Sci.*, 2016, **9**, 1931.

150 A., Vanchiappan, J. Gnanaraj, S. Madhavi and H.-K. Liu. *Chem. Eur. J.*, 2011, **17**, 14326.

151 M. Xu, S. Dalavi and B. L. Lucht, Electrolytes for Lithium-Ion Batteries with High-Voltage Cathodes [B]. *Lithium Batteries: Advanced Technologies and Applications,* 2013, 71.

152 L. Yang, B. Ravdel and B. L. Lucht, *Electrochem. Solid-State Lett.*, 2010, **13**, A95.

153 L. Xing, W. Li, C. Wang, F. Gu, M. Xu, C. Tan, J. Yi, *J. Phys. Chem. B*, 2009, **113**, 16596.

154 J.-H. Kim, N. P. W. Pieczonka, Z. Li, Y. Wu, S. Harris and B. R. Powell, *Electrochim. Acta*, 2013, **90**, 556.

155 N. P. W. Pieczonka, Z. Liu, P. Lu, K. L. Olson, J. Moote, B. R. Powell and J.-H. Kim, *J. Phys. Chem. C*, 2013, **117**, 15947.

156 S. Dalavi, M. Xu, B. Knight and B. L. Lucht, *Electrochem. Solid-State Lett.*, 2011, **15**, A28.

157 L. Yang, T. Markmaitree and B. L. Lucht, *J. Power Sources*, 2011, **196**, 2251.

158 S.-Y. Ha, J.-G. Han, Y.-M. Song, M.-J. Chun, S.-I. Han, W.-C. Shin and N.-S. Choi, *Electrochim. Acta*, 2013, **104**, 170.

159 M. Hu, J. Wei, L. Xing and Z. Zhou, *J. Appl. Electrochem.*, 2012, **42**, 291.

160 Z. D. Li, Y. C. Zhang, H. F. Xiang, X. H. Ma, Q. F. Yuan, Q. S. Wang and C. H. Chen, *J. Power Sources,* 2013, **240**, 471.

161 A. von Cresce and K. Xu, *J. Electrochem. Soc.*, 2011, **158**, A337.

162 A. Von Cresce and K. Xu, *ECS Trans.*, 2012, **41**, 17.

163 H. Rong, M. Xu, L. Xing and W. Li, *J. Power Sources*, 2014, **261**, 148.

164 Y.-M. Song, J.-G. Han, S. Park, K. T. Lee and N.-S. Choi, *J. Mater. Chem. A*, 2014, **2**, 9506.

165 G. Yan, X. Li, Z. Wang, H. Guo and C. Wang, *J. Power Sources*, 2014, **248**, 1306.

166 J. Zhang, J. Wang, J. Yang and Y. NuLi, *Electrochim. Acta*, 2014, **117**, 99.

167 L. Xia, Y. Xia and Z. Liu, *J. Power Sources*, 2015, **278**, 190.

168 G. Yan, X. Li, Z. Wang, H. Guo and X. Xiong, *J. Power Sources*, 2014, **263,** 231.

169 H. Lee, S. Choi, S. Choi, H.-J. Kim, Y. Choi, S. Yoon, J.-J. Cho, *Electrochem. Commun.*, 2007, **9**, 801.

170 F. Felix, J.-H. Cheng, S. Hy, J. Rick, F. M. Wang and B.-J. Hwang, *J. Phys. Chem. C*, 2013, 22619.

171 V. Tarnopolskiy, J. Kalhoff, M. Nádherná, D. Bresser, L. Picard, F. Fabre, M. Rey and S. Passerini, *J. Power Sources*, 2013, **236**, 39.

172 H. Bouayad, Z. Wang, N. Dupré, R. Dedryvère, D. Foix, S. Franger, J.-F. Martin, L. Boutafa, S. Patoux, D. Gonbeau and D. Guyomard, *J. Phys. Chem. C*, 2014, **118**, 4634.

173 N. P. W. Pieczonka, L. Yang, M. P. Balogh, B. R. Powell, K. R. Chemelewski, A. Manthiram, S. A. Krachkovskiy, G. R. Goward, M. Liu and J.-H. Kim, J. Phys. Chem. C, 2013, **117**, 22603.

174 K. Xu, S. Zhang and T. R. Jow, *Electrochem. Solid-State Lett.*, 2003, **6**, A117.

175 Q. Wu, W. Lu, M. Miranda, T. K. Honaker-Schroeder, K. Y. Lakhsassi and D. Dees, *Electrochem. Commun.*, 2012, **24**, 78.

176 M. Xu, L. Zhou, Y. Dong, Y. Chen, J. Demeaux, A. D. MacIntosh, A. Garsuch and B. L. Lucht, *Energy Environ. Sci.*, 2016, **9**, 1308.

177 E. Nanini-Maury, J. Światowska, A. Chagnes, S. Zanna, P. Tran-Van, P. Marcus and M. Cassir, *Electrochim. Acta*, 2014, **115**, 223.

178 M. Nagahama, N. Hasegawa and S. Okada, *J. Electrochem. Soc.*, 2010, **157**, A748.

179 L. Kavan, *Chem. Rev.*, 1997, **97**, 3061.

180 Y. Abu-Lebdeh and I. Davidson, *J. Electrochem. Soc.*, 2009, **156**, A60.

181 Y. Abu-Lebdeh and I. Davidson, *J. Power Sources*, 2009, **189**, 576.

182 A. J. Gmitter, I. Plitz and G. G. Amatucci, *J. Electrochem. Soc.*, 2012, **159**, A370.

183 K. Xu and C. A. Angell, *J. Electrochem. Soc.*, 1998, **145**, L70.

184 X.-G. Sun, C. Austen Angell, *Solid State Ionics*, 2004, **175**, 257.

185 X.-G. Sun, C. A. Angell, Electrochem. Commun., 2005, **7**, 261.

186 X. Sun and C. A. Angell, *Meeting Abstracts,* 2008, **MA2008-01**, 1417.

187 Y. Watanabe, S.-i. Kinoshita, S. Wada, K. Hoshino, H. Morimoto and S.-i. Tobishima, *J. Power Sources*, 2008, **179**, 770.

188 X. Sun and C. A. Angell, *Electrochem. Commun.*, 2009, **11**, 1418.

189 L. Mao, B. Li, X. Cui, Y. Zhao, X. Xu, X. Shi, S. Li and F. Li, *Electrochim. Acta*, 2012, **79**, 197.

190 C. Li, Y. Zhao, H. Zhang, J. Liu, J. Jing, X. Cui and S. Li, *Electrochim. Acta*, 2013, **104**, 134.

191 F. Wu, J. Xiang, L. Li, J. Chen, G. Tan and R. Chen, *J. Power Sources*, 2012, **202**, 322.

192 F. Wu, Q. Zhu, L. Li, R. Chen and S. Chen, *J. Mater. Chem. A*, 2013, **1**, 3659-3666.

193 A. Abouimrane, I. Belharouak and K. Amine, *Electrochem. Commun.*, 2009, **11**, 1073.

194 L. Xing, J. Vatamanu, O. Borodin, G. D. Smith and D. Bedrov, *J. Phys. Chem. C*, 2012, **116**, 23871.

195 T. Kitagawa, K. Azuma, M. Koh, A. Yamauchi, M. Kagawa, H. Sakata, H. Miyawaki, A. Nakazono, H. Arima and M. Yamagata, *Electrochemistry*, 2010, **78**, 345.

196 L. Hu, Z. Zhang, K. Amine, *Electrochem. Commun.*, 2013, **35**, 76.

197 Z. Zhang, L. Hu, H. Wu, W. Weng, M. Koh, P. C. Redfern, L. A. Curtiss and K. Amine, *Energy Environ. Sci.*, 2013, **6**, 1806.

198 L. Xia, Y. Xia, C. Wang, H. Hu, S. Lee, Q. Yu, H. Chen and Z. Liu, *ChemElectroChem*, 2015, **2**, 1707.

199 M. Ue, K. Ida and S. Mori, *J. Electrochem. Soc.*, 1994, **141**, 2989.

200 X. Zhang, R.-S. Kühnel, S. Passerini and A. Balducci, *J. Solution Chem.,* 2015, **44**, 528.

201 N. Shao, X.-G. Sun, S. Dai and D.-e. Jiang, *J. Phys. Chem. B*, 2011, **115**, 12120.

202 N. Shao, X.-G. Sun, S. Dai and D.-e. Jiang, *J. Phys. Chem. B*, 2012, **116**, 3235.

203 D. Kobayashi, M. Takehara, N. Nanbu, M. Ue and Y. Sasaki, *Meeting Abstracts*, 2008, **MA2008-02**,166.

204 Y. Sasaki, H. Satake, N. Tsukimori, N. Nanbu, M. Takehara and M. Ue, *Electrochemistry*, 2010, **78**, 467.

205 E. Markevich, G. Salitra, K. Fridman, R. Sharabi, G. Gershinsky, A. Garsuch, G. Semrau, M. A. Schmidt and D. Aurbach, *Langmuir*, 2014, **30**, 7414.

206 Y. Yamada, A. Yamada, *J. Electrochem. Soc.*, 2015, **162**, A2406.

207 Y. Yamada, K. Furukawa, K. Sodeyama, K. Kikuchi, M. Yaegashi, Y. Tateyama, A. Yamada, *J. Am. Chem. Soc.*, 2014, **136**, 5039.

208 S.-K. Jeong, H.-Y. Seo, D.-H. Kim, H.-K. Han, J.-G. Kim, Y. B. Lee, Y. Iriyama, T. Abe, Z. Ogumi, *Electrochem. Commun.*, 2008, **10**, 635.

209 L. Suo, Y.-S. Hu, H. Li, M. Armand, L. Chen, *Nat. Commun.*, 2013, **4**, 1481.

210 J. Qian, W. A. Henderson, W. Xu, P. Bhattacharya, M. Engelhard, O. Borodin, J. G. Zhang, *Nat. Commun.*, 2015, **6**, 6362.

211 Q. Ma, Z. Fang, P. Liu, J. Ma, X. Qi, W. Feng, J. Nie, Y.-S. Hu, H. Li, X. Huang, L. Chen and Z. Zhou, *ChemElectroChem*, 2016, **3**, 531.

212 J. O. Besenhard, *Carbon*, 1976, **14**, 111.

213 G. Nagasubramanian, *J. Power Sources*, 2003, **119–121**, 811.

214 M. Arakawa and J. Yamaki, *J. Electroanal. Chem.*, 1987, **219**, 273.

215 T. Abe, N. Kawabata, Y. Mizutani, M. Inaba and Z. Ogumi, *J. Electrochem. Soc.*, 2003, **150**, A257.

216 M. Nie, D. P. Abraham, D. M. Seo, Y. Chen, A. Bose and B. L. Lucht, *J. Phys. Chem. C*, 2013, **117**, 25381.

217 Y. Yamada, Y. Takazawa, K. Miyazaki and T. Abe, *J. Phys. Chem. C*, 2010, **114**, 11680.

218 Y. Yamada, M. Yaegashi, T. Abe, A. Yamada, *Chem. Commun.*, 2013, **49**, 11194.

219 Y. Yamada, K. Usui, C. H. Chiang, K. Kikuchi, K. Furukawa and A. Yamada, *ACS Appl. Mater. Interfaces*, 2014, **6**, 10892.

220 K. Sodeyama, Y. Yamada, K. Aikawa, A. Yamada, Y. Tateyama, *J. Phys. Chem. C*, 2014, **118**, 14091.

221 T. Doi, R. Masuhara, M. Hashinokuchi, Y. Shimizu, M. Inaba, *Electrochim. Acta*, 2016, **209**, 219.

222 J. Wang, Y. Yamada, K. Sodeyama, C. H. Chiang, Y. Tateyama and A. Yamada, *Nat. Commun.*, 2016, **7**, 12032.

223 K. Matsumoto, K. Inoue, K. Nakahara, R. Yuge, T. Noguchi and K. Utsugi, *J. Power Sources*, 2013, **231**, 234.

224 D. W. McOwen, D. M. Seo, O. Borodin, J. Vatamanu, P. D. Boyle and W. A. Henderson, *Energy Environ. Sci.*, 2014, **7**, 416.

225 Y. Yamada, C. H. Chiang, K. Sodeyama, J. Wang, Y. Tateyama, A. Yamada, *ChemElectroChem*, 2015, **2**, 1687.

226 K. Dokko, N. Tachikawa, K. Yamauchi, M. Tsuchiya, A. Yamazaki, E. Takashima, J.-W. Park, K. Ueno, S. Seki, N. Serizawa and M. Watanabe, *J. Electrochem. Soc.*, 2013, **160**, A1304.

227 K. Yoshida, M. Nakamura, Y. Kazue, N. Tachikawa, S. Tsuzuki, S. Seki, K. Dokko and M. Watanabe, *J. Am. Chem. Soc.*, 2011, **133**, 13121.

228 J.-W. Park, K. Yamauchi, E. Takashima, N. Tachikawa, K. Ueno, K. Dokko, M. Watanabe, *J. Phys. Chem. C*, 2013, **117**, 4431.

229 C. Zhang, A. Yamazaki, J. Murai, J.-W. Park, T. Mandai, K. Ueno, K. Dokko and M. Watanabe, *J. Phys. Chem. C*, 2014, **118**, 17362.

230 H. Moon, R. Tatara, T. Mandai, K. Ueno, K. Yoshida, N. Tachikawa, T. Yasuda, K. Dokko, M. Watanabe, *J. Phys. Chem. C*, 2014, **118**, 20246.

231 K. Ueno, K. Yoshida, M. Tsuchiya, N. Tachikawa, K. Dokko, M. Watanabe, *J. Phys. Chem. B*, 2012, **116**, 11323.

232 K. Ueno, J. Murai, K. Ikeda, S. Tsuzuki, M. Tsuchiya, R. Tatara, T. Mandai, Y. Umebayashi, K. Dokko and M. Watanabe, *J. Phys. Chem. C*, 2015, **120**, 15792.

233 W. H. Meyer, *Adv. Mater.*, 1998, **10**, 439.

234 Y. Zhu, S. Xiao, Y. Shi, Y. Yang, Y. Hou and Y. Wu, *Adv. Energy Mater.*, 2014, **4**, 1300647.

235 P. Zhang, L. C. Yang, L. L. Li, M. L. Ding, Y. P. Wu and R. Holzeb, *J. Membr. Sci.*, 2011, **379**, 80.

236 D. Zhou, L.-Z. Fan, H. Fan and Q. Shi, *Electrochim. Acta*, 2013, **89**, 334.

237 B. Scrosati, *Chem. Rec.*, 2001, **1**, 173.

238 R. Khurana, J. L. Schaefer, L. A. Archer and G. W. Coates, *J. Am. Chem. Soc.*, 2014, **136**, 7395.

239 H. J. Ha, E. H. Kil, Y. H. Kwon, J. Y. Kim, C. K. Lee and S. Y. Lee, *Energy Environ. Sci.*, 2012, **5**, 6491.

240 C. Liao, X. G. Sun, S. Dai, *Electrochim. Acta*, 2013, **87**, 889.

241 Y. S. Zhu, F. X. Wang, L. L. Liu, S. Y. Xiao, Z. Chang and Y. P. Wu, *Energy Environ. Sci.*, 2013, **6**, 618.

242 H. C. Gao, B. K. Guo, J. Song, K. Park, and J. B. Goodenough, *Adv. Energy Mater.*, 2015, **5**, 1402235.

243 Y. Zhu, F. Wang, L. Liu, S. Xiao, Y. Yang and Y. Wu, *Sci. Rep.*, 2013, **3**, 3187.

244 R. S. Carmichael, Practical Handbook of Physical Properties of Rocks and Minerals, *CRC Press: Boca Raton, FL*, 1989.

245 L. Wang, Y. Lu, J. Liu, M. Xu, J. Cheng, D. Zhang and J. B. Goodenough, *Angew. Chem. Int. Ed.*, 2013, **52**, 1964.

246 N. Yabuuchi, K. Kubota, M. Dahbi and S. Komaba, *Chem. Rev.*, 2014, **114**, 11636.

247 Y. Kim, K. H. Ha, S. M. Oh and K. T. Lee, *Chem. Eur. J.*, 2014, **20**, 11980.

248 S. Y. Hong, Y. Kim, Y. Park, A. Choi, N.-S. Choi and K. T. Lee, *Energy Environ. Sci.*, 2013, **6**, 2067.

249 Z. Li, D. Young, K. Xiang, W. C. Carter and Y.-M. Chiang, *Adv. Energy Mater.*, 2013, **3**, 290.

250 W. Wu, A. Mohamed and J. F. Whitacre, *J. Electrochem. Soc.*, 2013, **160**, A497.

251 A. Ponrouch, D. Monti, A. Boschin, B. Steen, P. Johansson and M. R. Palacín, *J. Mater. Chem. A*, 2015, **3**, 22.

252 D. Monti, E. Jónsson, M. R. Palacín, P. Johansson, *J. Power Sources*, 2014, **245**, 630.

253 N. Wongittharom, T.-C. Lee, C.-H. Wang, Y.-C. Wang, J.-K. Chang, *J. Mater. Chem. A*, 2014, **2**, 5655.

254 T. Hosokawa, K. Matsumoto, T. Nohira, R. Hagiwara, A. Fukunaga, S. Sakai, K. Nitta, *J. Phys. Chem. C*, 2016, **120**, 9628.

255 K. Vignarooban, R. Kushagra, A. Elango, P. Badami, B. E. Mellander, X. Xu, T. G. Tucker, C. Nam and A. M. Kannan, *Int. J. Hydrogen Energy*, 2016, **41**, 2829.

256 Y. Sasaki, M. Hosoya and M. Handa. *J. Power Sources*, 1997, **68**, 492.

257 M. Guignard, C. Didier, J. Darriet, P. Bordet, E. Elkaïm, C. Delmas, *Nat. Mater.*, 2013, **12**, 74.

258 Y. Kim, Y. Park, A. Choi, N.-S. Choi, J. Kim, J. Lee, J. H. Ryu, S. M. Oh and K. T. Lee, *Adv. Mater.*, 2013, **25**, 3045.

259 C.-Y. Yu, J.-S. Park, H.-G. Jung, K.-Y. Chung, D. Aurbach, Y.-K. Sun and S.-T. Myung, *Energy Environ. Sci.*, 2015, **8**, 2019.

260 R. Alcantara, P. Lavela, G. F. Ortiz, J. L. Tirado, *Electrochem. Solid-State Lett.*, 2005, **8**, A222.

261 A. Ponrouch, E. Marchante, M. Courty, J.-M. Tarascon, M. R. Palacín, *Energy Environ. Sci.*, 2012, **5**, 8572.

262 S. Komaba, W. Murata, T. Ishikawa, N. Yabuuchi, T. Ozeki, T. Nakayama, A. Ogata, K. Gotoh and K. Fujiwara, *Adv. Funct. Mater.*, 2011, **21**, 3859.

263 J. Y. Jang, H. Kim, Y. Lee, K. T. Lee, K. Kang, N.-S. Choi, *Electrochem. Commun.*, 2014, **44**, 74.

264 A. Ponrouch, R. Dedryvère, D. Monti, A. E. Demet, J. M. Ateba Mba, L. Croguennec, C. Masquelier, P. Johansson, M. R. Palacín, *Energy Environ. Sci.*, 2013, **6**, 2361.

265 D. I. Iermakova, R. Dugas, M. R. Palacín, A. Ponrouch, *J. Electrochem. Soc.*, 2015, **162**, A7060.

266 A. Plewa-Marczewska, T. Trzeciak, A. Bitner, L. Niedzicki, M. Dranka, G. Z. Żukowska, M. Marcinek, W. Wieczorek, *Chem. Mater.*, 2014, **26**, 4908.

267 C. Ge, L. Wang, L. Xue, Z.-S. Wu, H. Li, Z. Gong, X.-D. Zhang, *J. Power Sources*, 2014, **248**, 77.

268 A. Bhide, J. Hofmann, A. K. Durr, J. Janek and P. Adelhelm, *Phys Chem Chem Phys*, 2014, **16**, 1987.

269 X. Xia, W. M. Lamanna and J. R. Dahn, *J. Electrochem. Soc.*, 2013, **160**, A607.

270 G. G. Eshetu, S. Grugeon, H. Kim, S. Jeong, L. Wu, G. Gachot, S. Laruelle, M. Armand and S. Passerini, *ChemSusChem*, 2016, **9**, 462.

271 J. Chen, Z. Huang, C. Wang, S. Porter, B. Wang, W. Lie, H. K. Liu, *Chem. Commun.*, 2015, **51**, 9809.

272 S. M. Oh, S. T. Myung, C. S. Yoon, J. Lu, J. Hassoun, B. Scrosati, K. Amine, Y. K. Sun, *Nano Lett.*, 2014, **14**, 1620.

273 Z. Zeng, X. Jiang, R. Li, D. Yuan, X. Ai, H. Yang and Y. Cao, *Adv. Sci.*, 2016, http://dx.doi.org/10.1002/advs.201600066.

274 D. A. Stevens and J. R. Dahn, *J. Electrochem. Soc.*, 2000, **147**, 1271.

275 X. Xia, M. N. Obrovac and J. R. Dahn, Electrochem. *Solid-State Lett.*, 2011, **14**, A130.

276 S. S., Zhang, *J. Power Sources*, 2006, **162**, 1379.

277 S. Yoon, H. Kim, J.-J. Cho, Y.-K. Han and H. Lee, *J. Power Sources*, 2013, **244**, 711.

278 V. Etacheri, O. Haik, Y. Goffer, G. A. Roberts, I. C. Stefan, R. Fasching and D. Aurbach, *Langmuir*, 2011, **28**, 965.

279 L. Xia, Y. Xia, Z. Liu, *Electrochim. Acta*, 2015, **151**, 429.

280 S. Komaba, T. Ishikawa, N. Yabuuchi, W. Murata, A. Ito and Y. Ohsawa, *ACS Appl. Mater. Interfaces*, 2011, **3**, 4165.

281 A. Ponrouch, A. R. Goñi and M. R. Palacín, *Electrochem. Commun.*, 2013, **27,** 85.

282 J. Qian, Y. Chen, L. Wu, Y. Cao, X. Ai and H. Yang, *Chem. Commun.*,2012, **48**, 7070.

283 H. Lu, L. Wu, L. Xiao, X. Ai, H. Yang and Y. Cao, *Electrochim. Acta*, 2016, **190**, 402.

284 J. Qian, X. Wu, Y. Cao, X. Ai, H. Yang, *Angew. Chem. Int. Ed. Engl.*, 2013, **52**, 4633.

285 Y. Kim, Y. Kim, A. Choi, S. Woo, D. Mok, N.-S. Choi, Y. S. Jung, J. H. Ryu, S. M. Oh and K. T. Lee, *Adv. Mater.*, 2014, **26**, 4139.

286 S. A. Webb, L. Baggetto, C. A. Bridges and G. M. Veith, *J. Power Sources*, 2014, **248**, 1105.

287 J. Feng, Y. An, L. Ci, S. Xiong, *J. Mater. Chem. A*, 2015, **3**, 14539.

288 Y. Q. Yang, Z. Chang, M. X. Li, X. W. Wang and Y. P. Wu, *Solid State Ionics*, 2015, **269**, 1–7.

289 W. D. Zhou, H. C. Gao and J. B. Goodenough, *Adv. Energy Mater.*, 2016, **6**, 1501802.

290 H. Gao, W. Zhou, K. Park and J. B. Goodenough, *Adv. Energy Mater.*, 2016, **6**, 160047.

291 J. Muldoon, C. B. Bucur, T. Gregory, *Chem. Rev.*, 2014, **114**, 11683.

292 H. D. Yoo, I. Shterenberg, Y. Gofer, G. Gershinsky, N. Pour and D. Aurbach, Energy Environ. Sci., 2013, **6**, 2265.

293 D. Aurbach, I. Weissman, Y. Gofer, E. Levi, *The Chemical Record*, 2003, **3**, 61.

294 D. Aurbach, Y. Gofer, Z. Lu, A. Schechter, O. Chusid, H. Gizbar, Y. Cohen, V. Ashkenazi, M. Moshkovich, R. Turgeman and E. Levi, *J. Power Sources*, 2001, **97–98**, 28.

295 D. Aurbach, Y. Gofer, A. Schechter, O. Chusid, H. Gizbar, Y. Cohen, M. Moshkovich, R. Turgeman, *J. Power Sources*, 2001, **97–98**, 269.

296 J. Muldoon, C. B. Bucur, A. G. Oliver, T. Sugimoto, M. Matsui, H. S. Kim, G. D. Allred, J. Zajicek, Y. Kotani, *Energy Environ. Sci.*, 2012, **5**, 5941.

297 T. D. Gregory, R. J. Hoffman and R. C. Winterton, *J. Electrochem. Soc.*, 1990, **137**, 775.

298 Z. Lu, A. Schechter, M. Moshkovich, D. Aurbach, *J. Electroanal. Chem.*, 1999, **466**, 203.

299 D. Aurbach, Y. Gofer, Z. Lu, A. Schechter, O. Chusid, H. Gizbar, Y. Cohen, V. Ashkenazi, M. Moshkovich, R. Turgeman and E. Levi. *J. Power Sources*, 2001, **97–98**, 28.

300 L. P. Lossius and F. Emmenegger, *Electrochim. Acta*, 1996, **41**, 445.

301 Y. Gofer, R. Turgeman, H. Cohen and D. Aurbach, *Langmuir*, 2003, **19**, 2344.

302 L. W. Gaddum and H. E. French, *J. Am. Chem. Soc.*, 1927, **49**, 1295.

303 Y. S. Guo, F. Zhang, J. Yang and F. F. Wang, *Electrochem. Commun.*, 2012, **18**, 24.

304 Y. Vestfried, O. Chusid, Y. Goffer, P. Aped and D. Aurbach, *Organometallics*, 2007, **26**, 3130.

305 H. Gizbar, Y. Vestfrid, O. Chusid, Y. Gofer, H. E. Gottlieb, V. Marks and D. Aurbach, *Organometallics*, 2004, **23**, 3826.

306 F.-F. Wang, Y.-S. Guo, J. Yang, Y. Nuli, S.-i. Hirano, *Chem. Commun.*, 2012, **48**, 10763.

307 D. Aurbach, Z. Lu, A. Schechter, Y. Gofer, H. Gizbar, R. Turgeman, Y. Cohen, M. Moshkovich and E. Levi, *Nature*, 2000, **407**, 724.

308 O. Mizrahi, N. Amir, E. Pollak, O. Chusid, V. Marks, H. Gottlieb, L. Larush, E. Zinigrad and D. Aurbach, *J. Electrochem. Soc.*, 2008, **155**, A103.

309 D. Aurbach, H. Gizbar, A. Schechter, O. Chusid, H. E. Gottlieb, Y. Gofer and I. Goldberg, *J. Electrochem. Soc.*, 2002, **149**, A115.

310 Y. Gofer, O. Chusid, H. Gizbar, Y. Viestfrid, H. E. Gottlieb, V. Marks and D. Aurbach, *Electrochem. Solid-State Lett.*, 2006, **9**, A257.

311 D. Aurbach, G. S. Suresh, E. Levi, A. Mitelman, O. Mizrahi, O. Chusid and M. Brunelli, *Adv. Mater.*, 2007, **19**, 4260.

312 H. S. Kim, T. S. Arthur, G. D. Allred, J. Zajicek, J. G. Newman, A. E. Rodnyansky, A. G. Oliver, W. C. Boggess and J. Muldoon, *Nat. Commun.*, 2011, **2**, 427.

313 Y.-S. Guo, F. Zhang, J. Yang, F.-F. Wang, Y. NuLi, S.-I. Hirano, *Energy Environ. Sci.*, 2012, **5**, 9100.

314 S. Yagi, A. Tanaka, Y. Ichikawa, T. Ichitsubo and E. Matsubara, *J. Electrochem. Soc.,* 2013, **160**, C83.

315 R. Mohtadi, M. Matsui, T. S. Arthur, S. J. Hwang, *Angew. Chem. Int. Ed. Engl.*, 2012, **51**, 9780.

316 T. J. Carter, *Angew. Chem. Int. Ed.*, 2014, **53**, 3173.

317 O. Tutusaus, *Angew. Chem. Int. Ed.*, 2015, **54**, 7900.

318 C. Liu, Z. Yu, D. Neff, A. Zhamu, B. Z. Jang, *Nano Lett.*, 2010, **10**, 4863.

319 S. Makino, Y. Shinohara, T. Ban, W. Shimizu, K. Takahashi, N. Imanishi, W. Sugimoto, *Rsc Adv.*, 2012, **2**, 12144.

320 L. Yu, G. Z. Chen, *Faraday Discuss.*, 2016, DOI: 10.1039/C5FD00232J.

321 A. Basile, A. I. Bhatt, A. P. O'Mullane, *Nat. Commun.*, 2016, **7**, 11794.

322 J. Coetzer, *J. Power Sources*, 1986, **18**, 377.

323 J. Prakash, L. Redey, and D. R. Vissers, *J. Power Sources*, 1999, **84**, 63.

324 X. Lu, G. Li, J. Y. Kim, J. P. Lemmon, V. L. Sprenkle, and Z. Yang, *Energy Environ. Sci.*, 2013, **6**, 1837.

325 H. Kim, et al., Liquid Metal Batteries: Past, Present, and Future. *Chem. Rev.*, 2013, **113**, 2075.

326 E. A. Ukshe and N. G. Bukun, *Russian Chem. Rev.*, 1961, **30**, 90.

327 M. A. Bredig, J. W. Johnson and W. T. Smith, *J. Am. Chem. Soc.*, 1955, 77,

328 A. S. Dworkin, H. R. Bronstein and M. A. Bredig, *J, Phy. Chem.*, 1968, **72**, 1892.

329 C. E. Johnson and E. J. Hathaway, *J. Electrochem. Soc.*, 1971, **118**, 631.

330 E. R. Van Artsdalen and I. S. Yaffe, *J. Phy. Chem.*, 1955, **59**, 118.

331 B. L. Spatocco, T. Ouchi, G. Lambotte, P. J. Burke, D. R. Sadoway, *J. Electrochem. Soc.,* 2015, **162**, A2729.

332 D. J. Bradwell, H. Kim, A. H. C. Sirk, D. R. Sadoway, *J. Am. Chem. Soc.,* 2012, **134**, 1895.

333 H. Kim, D. A. Boysen, T. Ouchi, D. R. Sadoway, *J. Power Sources,* 2013, **241**, 239.

334 T. Ouchi, H. Kim, X. Ning, D. R. Sadoway, *J. Electrochem. Soc.,* 2014, **161**, A1898.

335 B. L. Spatocco, T. Ouchi, G. Lambotte, P. J. Burke, D. R. Sadoway, *J. Electrochem. Soc.,* 2015, **162**, A2729.

336 X. Ning, S. Phadke, B. Chung, H. Yin, P. Burke, D. R. Sadoway, *J. Power Sources,* 2015, **275**, 370.

337 A. Mehmeti, F. Santoni, M. Della Pietra, S. J. Mcphail, *J. Power Sources*, 2016, **308**, 97.

338 D. Fray, *Faraday Discuss.*, 2016, **190**, 11.

339 H. Morita, M. Kawase, Y. Mugikura, K. Asano, *J. Power Sources*, 2010, **195**, 6988.

340 S. Giddey, S. P. S. Badwal, A. Kulkarni, C. Munnings, *Prog. Energy Combusti.*, 2012, **38**, 360.

341 N. J. Cherepy, K. J. Fiet, R. Krueger, A. F. Jankowski, J. F. Cooper, *J. Electrochem. Soc.*, 2005, **152**, A80.

342 M. R. Predtechenskiĭ, Y. D. Varlamov, O. F. Bobrenok, S. N. Ul'yankin, *Doklady Physics*, 2009, **54**, 281.

343 M. R. Predtechensky, Y. D. Varlamov, O. F. Bobrenok, S. N. Ul'yankin, *J. Eng. Thermophys.*, 2009, **18**, 93.

344 M. R. Predtechensky, Y. D. Varlamov, S. N. Ul'yankin, Y. D. Dubov, *Thermophysics and Aeromechanics*, 2009, **16**, 601.

345 D. W. McKee and D. Chatterji, *Carbon*, 1975, **13**, 381.

346 P. G. Glugla and V. J. DeCarlo, *J. Electrochem. Soc.*, 1982, **129**, 1745.

347 D. Cao, Y. Sun and G. Wang, *J. Power Sources*, 2007, **167**, 250.

348 Y. K. Delimarskii, O. V. Gordis'kii and V. F. Grishchenko, *Dokl Akad Nauk* SSSR, 1964, **156**, 650

349 M. D. Ingram, B. Baron and G. J. Janz, *Electrochim. Acta*, 1966, **11**, 1629.

350 H. Kawamura and Y. Ito, *J. App. Electrochem*. 2000, **30**, 571.

351 S. Licht, B. Wang, S. Ghosh, H. Ayub, D. Jiang, J. Ganley, *J. Phys. Chem. Lett.*, 2010, **1**, 2363.

352 N. J. Siambun, H. Mohamed, D. Hu, D. Jewell, Y. K. Beng and G. Z. Chen, *J. Electrochem. Soc.*, 2011, **158**, H1117.

353 H. Yin, X. Mao, D. Tang, W. Xiao, L. Xing, H. Zhu, D. Wang and D. R. Sadoway, *Energy Environ. Sci.*, 2013, **6**, 1538.

354 H. V. Ijije, C. Sun and G. Z. Chen, *Carbon*, 2014, **73**, 163.

355 H. V. Ijije, R. C. Lawrence, N. J. Siambun, S. M. Jeong, D. A. Jewell, D. Hu and G. Z. Chen, *Faraday Discuss.*, 2014, **172**, 105.

356 H. V. Ijije, R. C. Lawrence and G. Z. Chen, *RSC Adv.*, 2014, **4**, 35808.

357 M. A. Hughes, J. A. Allen and S. W. Donne, SW, *Electrochim. Acta*, 2015, **176**, 1511.

358 J. W. Ren, J. Lau, M. Lefler and S. Licht, *J. Pgys. Chem. C*, 2015, **119**, 23342.

359 L. W. Hu, Y. Song,S. Q. Jiao, Y. J. Liu, J. B. Ge, H. D. Jiao, J. Zhu, J. X. Wang, H. M. Zhu and D. J. Fray, *ChemSusChem*, 2016, **9**, 588.

360 H. V. Ijije and G. Z. Chen, *Adv. Manufact.*, 2016, **4**, 23.

Entry for table of contents

Innovative salt solutions and liquid salts can advance batteries, supercapacitors, and supercapatteries for stationary, transport, seasonal and regional energy storage.

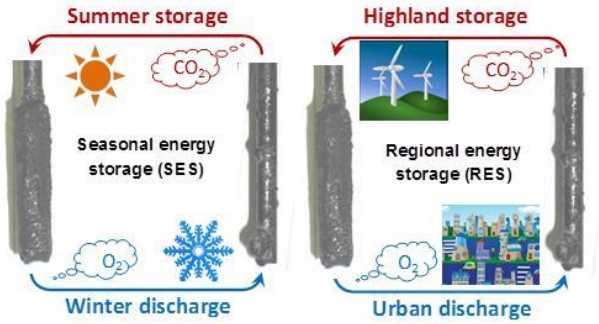

Photograph and biography of authors

From right to left: Dr. Lan Xia, Dr. Linpo Yu, Dr. Di Hu and Prof. George Z. Chen. The unique green building, solar panels and solar heaters in the background belong the Centre for Sustainable Energy Technologies at the University of Nottingham Ningbo China.

Lan Xia currently works as an Associate Research Fellow in Prof. George Z. Chen's group at the University of Nottingham Ningbo China (UNNC). She earned her PhD in physical chemistry from Wuhan University with Prof. Xin-Ping Ai in 2013. She then worked as a postdoctoral fellow with Prof. Zhao-Ping Liu at the Ningbo Institute of Materials Technology and Engineering (NIMTE), Chinese Academy of Sciences. Her research focuses on the self-actuating thermal protection mechanism for lithium ion batteries as well as design, synthesis and characterization of potential electrolyte solvents and electrolyte additives for batteries.

Linpo Yu is a Senior Research Fellow in Electrochemistry at the University of Nottingham Ningbo China. He is a member of the Royal Society of Chemistry. He received his BSc in Chemistry and PhD in Physical Chemistry (Electrochemistry) from Wuhan University in 2003 and 2008, respectively. He was a Research Assistant at Suzhou Institute of Nano-Tech and Nano-Bionics, CAS from 2008 to 2013. Then, he carried out postdoctoral research at the University of Nottingham in the UK for 2 years until he joined in the University of Nottingham Ningbo China in 2015. His main research interests include the supercapacitor and supercapattery electrode materials, ionic liquid electrolytes, and thermochromic materials.

Di Hu is assistant professor of chemical engineering in the University of Nottingham Ningbo Campus. His primary research background lies in the electrochemical production of pure metals and metal alloys via molten salt electrolysis. Dr Di Hu completed his BEng degree in Chemical Engineering and Technology at the China University of Mining and Technology (Beijing) in July 2006, and the MSc and PhD degrees in Chemical Engineering at the University of Nottingham in December 2007 and 2011, respectively. His PhD research was supervised by Prof. George Z. Chen on the subject of near-net-shape production of titanium alloy products via molten salt electrolysis.

George Zheng Chen (http://www.nottingham.ac.uk/~enzgzc), *CChem, FRSC, FRSA, FIMMM*, is professor of electrochemical technologies in both the Nottingham and Ningbo campuses of the University of Nottingham. He received both his Teaching Diploma (1981, Jiujiang Teacher Training College) and MSc (1985, Fujian Normal University, Prof. Qixin Zhang) in China. After obtaining his PhD in 1992 from University of London (Imperial College, Prof. John Albery, *FRS*), he worked in the Universities of Oxford (1992-1994), Leeds (1994-96) and Cambridge (1996-2003, Darwin), and in Jiangxi (1985-1988) and Wuhan (2000-2010, invited position) Universities. His research aims at electrochemical and liquid salts innovations for materials, energy and environment, producing 600+ documented outputs, including the Fray-Farthing-Chen Cambridge Process. (ORCID: 0000-0002-5589-5767).